Initiation, Progression and Malignant Transformation of Endogenous *Nras*$^{G12D/+}$-induced Chronic Myelomonocytic Leukemia

By

Jingfang Zhang

A dissertation submitted in partial fulfillment of

the requirements for the degree of

Doctor of Philosophy

(Oncology)

at the

UNIVERSITY OF WISCONSIN-MADISON

2015

Date of final oral examination: May 11th, 2015

The dissertation is approved by the following members of the Final Oral Committee:

Jing Zhang, Associate Professor, Oncology

Paul Lambert, Professor, Oncology

Emery Bresnick, Professor, Cell and Regenerative Biology

Norman Drinkwater, Professor, Oncology

Erik Ranheim, Professor (CHS), Pathology and Laboratory Medicine

Initiation, Progression and Malignant Transformation of Endogenous *Nras*$^{G12D/+}$-induced Chronic Myelomonocytic Leukemia

Jingfang Zhang

Under the supervision of Associate Professor Jing Zhang

at the University of Wisconsin - Madison

Abstract

Chronic myelomonocytic leukemia (CMML) is a devastating cancer that primarily occurs in the elderly with the median age ranging from 65 to 75 years. CMML is characterized by persistent monocytosis in peripheral blood. The clinical phenotypes of CMML are heterogeneous, ranging from predominantly myeloproliferative (MP-CMML) to predominantly myelodysplastic (MD-CMML). Approximately 15-20% of CMML cases evolve to acute myeloid leukemia (AML) soon after their initial diagnosis. The prognosis of CMML is poor with the median survival ranging from 15 to 20 months.

Oncogenic *NRAS* mutations are frequently indentified in CMML patients, especially in patients with MP-CMLL. Consistent with human studies, our lab previously developed a MP-CMML mouse model induced by *Nras*$^{G12D/+}$ expressed from its endogenous locus. Over 90% of recipient mice transplanted with *Nras*$^{G12D/+}$ bone marrow cells develop MP-CMML-like phenotypes with a prolonged latency. In this mouse model, *Nras*$^{G12D/+}$-HSCs are leukemia initiating cells (LICs). And hyperactivation of granulocyte-macrophage colony stimulating factor (GM-CSF) signaling, which is frequently associated with human CMML patients, is acquired during CMML progression. These results suggest that hyperactivation of GM-CSF signaling might be

essential for CMML initiation and/or progression. To further test this hypothesis, we deleted GM-CSF receptor βc subunit in *Nras*$^{G12D/+}$ mice. Our results indicate that deletion of *βc* abolishes GM-CSF signaling, but neither affects *Nras*$^{G12D/+}$ HSC functions, nor abrogates *Nras*$^{G12D/+}$-induced CMML. However, loss of βc-mediated GM-CSF signaling did slow down CMML progression, as demonstrated by reduced splenmegaly, loss of spontaneous colony formation, and prolonged the survival of recipient mice with *Nras*$^{G12D/+}$ cells. Together, our data suggest that inhibiting GM-CSF signaling in MP-CMML patients might transiently mitigate disease phenotypes but not eradicate the disease.

Nras$^{G12D/+}$-induced CMML in mice never spontaneously transform to AML. We tested the potential genetic interaction between loss of *p53* and endogenous oncogenic Nras signaling in promoting CMML to AML. For this purpose, we generated conditional *Nras*$^{G12D/+}$; *p53*$^{-/-}$ mice. The recipient mice transplanted with *Nras*$^{G12D/+}$; *p53*$^{-/-}$ bone marrow cells developed a highly penetrant AML. Our results demonstrate that loss of *p53* profoundly impacts on *Nras*$^{G12D/+}$ MPs to promote leukemogenesis, as demonstrated by increased quiescence and self-renewal in *Nras*$^{G12D/+}$; *p53*$^{-/-}$ MPs. These mutant MPs are transformed to AML initiating cells (referred as AML-MPs). The distinct transcriptome of AML-MPs is mainly driven by loss of *p53*. Moreover, oncogenic *Nras* is overexpressed in AML-MPs through genetic and epigenetic mechanisms leading to hyperactivation of ERK1/2 signaling. Together, our results indicate that loss of *p53* synergizes with enhanced oncogenic Nras signaling to promote the leukemogenic transformation of MPs and drive the evolution of CMML to AML.

Table of contents

List of figures

Chapter 1

Chapter 2

Chapter 3

List of tables

Chapter 3

Acknowledgments

After the PhD training in McArdle Laborotory for Cancer Research at the University of Wisconsin-Madison, I feel I made a big step towards my goal as an independent scientist. This could not be accomplished without other people's help, encouragement and inspiration. I own so many thanks to my teachers, my work mates, my friends and my family.

First of all, I would like to thank Dr. Jing Zhang for her outstanding mentoring. It was her to introduce me to this fascinating research field: hematopoiesis and leukemia. Her hardworking, patience and sharp thinking made my PhD training effective and meaningful. I learned a lot from her not only through direct instructions but more often through witnessing how she performs in her research career: to be creative and more importantly critical in science. I am sure this experience will benefit me throughout my life.

Secondly, I would like to show my great appreciation to all my committee members, Drs. Paul Lambert, Emery Bresnick, Erik Ranheim and Norman Drinkwater. I benefit a lot from their inspiring questions, which made me think deeper and wider.

Thirdly, I would like to thank all my collaborators, especially Li Lu, a Postdoc in Dr. Xuehua's Lab, without her help in bioinformatics this thesis could not be finished in time. Also, I would like to thank my lab members in the Zhang lab, current and past. They are always helpful and like to share ideas and opinions with me.

Last but not least, I would like to thank my parents, my husband and my lovely daughter. Their love and unconditional supports inspire me to work towards my career goal.

Abbreviations

AML	Acute myeloid leukemia
βc	Common β subunit
CFU-GM	Colony forming unit-granulocyte macrophage
CMML	Chronic myelomonocytic leukemia
CMP	Common myeloid progenitor
GAP	GTPase activating protein
GEF	Guanine nucleotide exchange factor
GM-CSF	Granulocyte-macrophage colony stimulating factor
GMP	Granulocyte-monocyte progenitor
HSC	Hematopoietic stem cell
IL-3	Interleukin-3
IL-5	Interleukin-5
JAK2	Janus kinase 2
JMML	Juvenile myelomonocytic leukemia
LIC	Leukemia initiating cell
LT-HSC	Long term-HSC
Nf1	Neurofibromatosis type 1
MEP	Megakaryocyte-erythroid progenitor
MD-CMML	Myelodysplastic-CMML
MP-CMML	Myeloproliferative-CMML
MDS/MPN	Myelodysplastic/myeloproliferative neoplasm
MP	Myeloid progenitor

MPN	Myeloproliferative neoplasm
MPP	Multipotent progenitor
pI-pC	Polyinosinic-polycytidylic acid
Stat5	Signal transducer and activator of transcriptions 5
T-ALL	T-cell lymphoblastic leukemia/lymphoma
UPD	Uniparental disomy
WHO	World Health Organization

Chapter 1

Introduction

1.1 Chronic myelomonocytic leukemia (CMML)

Chronic myelomonocytic leukemia (CMML) is a rare disease with approximate 0.3 cases per 100,000 people per year in United States [1]. CMML primarily occurs in the elderly with the median age ranging from 65 to 75 years [2]. CMML has a gender bias towards male with a male/female ratio of approximately 2:1, the reason for which remains largely unknown. The main feature of CMML is persistent monocytosis in peripheral blood. Monocytes constitute 2-10% of white blood cells in the human body with over half of them stored in spleen. Monocytes are the precursor of macrophages and dendritic cells, and play an important role in innate immune response. Upon infection, monocytes move rapidly to the affected area and differentiate quickly into macrophages to pursue their role in immune defense. Persistent clonal monocytosis is often associated with hematopoietic stem cell (HSC) disorders and is common in CMML [3].

In addition to the myeloproliferative feature (monocytosis), CMML also displays variable degrees of myelodysplastic phenotypes, which manifest as dysplasia in one or more myeloid lineages. Therefore, in 2008, CMML and its counterpart disease, juvenile myelomonocytic leukemia (JMML), which mainly occurs in children between birth and 6 years of age, were classified as mixed myelodysplastic/myeloproliferative neoplasm (MDS/MPN) by the World Health Organization (WHO) [4]. Now the widely accepted diagnostic criteria for CMML include: persistent monocytosis in peripheral blood with counts > 1 x 10^9/l; absence of *BCR-ABL* fusion gene and absence of rearrangements of *PDGFRA* and *PDGFRB* genes; less than 20% myeloblasts and promonocytes in the peripheral blood or bone marrow; and dysplasia in one or more myeloid lineages. If myelodysplasia is absent or minimal, a diagnosis of CMML still can be made if other

requirements are met, and a molecular genetic abnormality is present or persistent monocytosis for more than three months and other causes of monocytosis have been ruled out. Based on blast count in peripheral blood and bone marrow, the WHO further sub-classified CMML into CMML-1 (< 5% peripheral blasts, < 10% medullary blasts) and CMML-2 (5-19% peripheral blasts, 10-19% medullary blasts). CMML-2 has a poorer prognosis and higher risk of transforming to acute myeloid leukemia (AML) compared with CMML-1.

Although several large cohort studies of CMML patients have been performed in the United States and Europe, a widely accepted prognostic model is not available yet. One of the most recently developed prognostic scoring systems was proposed by Mayo Clinic [5]. This system uses four independent risk factors including increased absolute monocyte count (> 10 x 10^9/l), presence of circulating immature myeloid cells, decreased hemoglobin (< 10 g/dl) and decreased platelet count (< 100 x 10^9/l) to stratify CMML patients into three categories: low risk (0 risk factors), intermediate risk (1 risk factor) and high risk (2 or more risk factors), with median survivals of 32, 18 and 10 months, respectively.

Cytogenetic abnormalities are observed in 20-40% of CMML patients in different studies and are associated with poor prognosis and high risk of AML transformation [5-7]. The recently proposed Spanish cytogenetic risk stratification system classified CMML patients into three groups: high risk with trisomy 8, complex karyotype or abnormalities of chromosome 7, low risk with normal karyotype or loss of Y chromosome, and intermediate risk that include all other chromosomal abnormalities [7].

In addition, molecular aberrations are detected in approximately 90% of CMML

patients [8]. Unlike JMML, which is mainly caused by deregulation of Ras signaling [2], the molecular pathogenesis of CMML is more heterogeneous. Based on recently published sequencing results, mutated genes identified in CMML could be classified into four different categories [3, 8]. The first class includes cytokine receptors and genes involved in Ras signaling, such as *NRAS*, *CBL*, *JAK2*, *KRAS*, and *FLT3*, which mainly regulate cell proliferation and survival. Oncogenic *NRAS* and *KRAS* are among the most frequently identified mutations in this category and often associated with myeloproliferative-CMML(MP-CMML)-like phenotypes [9]. The second class is transcription factors that regulate hematopoietic stem and progenitor cell functions, for example, *RUNX1* and *TP53*. The third class is genes involved in epigenetic regulation of gene transcription, such as *ASXL1*, *TET2*, *IDH2*, *EZH2*, *DNMT3A*, *IDH1*. In addition, mutations involved in spliceosome components are frequently identified in CMML patients, including *SRSF2*, *SF3B1*, *ZRSF2* and *U2AF1*.

One reason rendering CMML a devastating disease is that approximately 15-20% of CMML patients transform to AML soon after their initial diagnosis [10]. However, the molecular mechanism of this malignant transformation remains largely unknown. A recent study demonstrated that recurrent genetic alterations in post-myeloproliferative neoplasm (MPN, mainly driven by $JAK2^{V617F}$ mutation) AML include *ASXL1*, *IDH2*, *SRSF2*, *TP53* and *CALR***,** which occur at a much lower frequency in de novo AML [11]**.** However, involvement of these genetic lesions in CMML transformation to AML has not been shown.

Currently, there is no effective treatment for CMML, though several agents and on-going clinical trials might provide partial benefits to certain groups of CMML patients.

For example, myelosuppressive agents, such as hydroxycarbamide, can be used to reduce splenomegaly and elevated blood counts [12]. Hypomethylating agents, such as 5-Azacitidine and decitabine, have been recently approved for use in patients with MDS and CMML [3]. GSK212, an MEK inhibitor, is currently in clinical trial for CMML patients with *RAS* mutations (Trial #: NCT00920140). Allogeneic stem cell transplantation remains the best option. However, it is not suitable for most CMML patients given their old age. Therefore, it is urgent to find effective therapeutic targets for CMML patients.

1.2 Hyperactive GM-CSF signaling in CMML

Granulocyte-macrophage colony stimulating factor (GM-CSF) plays an important role in regulating survival, proliferation, differentiation and activation of various hematopoietic cells, especially macrophages and granulocytes [13]. GM-CSF receptor is composed of α (GM-CSFRα) and β subunit (GM-CSFRβc). β subunit is usually named as common β (βc) subunit because it is shared by other two cytokine receptors, interleukin-3 (IL-3) receptor and interleukin-5 (IL-5) receptor. Mice deficient for *Gmcsf* or *βc* are grossly normal and show no significant alterations in hematopoiesis [12, 14, 15], suggesting that GM-CSF signaling is dispensable for normal hematopoiesis.

Upon ligand binding, GM-CSF receptor and its ligand form a dodecamer or higher order complex and its associated Janus kinase 2 (JAK2) is activated. Activated JAK2 in turn phosphorylates signal transducer and activator of transcriptions 5 (Stat5) and GM-CSFR βc subunit. Phosphorylated receptor recruits adaptor proteins and further activates the Ras/Raf/MEK/ERK pathway.

Ras proteins are small GTPases and there are three *RAS* genes in human, *Kras*, *Nras* and *Hras*. Ras proteins act as molecular switches by cycling between active GTP-bound and inactive GDP-bound forms. Adaptor proteins activate guanine nucleotide exchange factors (GEFs), which subsequently activate Ras by stimulating their disassociation from GDP and loading of GTP. Conversely, activated Ras-GTP is turned off by its intrinsic GTPase activity and this process is accelerated by GTPase activating proteins (GAPs).

Oncogenic mutations in *KRAS* and *NRAS*, but rarely in *HRAS*, are identified in myeloid diseases including JMML, CMML, and AML [16]. Mutations in *RAS* and its regulatory components, such as *CBL*, *PTPN11*, *NF1*, are identified in approximately 90% of JMML [2] and about 40% of CMML [8], and oncogenic *Ras* mutations are specifically enriched in MP-CMML (~40%) [9]. Several hotspots have been identified for *RAS* mutations, including G12, G13 and Q61 codons. Substitutions at these residues lock Ras in the activated GTP-bound form by decreasing or abolishing GTP hydrolysis to GDP. Noticeably, uniparental disomy (UPD) of oncogenic *RAS* allele is observed during JMML/CMML development [17].

One cellular feature of JMML and CMML is forming increased numbers of colony forming unit-granulocyte macrophage colonies (CFU-GM) in the absence or presence of GM-CSF [18-21]. This abnormal cell growth could be due to increased secretion of GM-CSF and/or hypersensitivity of patient progenitor cells to GM-CSF stimulation. Previous reports showed that serum level of GM-CSF in CMML patients is low or even undetectable [20, 22]. On the other hand, a recent study identified hyperactivated JAK2/Stat5 signaling in JMML and CMML patient samples upon GM-

CSF stimulation [19]. Consistent with this finding, our lab also found that recipient mice transplanted with *Nras*$^{G12D/+}$ bone marrow cells gain hyperactivation of GM-CSF-evoked JAK2/Stat5 and Ras/Raf/MEK/ERK signaling during MP-CMML development [16]. In addition, human CMML cells can only engraft into immunodeficient mice expressing human GM-CSF transgene [21]. All these findings indicate that JMML/CMML cells are hypersensitive to GM-CSF, which may contribute to abnormal leukemia cell proliferation.

Inhibiting GM-CSF signaling has been evaluated as a potential treatment for JMML/MP-CMLL. E21R, a GM-CSF analogue, selectively binds GM-CSFRα subunit, antagonizes GM-CSF signaling, and induces apoptosis in hematopoietic cells cultured *in vitro* [23]. Short-term treatment of E21R not only markedly reduces JMML xenograft growth in immunodeficient mice but also receives transient clinical response in a patient with end-stage JMML [24, 25]. E21R has also been demonstrated to inhibit CMML cell growth *in vitro* [21].

The long-term effects of inhibiting GM-CSF signaling on JMML development have also been evaluated in *Nf1*$^{-/-}$ mouse model. Neurofibromatosis type 1 (Nf1) is a Ras GAP that accelerates the hydrolysis of Ras-GTP into Ras-GDP and thus serves as a negative regulator of Ras signaling. Children with NF1 syndrome are predisposed to JMML and *Nf1*-deficient mice develop JMML-like phenotypes. To completely abolish GM-CSF signaling, *Nf1*$^{-/-}$ mice were bred to *βc*$^{-/-}$ background. The obtained results are controversial. The recipient mice transplanted with *Nf1*$^{-/-}$; *βc*$^{-/-}$ fetal liver cells do not develop significant JMML over one year, while using Mx1-Cre to inactivate the *Nf1* allele in adult *βc*$^{-/-}$ hematopoitic system attenuates JMML-like phenotype but does not abrogate it [26].

1.3 *Nras*$^{G12D/+}$-induced CMML mouse model

Recently, our lab developed a CMML mouse model induced by endogenous *Nras*$^{G12D/+}$ [16]; recipient mice transplanted with bone morrow cells expressing *Nras*$^{G12D/+}$ develop a highly penetrant CMML (above 90%) after a prolonged latency. In this model, *Nras*$^{G12D/+}$ HSCs are required to initiate and maintain CMML and thus serve as leukemia initiating cells (LICs). *Nras*$^{G12D/+}$ HSCs undergo moderate hyperproliferation with increased self-renewal and display a myeloid lineage differentiation bias. These phenotypes are associated with hyperactivation of ERK1/2 in HSCs and can be partially rescued by down-regulating ERK1/2 signaling [27].

Myeloid progenitor (MP) compartment is moderately expanded in *Nras*$^{G12D/+}$ mice. This is not due to hyperproliferation of MPs but is mainly caused by biased *Nras*$^{G12D/+}$ HSC differentiation. Although hyperactivated GM-CSF signaling is not observed in *Nras*$^{G12D/+}$ MPs after acute induction of the oncogene, they form spontaneous colonies without exogenous cytokine stimulation. The abnormal GM-CSF signaling is only observed during CMML development, which in some cases is associated with UPD of oncogenic *Nras* allele. However, based on the observations that secondary recipient mice transplanted with CMML bone marrow cells require a long latency similar to that in the primary recipient mice and only *Nras*$^{G12D/+}$ HSCs could re-establish CMML in irradiated recipients, we believe that *Nras*$^{G12D/+}$ MPs play an important role in driving CMML formation but are not fully transformed to LICs yet.

Based on these results, we propose a model for CMML development (Figure 1-1). While *Nras*$^{G12D/+}$ HSCs proliferate and differentiate, additional mutations accumulate in

MPs, for example UPD of *Nras*$^{G12D/+}$ allele, which leads to hyperactivated GM-CSF signaling. The aberrant cytokine signaling in turn drives inappropriate myeloid progenitor/precursor cell survival, proliferation and differentiation, which subsequently result in persistent monocytosis. However, more concrete evidence is required to determine whether aberrant GM-CSF signaling plays an important role in CMML initiation and/or progression. Additionally, none of our *Nras*$^{G12D/+}$-induced CMML mice spontaneously transforms to AML, suggesting that additional genetic alterations are required to cooperate with oncogenic *Nras* in this process.

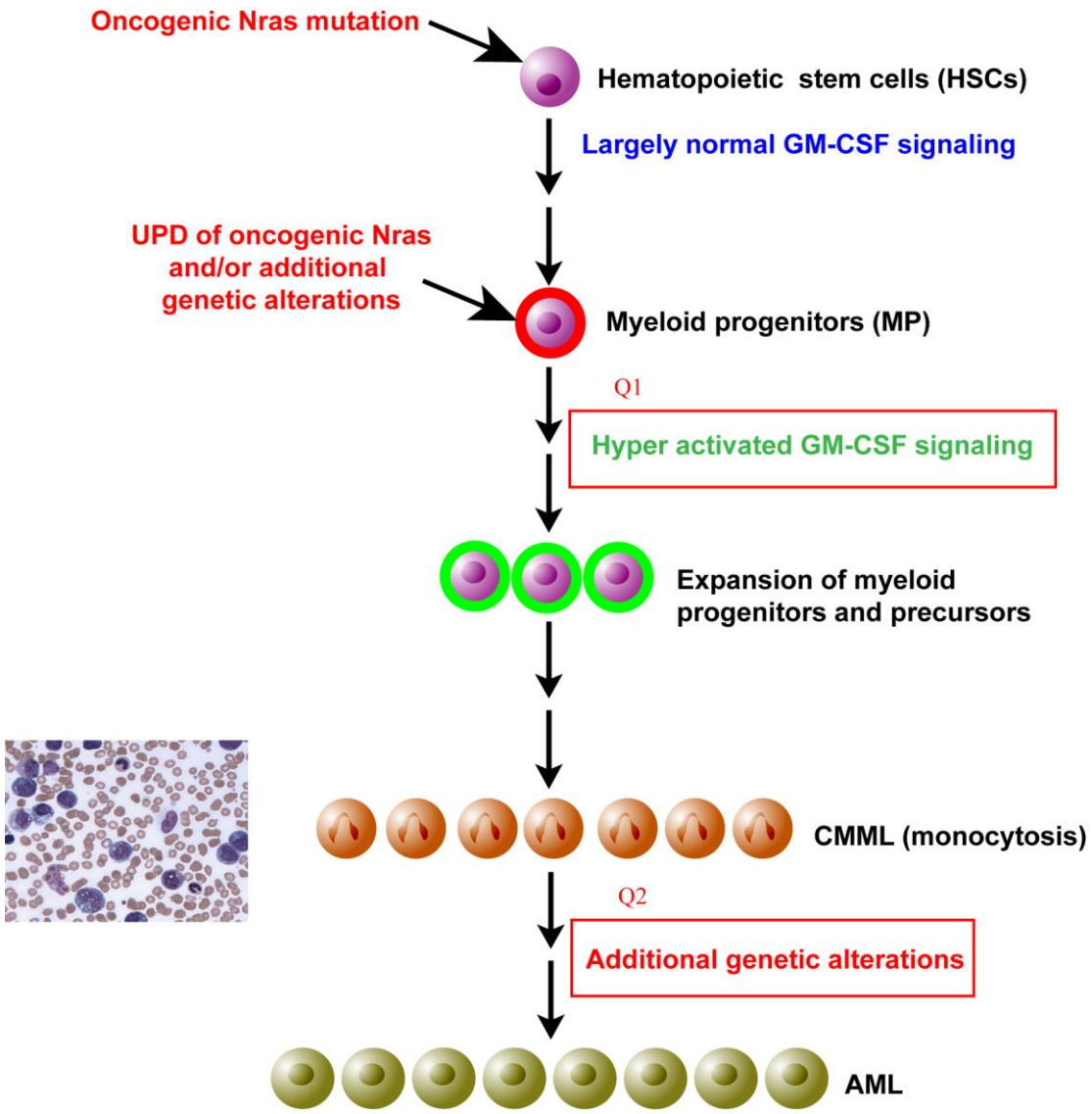

Figure 1-1. A mouse model of CMML

1.4 Synopsis of this research

The goal of this thesis is to address two important questions in CMML development and transformation. The first one is whether GM-CSF signaling plays an essential role in *Nras*$^{G12D/+}$-induced CMML initiation and/or progression. The second one is whether loss

of *p53* synergizes with oncogenic *Nras*$^{G12D/+}$ to promote malignant transformation of CMML to AML.

To address the first question, we further deleted GM-CSF receptor βc subunit in *Nras*$^{G12D/+}$ mice. Our results show that deletion of *βc* abolishes GM-CSF signaling but does not affect the function of *Nras*$^{G12D/+}$-HSCs, which serve as LICs. Not surprisingly, recipient mice with *Nras*$^{G12D/+}$*; βc*$^{-/-}$ bone marrow cells still develop CMML but with significantly prolonged latency. These results indicate that abolishing GM-CSF signaling is inadequate to inhibit CMML initiation, but it slows down the disease progression.

Despite our wealth of knowledge in pathogenic mechanisms driving CMML formation, little is known about the cellular and molecular mechanisms underlying the malignant transformation of CMML to AML. We tested potential genetic interaction between oncogenic *Nras* and *p53* deficiency in promoting this malignant transformation. We demonstrate that loss of *p53* induces increased self-renewal in MPs associated with their increased quiescence in G0 phase. And loss of *p53* induces further expansion of *Nras*$^{G12D/+}$ MPs *in vivo*. In addition, a fraction of these MPs acquire overexpression of oncogenic *Nras* through genetic and epigenetic mechanisms and are transformed to AML initiating cells. Together, our study identifies a significant synergy between p53 loss and enhanced oncogenic Nras signaling in promoting CMML transformation to AML.

1.5 Reference

1. Rollison, D.E., et al., Epidemiology of myelodysplastic syndromes and chronic myeloproliferative disorders in the United States, 2001-2004, using data from the NAACCR and SEER programs. Blood, 2008. **112**(1): p. 45-52.
2. Emanuel, P.D., Juvenile myelomonocytic leukemia and chronic myelomonocytic leukemia. Leukemia, 2008. **22**(7): p. 1335-42.
3. Patnaik, M.M., et al., Chronic myelomonocytic leukaemia: a concise clinical and pathophysiological review. Br J Haematol, 2014. **165**(3): p. 273-86.
4. Vardiman, J.W., et al., The 2008 revision of the World Health Organization (WHO) classification of myeloid neoplasms and acute leukemia: rationale and important changes. Blood, 2009. **114**(5): p. 937-51.
5. Patnaik, M.M., et al., Mayo prognostic model for WHO-defined chronic myelomonocytic leukemia: ASXL1 and spliceosome component mutations and outcomes. Leukemia, 2013. **27**(7): p. 1504-10.
6. Onida, F., et al., Prognostic factors and scoring systems in chronic myelomonocytic leukemia: a retrospective analysis of 213 patients. Blood, 2002. **99**(3): p. 840-9.
7. Such, E., et al., Cytogenetic risk stratification in chronic myelomonocytic leukemia. Haematologica, 2011. **96**(3): p. 375-83.
8. Itzykson, R., et al., Prognostic score including gene mutations in chronic myelomonocytic leukemia. J Clin Oncol, 2013. **31**(19): p. 2428-36.

9. Ricci, C., et al., RAS mutations contribute to evolution of chronic myelomonocytic leukemia to the proliferative variant. Clin Cancer Res, 2010. **16**(8): p. 2246-56.

10. Germing, U., A. Kundgen, and N. Gattermann, Risk assessment in chronic myelomonocytic leukemia (CMML). Leuk Lymphoma, 2004. **45**(7): p. 1311-8.

11. Rampal, R., et al., Genomic and functional analysis of leukemic transformation of myeloproliferative neoplasms. Proc Natl Acad Sci U S A, 2014. **111**(50): p. E5401-10.

12. Wattel, E., et al., A randomized trial of hydroxyurea versus VP16 in adult chronic myelomonocytic leukemia. Groupe Francais des Myelodysplasies and European CMML Group. Blood, 1996. **88**(7): p. 2480-7.

13. Hercus, T.R., et al., The granulocyte-macrophage colony-stimulating factor receptor: linking its structure to cell signaling and its role in disease. Blood, 2009. **114**(7): p. 1289-98.

14. Nishinakamura, R., et al., Mice deficient for the IL-3/GM-CSF/IL-5 beta c receptor exhibit lung pathology and impaired immune response, while beta IL3 receptor-deficient mice are normal. Immunity, 1995. **2**(3): p. 211-22.

15. Robb, L., et al., Hematopoietic and lung abnormalities in mice with a null mutation of the common beta subunit of the receptors for granulocyte-macrophage colony-stimulating factor and interleukins 3 and 5. Proc Natl Acad Sci U S A, 1995. **92**(21): p. 9565-9.

16. Wang, J., et al., Endogenous oncogenic Nras mutation promotes aberrant GM-CSF signaling in granulocytic/monocytic precursors in a murine model of chronic myelomonocytic leukemia. Blood, 2010. **116**(26): p. 5991-6002.

17. Kong, G., et al., Combined MEK and JAK inhibition abrogates murine myeloproliferative neoplasm. J Clin Invest, 2014. **124**(6): p. 2762-73.

18. Emanuel, P.D., et al., Selective hypersensitivity to granulocyte-macrophage colony-stimulating factor by juvenile chronic myeloid leukemia hematopoietic progenitors. Blood, 1991. **77**(5): p. 925-9.

19. Kotecha, N., et al., Single-cell profiling identifies aberrant STAT5 activation in myeloid malignancies with specific clinical and biologic correlates. Cancer Cell, 2008. **14**(4): p. 335-43.

20. Cambier, N., et al., Chronic myelomonocytic leukemia: from biology to therapy. Hematol Cell Ther, 1997. **39**(2): p. 41-8.

21. Ramshaw, H.S., et al., Chronic myelomonocytic leukemia requires granulocyte-macrophage colony-stimulating factor for growth in vitro and in vivo. Exp Hematol, 2002. **30**(10): p. 1124-31.

22. Verhoef, G.E., et al., Measurement of serum cytokine levels in patients with myelodysplastic syndromes. Leukemia, 1992. **6**(12): p. 1268-72.

23. Iversen, P.O., et al., The apoptosis-inducing granulocyte-macrophage colony-stimulating factor (GM-CSF) analog E21R functions through specific regions of the heterodimeric GM-CSF receptor and requires interleukin-1beta-converting enzyme-like proteases. J Biol Chem, 1997. **272**(15): p. 9877-83.

24. Iversen, P.O., et al., Inhibition of granulocyte-macrophage colony-stimulating factor prevents dissemination and induces remission of juvenile myelomonocytic leukemia in engrafted immunodeficient mice. Blood, 1997. **90**(12): p. 4910-7.

25. Bernard, F., et al., Transient hematologic and clinical effect of E21R in a child with end-stage juvenile myelomonocytic leukemia. Blood, 2002. **99**(7): p. 2615-6.

26. Kim, A., et al., Beta common receptor inactivation attenuates myeloproliferative disease in Nf1 mutant mice. Blood, 2007. **109**(4): p. 1687-91.

27. Wang, J., et al., Nras(G12D/+) promotes leukemogenesis by aberrantly regulating hematopoietic stem cell functions. Blood, 2013. **121**(26): p. 5203-7.

Chapter 2

Deficiency of *β common receptor* attenuates the progression of myeloproliferative neoplasm in *Nras*$^{G12D/+}$ mice

Juan Du, a previous postdoctoral in our lab, helped to generate the compound mouse *Nras*$^{G12D/+}$; $\beta c^{-/-}$. Erik Ranheim, a professor in Pathology and Laboratory Medicine, helped to check all the tissue sections.

2.1 Abstract

Activating Ras signaling is a major driver in juvenile and the myeloproliferative variant of chronic myelomonocytic leukemia (JMML/MP-CMML). Numerous studies suggest that GM-CSF signaling plays a central role in establishing and maintaining JMML/MP-CMML phenotypes in human and mouse. However, it remains elusive how GM-CSF signaling impacts on JMML/MP-CMML initiation and progression. Here, we investigate this issue in a well-characterized MP-CMML model induced by endogenous *Nras*$^{G12D/+}$ mutation. In this model, *Nras*$^{G12D/+}$ hematopoietic stem cells (HSCs) are required to initiate and maintain CMML phenotypes and serve as CMML initiating cells. We show that the common β chain of the GM-CSF receptor (βc) is dispensable for *Nras*$^{G12D/+}$ HSC function; loss of *βc* does not affect the expansion, increased self-renewal, or myeloid differentiation bias in *Nras*$^{G12D/+}$ HSCs. Therefore, *βc*$^{-/-}$ does not abrogate CMML in *Nras*$^{G12D/+}$ mice. However, *βc* deficiency indeed significantly reduces *Nras*$^{G12D/+}$-induced splenomegaly and spontaneous colony formation and prolongs the survival of CMML-bearing mice, suggesting that GM-CSF signaling plays an important role in promoting CMML progression. Together, our results suggest that inhibiting GM-CSF signaling in JMML/MP-CMML patients might transiently alleviate disease symptoms but would not eradicate the disease.

2.2 Introduction

Juvenile and chronic myelomonocytic leukemia (JMML and CMML) belong to the group of "mixed myelodysplastic/myeloproliferative diseases" (MDS/MPD) [2, 25]. CMML primarily occurs in the elderly with median ages at presentation ranging from 65 to 75

years, whereas JMML exclusively affects children, typically under the age of 4 years. Despite the demographic difference, CMML and JMML share similar clinical features, including monocytosis, hepatosplenomegaly, and the absence of the *BCR-ABL* fusion gene. At the molecular level, activating Ras signaling is a central theme in JMML and in the myeloproliferative variant of CMML (MP-CMML) [2, 26-29]. Consistent with human studies, mice harboring an oncogenic *Ras* allele and mice deficient of *Nf1*, a negative regulator of Ras signaling, develop JMML/MP-CMML like phenotypes [30-38].

A cellular characteristic of both JMML and CMML is the formation of excess numbers of colony forming unit-granulocyte macrophage (CFU-GM) colonies in semi-solid cultures in the absence and presence of subsaturating concentrations of granulocyte-macrophage colony stimulating factor (GM-CSF) [15, 17, 39]. GM-CSF is an important hematopoietic cytokine that regulates the survival, proliferation, differentiation and activation of various hematopoietic cell types, especially macrophages and granulocytes [11]. Upon binding to its heteromeric receptor, which is composed of α (GM-CSFRα) and β subunit, the biological activities of GM-CSF are exerted through the Janus kinase 2 (Jak2)/ signal transducer and activator of transcriptions 5 (Stat5) and Ras/Raf/MEK/ERK pathways [40]. Despite hypersensitivity of JMML/CMML myeloid progenitors to GM-CSF, mice deficient of GM-CSF or its receptor develop normally and show no significant alterations of hematopoiesis [11, 40], suggesting that GM-CSF signaling is dispensable for normal hematopoiesis. Therefore, antagonizing GM-CSF signaling has been explored as a potential strategy for treating JMML/MP-CMML.

Several studies suggest that GM-CSF signaling plays a central role in establishing and maintaining JMML/MP-CMML like phenotypes. In a recent study of GM-CSF

signaling in JMML and CMML patient samples, an aberrant Stat5 signaling signature was identified in a subpopulation of monocytic cells defined as $CD33^{+}$ $CD14^{+}$ $CD34^{-}$ $CD38^{lo}$ cells [16]. This subset of cells can be used to monitor disease status at diagnosis, remission, relapse, and malignant transformation to an acute phase. Consistent with this notion, we found that recipients transplanted with $Nras^{G12D/+}$ cells acquire hypersensitivity to GM-CSF (both the Jak2/Stat5 and Ras/Raf/MEK/ERK pathways are hyperavtivated upon GM-CSF stimulation) during MP-CMML progression, which in some cases attribute to uniparental disomy of the oncogenic *Nras* allele [33]. Short-term inhibition of GM-CSF not only induces remission of JMML in engrafted immunodeficient mice [20] but also achieves transient clinical response in an end-stage JMML patient [21].

The long-term effects of inhibiting GM-CSF on JMML are evaluated in $Nf1^{-/-}$ model. Four of six $Gmcsf^{-/-}$ mice transplanted with $Nf1^{-/-}$; $Gmcsf^{-/-}$ fetal liver cells develop JMML-like phenotypes with prolonged latency [41], which is postulated to be due to the residual activity of pre-formed GM-CSF receptor in the absence of GM-CSF [42]. Subsequently, a study using the *Mx1-Cre* transgene to inactivate a conditional *Nf1* allele in $\beta c^{-/-}$ hematopoietic cells shows that the severity of JMML-like phenotypes are reduced but not abrogated, while mice transplanted with $Nf1^{-/-}$; $\beta c^{-/-}$ stem cells do not develop significant JMML over one year [24]. Therefore, it remains elusive how GM-CSF signaling impacts on JMML/MP-CMML initiation and progression.

We addressed this question using the well-characterized MP-CMML model induced by oncogenic *Nras* [33-35, 43, 44]. In this model, acute expression of oncogenic Nras from its endogenous locus leads to expanded hematopoietic stem cell (HSC)

compartment, increased HSC self-renewal, and myeloid differentiation bias in mutant HSCs. The myeloid progenitor (MP) compartment is expanded without significant hyperactivation of GM-CSF signaling or hyperproliferation in these cells, suggesting that increased number of MPs is largely due to the increased myeloid differentiation potential of *Nras*$^{G12D/+}$ HSCs. Consistent with this notion, ~95% of recipients transplanted with *Nras*$^{G12D/+}$ bone marrow cells develop MP-CMML like phenotypes after a long latency. *Nras*$^{G12D/+}$ HSCs are required to initiate and maintain the disease phenotypes and thus serve as CMML initiating cells, while MPs acquire secondary genetic hits to gain hypersensitivity to GM-CSF and push monocytosis to develop in vivo.

We chose a genetic approach to stably delete GM-CSF signaling in *Nras*$^{G12D/+}$ mice. The GM-CSF receptor shares a common β subunit (βc) with IL-3 and IL-5 receptors [45]. The GM-CSFRα and IL-5 receptor α subunits only pair with βc, while IL-3 receptor α subunit forms heterodimers with both βc and an IL-3 specific β subunit in mouse [46]. Therefore, *βc*$^{-/-}$ bone marrow cells respond to IL-3 but not GM-CSF. Here, we report that *Nras*$^{G12D/+}$*; βc*$^{-/-}$ HSCs are very similar as *Nras*$^{G12D/+}$ HSCs; both of them show comparably increased numbers, increased self-renewal, and increased myeloid differentiation bias resulting in expanded MP compartment. These results suggest that *βc* is dispensable for *Nras*$^{G12D/+}$ HSCs, the CMML initiating cells. Therefore, deletion of *βc* does not abrogate CMML formation in recipients transplanted with *Nras*$^{G12D/+}$ cells. However, loss of βc-mediated GM-CSF signaling indeed attenuates CMML progression as demonstrated by reducing splenomegaly, abolishing spontaneous colony formation, and prolonging the survival of recipients with *Nras*$^{G12D/+}$ cells. Our data suggest that

inhibiting GM-CSF signaling in JMML/MP-CMML patients might provide transient symptomatic improvements but would not eradicate the disease.

2.3 Materials and methods

Mice

All mouse lines were maintained on a pure C57BL/6 genetic background (>N10). The conditional *Nras*$^{LSL\ G12D/+}$ allele is described in (11). *Nras*$^{LSL\ G12D/+}$ mice were crossed to Mx1-Cre mice to generate mice carrying both alleles (*Nras*$^{LSL\ G12D/+}$*; Mx1-Cre*). The common β subunit knockout mice (*βc*$^{-/-}$) were obtained from Jackson Laboratories (stock number 005940). *Nras*$^{LSL\ G12D/+}$*; βc*$^{-/-}$ mice were crossed to *Mx1-Cre; βc*$^{-/-}$ to generate compound mice *Nras*$^{LSL\ G12D/+}$*; Mx1-Cre; βc*$^{-/-}$. Genotyping of *Nras*$^{G12D/+}$ and *Mx1-Cre* was done as previously described [33]. Genotyping of *βc* was performed per the instructions of Jackson Laboratory. CD45.1^{+} congenic recipient mice were purchased from NCI.

To induce Cre expression, 5-7 week old mice were injected intraperitoneally with 100 μg of polyinosinic-polycytidylic acid (pI-pC; GE Healthcare) every other day for two doses. The day of first pI-pC injection was defined as Day 1. All animal experiments were conducted in accordance with the *Guide for the Care and Use of Laboratory Animals* and approved by an Animal Care and Use Committee at UW-Madison. The program is accredited by the Association for Assessment and Accreditation of Laboratory Animal Care.

Murine bone marrow transplantation

2.5×10^5 total bone marrow cells ($CD45.2^+$) were mixed with same number of congenic bone marrow cells ($CD45.1^+$) and injected into individual lethally irradiated mice as described previously [33].

Flow cytometric analysis of hematopoietic tissues

For lineage analysis of peripheral blood, bone marrow, and spleen, flow cytometric analyses were performed as previously described [32]. HSCs, MPPs, LSK and MPs in bone marrow and spleen were analyzed as previously described [35, 43]. Stained cells were analyzed on a FACS Calibur or LSRII (BD Biosciences).

Directly conjugated or biotin conjugated antibodies specific for the following surface antigens were purchased from eBioscience: CD45.1 (A20), CD45.2 (104), Mac-1 (M1/70), Gr-1 (RB6-8C5), CD3 (145-2C11), CD4 (RM4-5), CD8 (53-6.7), CD19 (eBio1D3), Thy1.2 (53-2.1), TER119 (TER-119), B220 (RA3-6B2), IgM (eB121-15F9), IL-7Rα (B12-1), CD41 (eBioMWReg30), CD48 (HM48-1), Sca1 (D7), cKit (2B8), and CD34 (RAM34). FcγRII/III (2.4G2) was purchased from BD Biosciences. CD150 (TC15-12F12.2) was purchased from Biolegend.

Colony assay

A total of 5×10^4 bone marrow cells were plated in duplicate in semisolid medium MethoCult M3234 (StemCell Technologies) supplemented with mouse GM-CSF or IL-3 (Peprotech, Rocky Hill, NJ) according to the manufacture's protocol. The colonies were counted after 7-10 days in culture.

Flow cytometric analysis of phospho-ERK and phospho-Stat5

Phosphorylated ERK1/2 and STAT5 were analyzed in defined $Lin^{-/low}$ $c\text{-}Kit^{+}$ and $Lin^{-/low}$ $c\text{-}Kit^{-}$ cells essentially as previously described [33]. Surface proteins were detected with FITC-conjugated antibodies (BD Biosciences unless specified) against B220 (6B2), Gr-1 (RB6-8C5), CD3 (17A2, Biolegend), CD4 (RM4-5), CD8 (53-6.7), and TER119, and PE-conjugated anti-CD117/c-Kit antibody (eBiosciences, San Diego, CA). p-ERK1/2 was detected by a primary antibody against pERK (Thr202/Tyr204; Cell signaling Technology) followed by APC conjugated donkey anti-rabbit F(ab')2 fragment (Jackson ImmunoResearch). p-Stat5 (pY694) was detected by Alexa 647 conjugated primary antibody against phospho Stat5 (BD Biosciences).

Complete blood count and histopathology

Complete blood count analysis was performed using a Hemavet 950FS (Drew Scientific). Mouse tissues were fixed in 10% neutral buffered formalin (Sigma-Aldrich) and further processed at the UWCCC Histology Lab.

Immunohistochemistry

Paraffin sections were deparafinnized, rehydrated, and stained for pan-cytokeratin (Thermo Scientific) in the UWCCC TRIP lab.

Statistics

Unpaired 2-tailed Student's t tests were used to determine the significance between 2 data sets. A *P* value less than 0.05 was considered significant.

2.4 Results

Deletion of *βc* decreases oncogenic Nras-induced splenomegaly

To investigate whether deletion of *βc* affects the hematopoietic phenotypes induced by oncogenic Nras, we generated *Mx1-Cre*, $Nras^{LSL\ G12D/+}$*; Mx1-Cre* and $Nras^{LSL\ G12D/}$*;* $\beta c^{-/-}$*; Mx1-Cre* mice (Figure 2-1A and 1B). At 5-7 weeks old, these mice were administrated with pI-pC, which stimulates endogenous interferon production and induces Cre expression in the hematopoitic tissues from the interferon-inducible promoter Mx1 [47]. The Cre recombinease subsequently removed the stop cassette and induced oncogenic Nras expression from its endogenous locus. The day of the first pI-pC injection is defined as Day 1. After two rounds of pI-pC injection, all mice were sacrificed on Day 12. We refer to the pI-pC treated compound mice as $Nras^{G12D/+}$ and $Nras^{G12D/+}$*;* $\beta c^{-/-}$ mice, respectively, and pI-pC treated *Mx1-Cre* mice as control mice throughout this chapter.

After acute induction of oncogenic Nras expression in hematopoietic tissues, both $Nras^{G12D/+}$ and $Nras^{G12D/+}$*;* $\beta c^{-/-}$ mice were grossly normal, with unremarkable white blood cell counts, hematocrit, platelet counts (Figure 2-1D) and normal myeloid differentiation in bone marrow and peripheral blood (Figure 2-1E). However, $Nras^{G12D/+}$ mice showed moderately but significantly enlarged spleen compared with control mice (Figure 2-1C). Flow cytometric analysis demonstrated that the percentages of granulocytes (Mac^+ $Gr1^+$) and monocytes ($Mac1^+$ $Gr1^-$) were significantly increased in $Nras^{G12D/+}$ spleens compared with those in control spleens (Figure 2-1E). Noticeably, the splenomegaly and percentage of splenic monocytes were significantly reduced in $Nras^{G12D/+}$*;* $\beta c^{-/-}$ mice compared with those in $Nras^{G12D/+}$ mice (Figure 2-1C and 1E).

These results indicate that deletion of *βc* decreases oncogenic *Nras*-induced monocytic cell expansion in spleen, which might contribute to the reduced splenomegaly in $Nras^{G12D/+}$; $\beta c^{-/-}$ mice.

Loss of *βc* abolishes GM-CSF signaling but preserves IL-3 signaling in $Nras^{G12D/+}$ cells

To determine whether loss of *βc* affects cytokine signaling in $Nras^{G12D/+}$ cells, we studied GM-CSF signaling and IL-3 signaling in $Lin^{low/-}$ $cKit^{+}$ cells (enriched for MPs) and $Lin^{low/-}$ $cKit^{-}$ cells (enriched for myeloid precursors) from control, $Nras^{G12D/+}$ and $Nras^{G12D/+}$; $\beta c^{-/-}$ mice (Figure 2-2). We found that GM-CSF- and IL-3-evoked ERK1/2 and STAT5 activation in $Nras^{G12D/+}$ MPs were largely comparable to those in control cells, while $Nras^{G12D/+}$ myeloid precursors showed moderate but significant hyperactivation upon stimulation with saturated concentrations of cytokines. In the absence of βc, GM-CSF signaling was completely abolished in $Nras^{G12D/+}$; $\beta c^{-/-}$ cells (Figure 2-2A), whereas IL-3 signaling remained intact (Figure 2-2B).

***βc* is dispensable for $Nras^{G12D/+}$ HSCs**

Because $Nras^{G12D/+}$ HSCs serve as CMML initiating cells [43], we investigated whether deletion of *βc* affects their functions in leukemogenesis. We first examined the HSC compartment in control, $Nras^{G12D/+}$ and $Nras^{G12D/+}$; $\beta c^{-/-}$ mice on Day 12. HSCs were defined as Lin^{-} $CD41^{-}$ $CD48^{-}$ $cKit^{+}$ $Sca1^{+}$ $CD150^{+}$ cells [48, 49]. The absolute HSC numbers in bone marrow and spleen of $Nras^{G12D/+}$; $\beta c^{-/-}$ mice were moderately but significantly increased compared with those in control mice but comparable to those in

Nras$^{G12D/+}$ mice (Figure 2-3A). Concomitantly, the compartments of multipotent progenitor (MPP, defined as Lin$^-$ CD41$^-$ CD48$^-$ c-Kit$^+$ Sca1$^+$ CD150$^-$) and [48] and LSK (Lin$^-$ sca1$^+$ c-kit$^+$) cells in bone marrow and/or spleen of *Nras*$^{G12D/+}$*; βc*$^{-/-}$ mice were also expanded but indistinguishable from those in *Nras*$^{G12D/+}$ mice (Figure 2-3B and 3C). These results indicate that deletion of *βc* does not affect oncogenic *Nras*-induced HSC expansion.

To investigate further whether deletion of *βc* affects increased self-renewal of *Nras*$^{G12D/+}$ HSCs [43], we transplanted 2.5 x 10^5 total bone marrow cells (CD45.2$^+$) isolated from control, *Nras*$^{G12D/+}$, and *Nras*$^{G12D/+}$*; βc*$^{-/-}$ mice, accompanied with same number of congenic competitors (CD45.1$^+$) into lethally irradiated recipient mice (CD45.1$^+$). We found that over one year of time, donor derived blood cells in recipients transplanted with *Nras*$^{G12D/+}$*; βc*$^{-/-}$ cells were stably maintained at a much higher reconstitution rate compared with those in recipients with control cells but at a similar level as recipients with *Nras*$^{G12D/+}$ cells (Figure 2-3D). These data suggest that deletion of *βc* does not affect increased self-renewal of *Nras*$^{G12D/+}$ HSCs. Together, our results demonstrate that βc is dispensable for *Nras*$^{G12D/+}$ HSCs.

Loss of *βc* abolishes oncogenic *Nras*-induced spontaneous colony formation

To test whether loss of *βc* affects MP expansion in *Nras*$^{G12D/+}$ mice, we analyzed the MP (Lin$^-$ IL7Rα$^-$ Sca1$^-$ cKit$^+$) compartment in control, *Nras*$^{G12D/+}$ and *Nras*$^{G12D/+}$*; βc*$^{-/-}$ mice. The absolute numbers of MPs, including common myeloid progenitors (CMPs), granulocyte-monocyte progenitors (GMPs) and megakaryocyte-erythroid progenitors (MEPs), in *Nras*$^{G12D/+}$ and *Nras*$^{G12D/+}$*; βc*$^{-/-}$ bone marrow were comparable with each

other and both significantly higher than those in control bone marrow (Figure 2-4A). A similar trend was also observed in spleen (Figure 2-4A). Our data indicate that deletion of *βc* does not affect oncogenic *Nras*-induced MP expansion.

We and others previously reported that bone marrow cells from $Nras^{G12D/+}$ mice form significant number of colonies in the absence of cytokines [33, 34]. To determine whether the spontaneous colony formation of $Nras^{G12D/+}$ cells depends on βc-mediated signaling, we isolated bone marrow cells from control, $Nras^{G12D/+}$ and $Nras^{G12D/+}; \beta c^{-/-}$ mice and plated them in semi-solid media in the absence of cytokines. Consistent with previous reports, $Nras^{G12D/+}$ cells formed significant number of colonies, while $Nras^{G12D/+}; \beta c^{-/-}$ cells formed much lower number of colonies (Figure 2-4B). In the presence of mGM-CSF or mIL-3, $Nras^{G12D/+}$ cells formed significantly more and bigger colonies than control cells (Figure 2-4B). As expected, $Nras^{G12D/+}; \beta c^{-/-}$ cells did not form significant number of colonies in the presence of mGM-CSF but formed comparable number and size of colonies as $Nras^{G12D/+}$ cells in the presence of mIL-3, consistent with our signaling studies (Figure 2-4B). Our results suggest that the spontaneous colony formation of $Nras^{G12D/+}$ cells largely depends on βc-mediated GM-CSF signaling.

_βc_ deficiency significantly delays the progression of oncogenic _Nras_-induced leukemias in a cell autonomous manner

To investigate whether *βc* deficiency attenuates oncogenic *Nras*-induced leukemogenesis in a hematopoietic cell-specific manner, we transplanted bone marrow cells from control, $Nras^{G12D/+}$ and $Nras^{G12D/+}; \beta c^{-/-}$ mice together with competitor cells into lethally irradiated mice (Figure 2-5). Consistent with our previous report [33], ~97% of recipients

transplanted with *Nras*$^{G12D/+}$ cells developed a CMML-like disease and ~7% developed acute T-cell lymphoblastic leukemia/lymphoma (T-ALL). Similarly, ~94% of recipients with *Nras*$^{G12D/+}$*; βc*$^{-/-}$ cells developed a CMML-like disease and ~12% developed T-ALL (Figure 2-5B). Some mice developed both diseases. However, recipients transplanted with *Nras*$^{G12D/+}$*; βc*$^{-/-}$ cells survived significantly longer than those with *Nras*$^{G12D/+}$ cells (median survival: 537 days vs 357 days) (Figure 2-5A). Despite different survival curves, both groups of mice with CMML displayed similar disease phenotypes at the moribund stage, including markedly enlarged spleen (Figure 2-5C) with significant extramedullary hematopoiesis (Figure 2-5F), increased white blood cell counts and anemia (Figure 2-5D), and a predominant expansion of granulocytes and/or monocytes in hematopoietic tissues (Figure 2-5E). These results indicate that deletion of *βc* cannot abrogate oncogenic *Nras*-induced CMML formation but it does significantly delay CMML progression.

Deletion of *βc* in *Nras*$^{G12D/+}$ mice promotes hepatic histiocytic sarcomas with atypical morphology

Our previous results show that ~50% of primary *Nras*$^{G12D/+}$ mice (7 out of 15) died with hepatic histiocytic sarcoma within a year after pI-pC injections [33]. While the median survival of *Nras*$^{G12D/+}$*; βc*$^{-/-}$ mice was indistinguishable from that of *Nras*$^{G12D/+}$ mice, the disease latency was prolonged (Figure 2-6). Like *Nras*$^{G12D/+}$ mice, most of *Nras*$^{G12D/+}$*; βc*$^{-/-}$ mice (6 out of 8) developed CMML-like phenotypes with increased monocytosis in peripheral blood (Figure 2-6C). Two out of three *Nras*$^{G12D/+}$*; βc*$^{-/-}$ mice also developed multiple hepatic tumor nodules with varying morphology but consisting of histiocyte-like cells ranging from small and monotonous to large and multinucleated. Because the

tumors also entrapped steatotic hepatocytes and residual sinusoidal endothelial channels (Figure 2-7A), we initially considered whether this might represent a non-hematopoietic tumor type, but negative pan-keratin staining (Figure 2-7B) and the overall morphologic features favor a histiocytic/monocytic derived neoplasm. We speculate that the morphologic differences between these tumors and those we have previously described in *Nras*$^{G12D/+}$ mice may be secondary to their inability to normally respond to GM-CSF derived signal.

2.5 Discussion

In this manuscript, we show that *βc* deficiency indeed abolishes GM-CSF signaling in *Nras*$^{G12D/+}$ cells but IL-3 signaling is preserved. Consequently, loss of *βc* does not affect *Nras*$^{G12D/+}$ HSC functions and therefore does not abrogate CMML in *Nras*$^{G12D/+}$ mice. However, deletion of *βc* does significantly slow down the progression of CMML and prolong the survival of recipients transplanted with *Nras*$^{G12D/+}$ cells (Figure 2-8).

We previously reported that in *Nras*$^{G12D/+}$-induced CMML model, mutant HSCs are required to initiate and maintain CMML-like phenotypes and serve as CMML initiating cells [43]. Consistent with an earlier report that *βc* is dispensable for normal HSCs [23], we found that *βc* is dispensable for *Nras*$^{G12D/+}$ HSCs as well; loss of *βc* does not affect the expansion, increased self-renewal, and myeloid differentiation bias in *Nras*$^{G12D/+}$ HSCs (Figures 2-3 and 4). We believe that *βc* is also dispensable for *Nf1*$^{-/-}$ HSCs. Therefore, it is not surprising that MP compartment remains expanded in *Nras*$^{G12D/+}$*; βc*$^{-/-}$ and *Nf1*$^{-/-}$*; βc*$^{-/-}$ mice and deletion of *βc* does not abrogate CMML in these animals [24].

Despite potential compensation of other cytokine signaling (e.g. IL-3, G-CSF, and M-CSF) in the absence of βc-mediated GM-CSF signaling, *βc* deficiency indeed significantly reduces *Nras*$^{G12D/+}$-induced splenomegaly and spontaneous colony formation and prolongs the survival of CMML mice, suggesting that GM-CSF signaling plays an important role in promoting CMML progression. Our result is consistent with previous human and mouse studies [16, 20, 21, 33, 50]. However, in t(8;21)-induced acute myeloid leukemia (AML), GM-CSF is found to reduce the replating ability of RUNX1-ETO-expressing cells and therefore have a negative impact on leukemogenesis; expression of RUNX1-ETO in *βc*$^{-/-}$ cells leads to a high penetrance of AML [51]. Therefore, hyperactive GM-CSF signaling potentially opposes AML formation by inhibiting transformation of MPs to AML initiating cells. This might explain the absence of spontaneous AML in oncogenic Ras models and low incidence of transformation to AML in JMML patients. Although we and others did not see AML genesis in *Nras*$^{G12D/+}$; *βc*$^{-/-}$ and *Nf1*$^{-/-}$; *βc*$^{-/-}$ mice, we could not rule out the possibility that long-term inhibition of GM-CSF signaling in JMML/CMML patients might increase their risk to develop AML.

2.6 Figures and legends

Figure 2-1. Loss of *βc* decreases *Nras*$^{G12D/+}$-induced splenomegaly. Mice were treated with pI-pC and euthanized on Day 12 for analysis as described in Materials and Methods. (A) Schematic illustration of the strategy to generate experimental mice. (B) Genotyping analysis of genomic DNA to detect different alleles in representative control, *Nras*$^{G12D/+}$ and *Nras*$^{G12D/+}$*; βc*$^{-/-}$ mice. (C) The ratio of spleen weight to body weight (BW) of control, *Nras*$^{G12D/+}$ and *Nras*$^{G12D/+}$*; βc*$^{-/-}$ mice. (D) Complete blood count was performed on peripheral blood samples collected from control, *Nras*$^{G12D/+}$ and *Nras*$^{G12D/+}$*; βc*$^{-/-}$ mice. The range and median of the data were shown. (E) Flow cytometry analysis of bone marrow (BM), peripheral blood (PB) and spleen (SP) cells using myeloid lineage-specific markers. Data are presented as mean ± SD. * $P < 0.05$; ** $P < 0.01$.

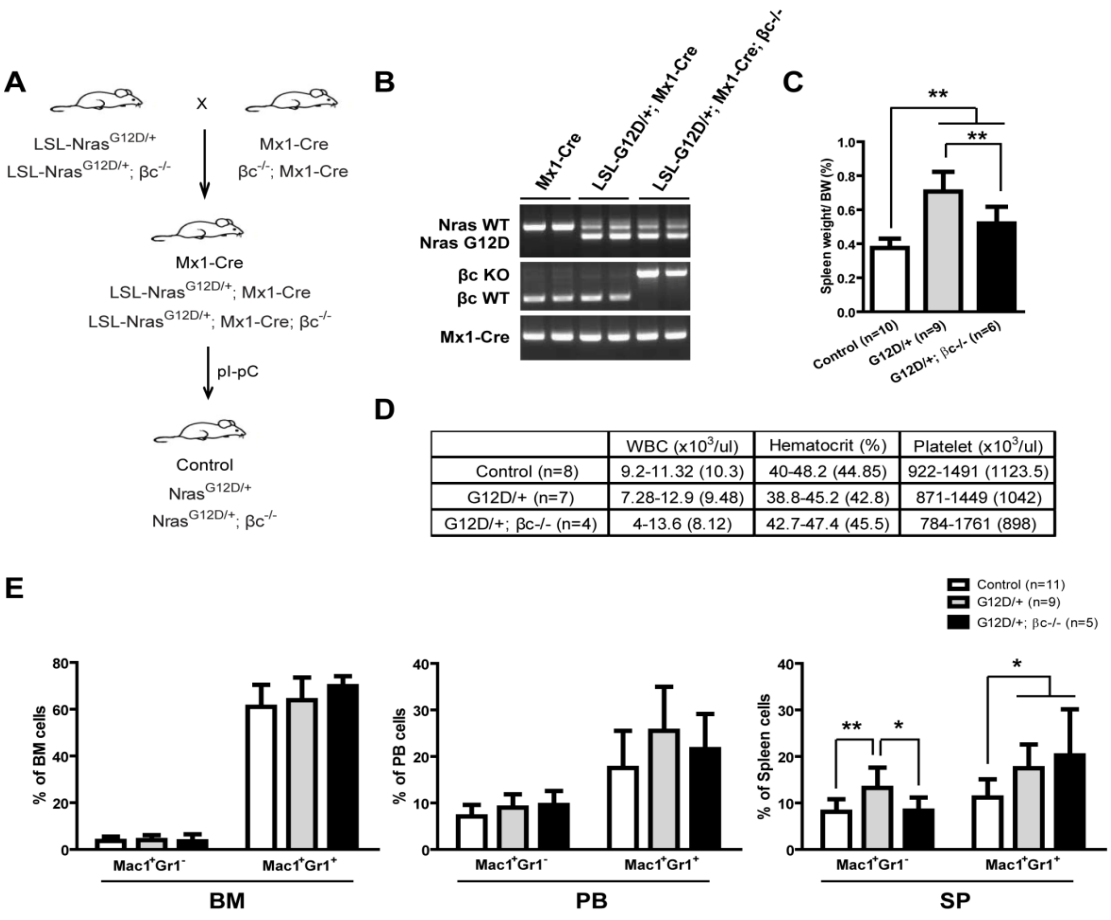

	WBC (x10^3/ul)	Hematocrit (%)	Platelet (x10^3/ul)
Control (n=8)	9.2-11.32 (10.3)	40-48.2 (44.85)	922-1491 (1123.5)
G12D/+ (n=7)	7.28-12.9 (9.48)	38.8-45.2 (42.8)	871-1449 (1042)
G12D/+; βc-/- (n=4)	4-13.6 (8.12)	42.7-47.4 (45.5)	784-1761 (898)

Figure 2-2. *βc* deficiency abolishes GM-CSF signaling but preserves IL-3 signaling in *Nras*$^{G12D/+}$ cells. Total bone marrow cells isolated from control, *Nras*$^{G12D/+}$ or *Nras*$^{G12D/+}$; *βc*$^{-/-}$ mice on Day 12 were serum and cytokine starved for 2 hours and stimulated with various concentrations of mGM-CSF (0, 0.16 and 2 ng/ml) (A) or mIL-3 (0, 1, 10 ng/ml) (B) at 37°C for 10 minutes. Levels of p-ERK1/2 and p-Stat5 were measured using phosphospecific flow cytometry. Non-neutrophil bone marrow cells were gated for data analysis. Myeloid progenitors are enriched in Lin$^{-/low}$ c-Kit^{+} cells (Pro), whereas myeloid precursors are enriched in Lin$^{-/low}$ cKit^{-} cells (Pre). Data are presented as mean ± SD. * $P < 0.05$; ** $P < 0.01$; *** $P < 0.001$.

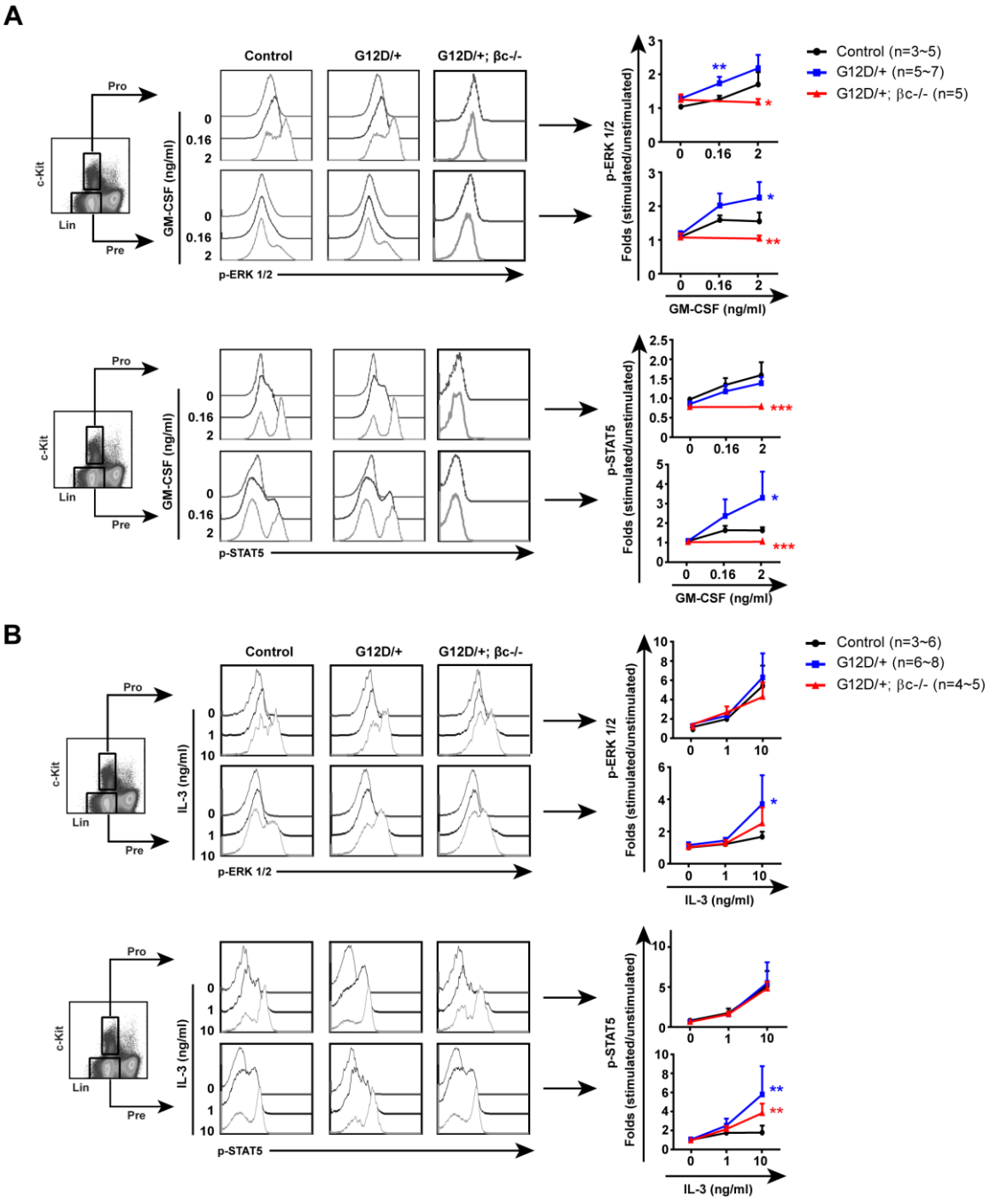
A
Control
G12D/+
G12D/+; βc-/-
Pro
Pre
c-Kit
Lin
GM-CSF (ng/ml)
0
0.16
2
p-ERK 1/2
Folds (stimulated/unstimulated)
GM-CSF (ng/ml)
Control (n=3~5)
G12D/+ (n=5~7)
G12D/+; βc-/- (n=5)
p-STAT5
B
IL-3 (ng/ml)
0
1
10
Control (n=3~6)
G12D/+ (n=6~8)
G12D/+; βc-/- (n=4~5)

Figure 2-3. Deletion of *βc* does not affect *Nras*$^{G12D/+}$ HSCs. Mice were treated with pI-pC and euthanized on Day 12 for analysis as described in Materials and Methods. (A) Lin$^-$ CD41$^-$ CD48$^-$ c-Kit$^+$ Scar-1$^+$ CD150$^+$ HSCs, (B) Lin$^-$ CD41$^-$ CD48$^-$ c-Kit$^+$ Scar-1$^+$ CD150$^-$ MPPs, and (C) Lin$^-$ c-Kit$^+$ Scar-1$^+$ (LSK) cells from bone marrow (BM) and spleen (SP) were quantified using flow cytometry. (D) 2.5 x 10^5 bone marrow cells from control, *Nras*$^{G12D/+}$ or *Nras*$^{G12D/+}$*; βc*$^{-/-}$ mice were transplanted with same number of competitor cells into lethally irradiated mice. The percentages of donor-derived cells (CD45.2$^+$) in the peripheral blood of recipient mice were examined at multiple time points after transplantation. Data are presented as mean ± SD. * $P < 0.05$; ** $P < 0.01$; *** $P < 0.001$.

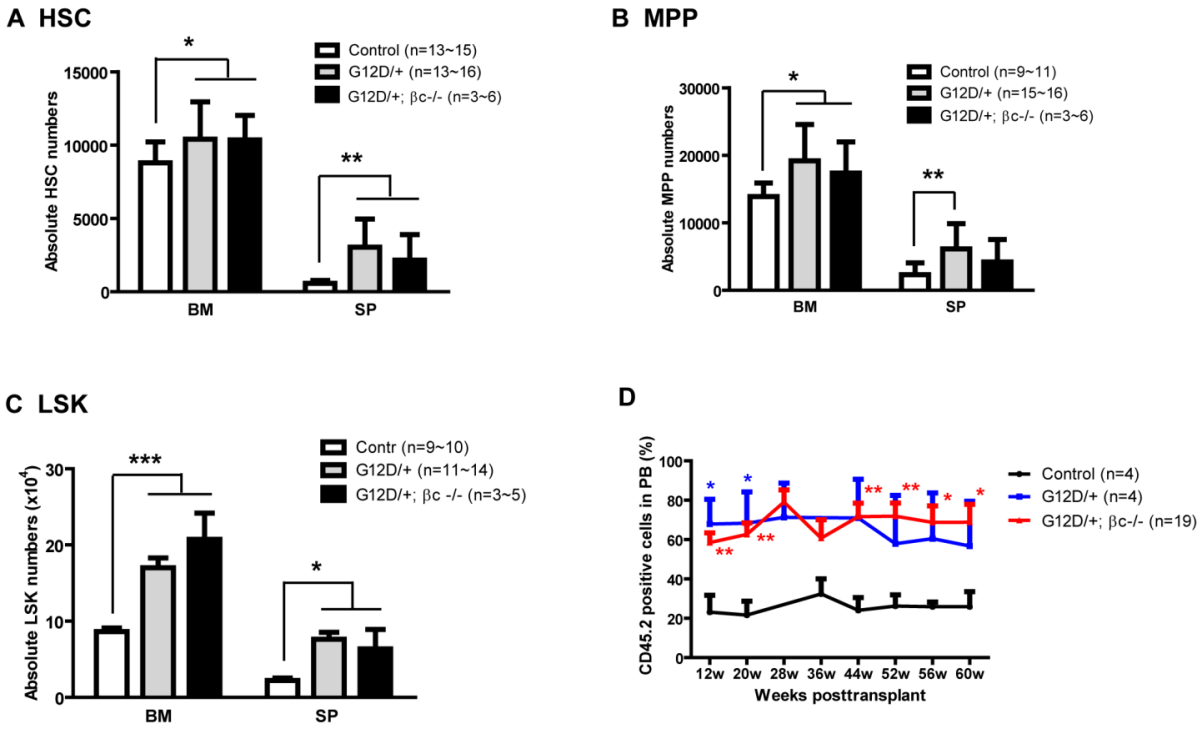

Figure 2-4. Loss of *βc* greatly reduces *Nras*$^{G12D/+}$-induced spontaneous colony formation. Mice were treated with pI-pC and euthanized on Day 12 for analysis as described in Materials and Methods. (A) Quantification of myeloid progenitors (MPs) in bone marrow (BM) and spleen (SP). CMP, common myeloid progenitor; GMP, granulocyte-monocyte progenitor; and MEP, megakaryocyte-erythroid progenitors. (B) 5 x 10^4 bone marrow cells isolated from control, *Nras*$^{G12D/+}$ or *Nras*$^{G12D/+}$*; βc*$^{-/-}$ mice were plated in semisolid medium without cytokine or with 0.2 ng/ml mGM-CSF or 10 ng/ml mIL-3. Colonies were counted 7-10 days after culture.

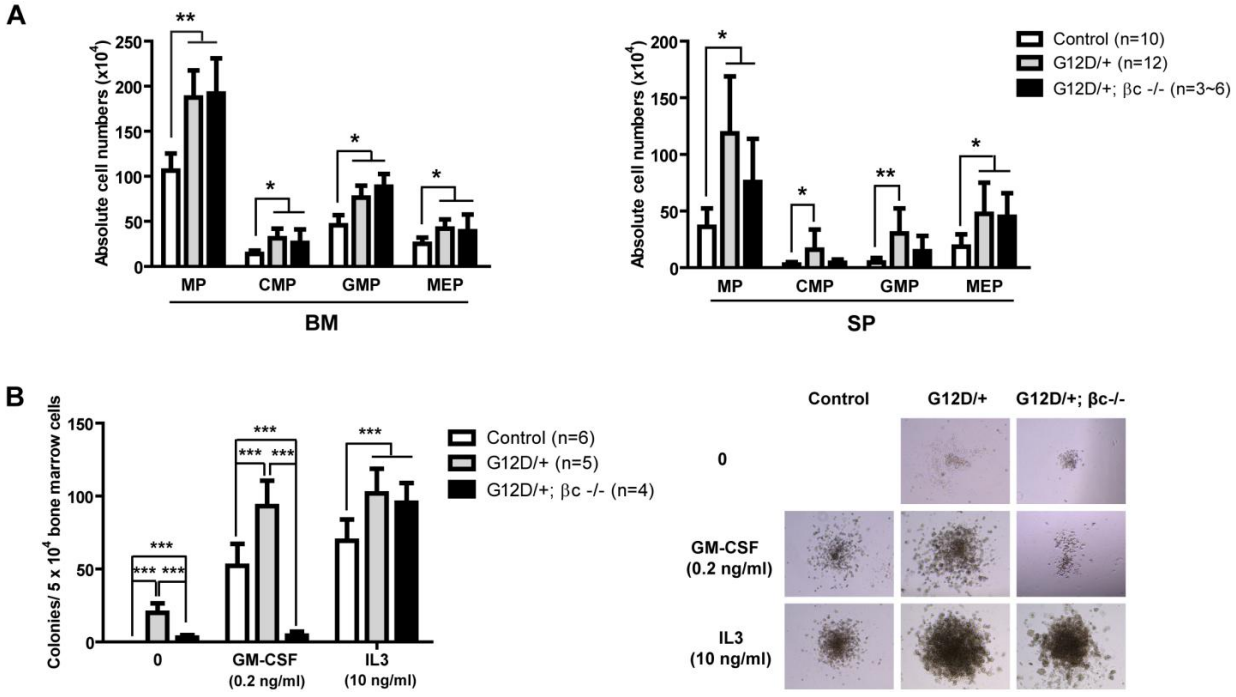

Figure 2-5. Deletion of *βc* slows down the progression of *Nras*$^{G12D/+}$-induced hematopoietic malignancies. Lethally irradiated mice were transplanted with 2.5 x 10^5 total bone marrow cells from control, *Nras*$^{G12D/+}$ or *Nras*$^{G12D/+}$*; βc*$^{-/-}$ mice along with same number of competitor cells. (A) Kaplan-Meier comparative survival analysis of reconstituted mice. Cumulative survival was plotted against days after transplantation. *P* value was determined by the log-rank test. (B) Disease incidence in recipient mice transplanted with *Nras*$^{G12D/+}$ or *Nras*$^{G12D/+}$*; βc*$^{-/-}$ cells. (C) Spleen and liver weight of moribund CMML-*Nras*$^{G12D/+}$ or CMML-*Nras*$^{G12D/+}$*; βc*$^{-/-}$ mice. (D) Complete blood count was performed on peripheral blood samples collected from moribund CMML-*Nras*$^{G12D/+}$ or CMML-*Nras*$^{G12D/+}$*; βc*$^{-/-}$ mice and age-matched control mice. (E) Flow cytometry analysis of bone marrow (BM), peripheral blood (PB) and spleen (SP) cells from control and moribund CMML-*Nras*$^{G12D/+}$ and CMML-*Nras*$^{G12D/+}$*; βc*$^{-/-}$ mice using myeloid lineage-specific markers. (F) Representative spleen histologic H&E sections from moribund CMML-*Nras*$^{G12D/+}$ and CMML-*Nras*$^{G12D/+}$*; βc*$^{-/-}$ mice and age-matched control mice. Data are presented as mean ± SD. * $P < 0.05$; ** $P < 0.01$; *** $P < 0.001$.

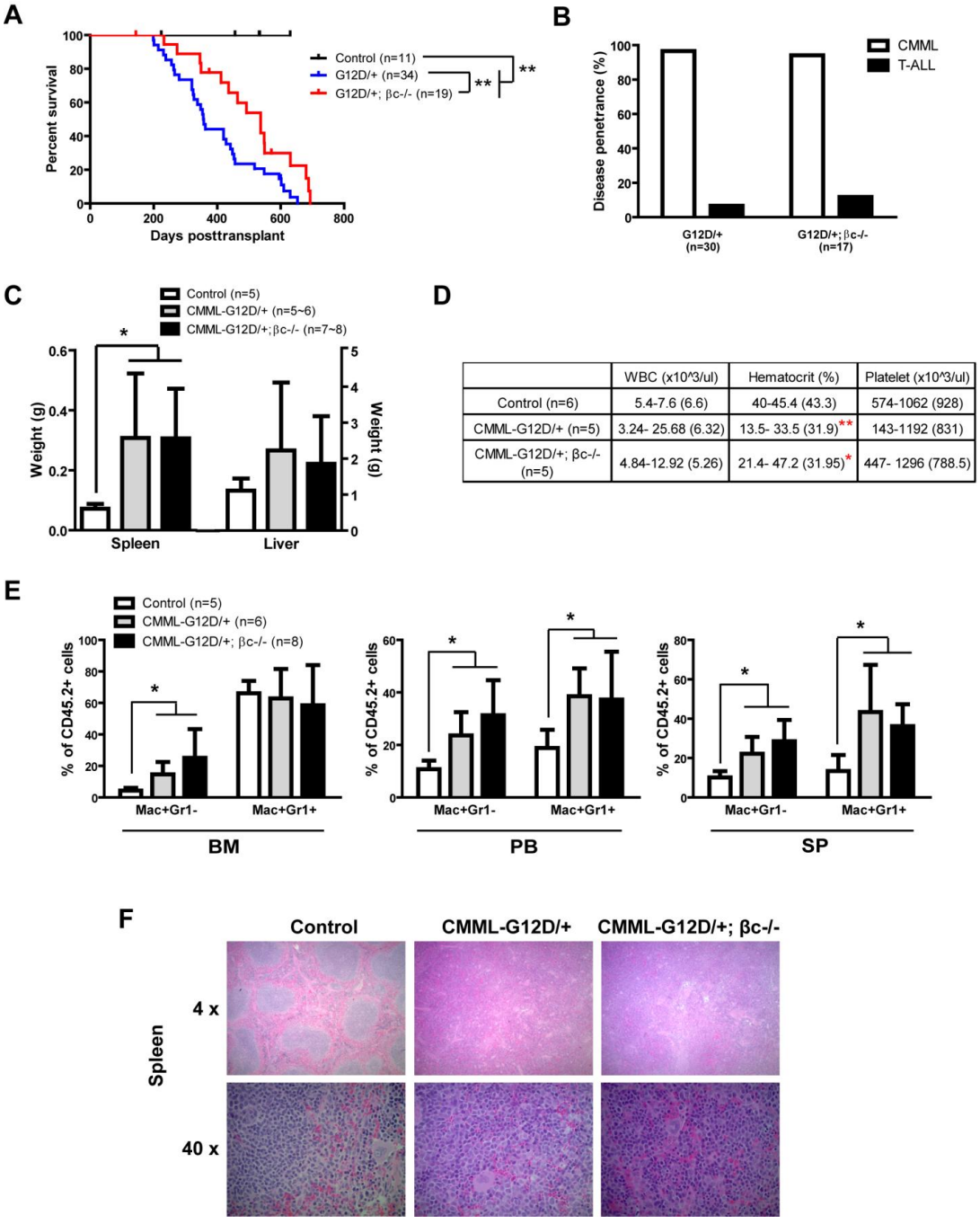

	WBC (x10^3/ul)	Hematocrit (%)	Platelet (x10^3/ul)
Control (n=6)	5.4-7.6 (6.6)	40-45.4 (43.3)	574-1062 (928)
CMML-G12D/+ (n=5)	3.24- 25.68 (6.32)	13.5- 33.5 (31.9)**	143-1192 (831)
CMML-G12D/+; βc-/- (n=5)	4.84-12.92 (5.26)	21.4- 47.2 (31.95)*	447- 1296 (788.5)

Figure 2-6. *Nras*$^{G12D/+}$; *βc*$^{-/-}$ mice develop CMML-like phenotypes after a prolonged latency. (A) Kaplan-Meier comparative survival analysis of non-transplanted control, *Nras*$^{G12D/+}$ and *Nras*$^{G12D/+}$; *βc*$^{-/-}$ mice. Cumulative survival was plotted against weeks after the last pI-pC injection. P value was determined by the log-rank test. (B) Spleen weights of moribund *Nras*$^{G12D/+}$; *βc*$^{-/-}$ mice and age-matched control mice. Data are presented as mean + SD. (C) Representative flow analysis of myeloid cells from moribund *Nras*$^{G12D/+}$; *βc*$^{-/-}$ mice and age-matched control mice. n.s., not significant; * P < 0.05.

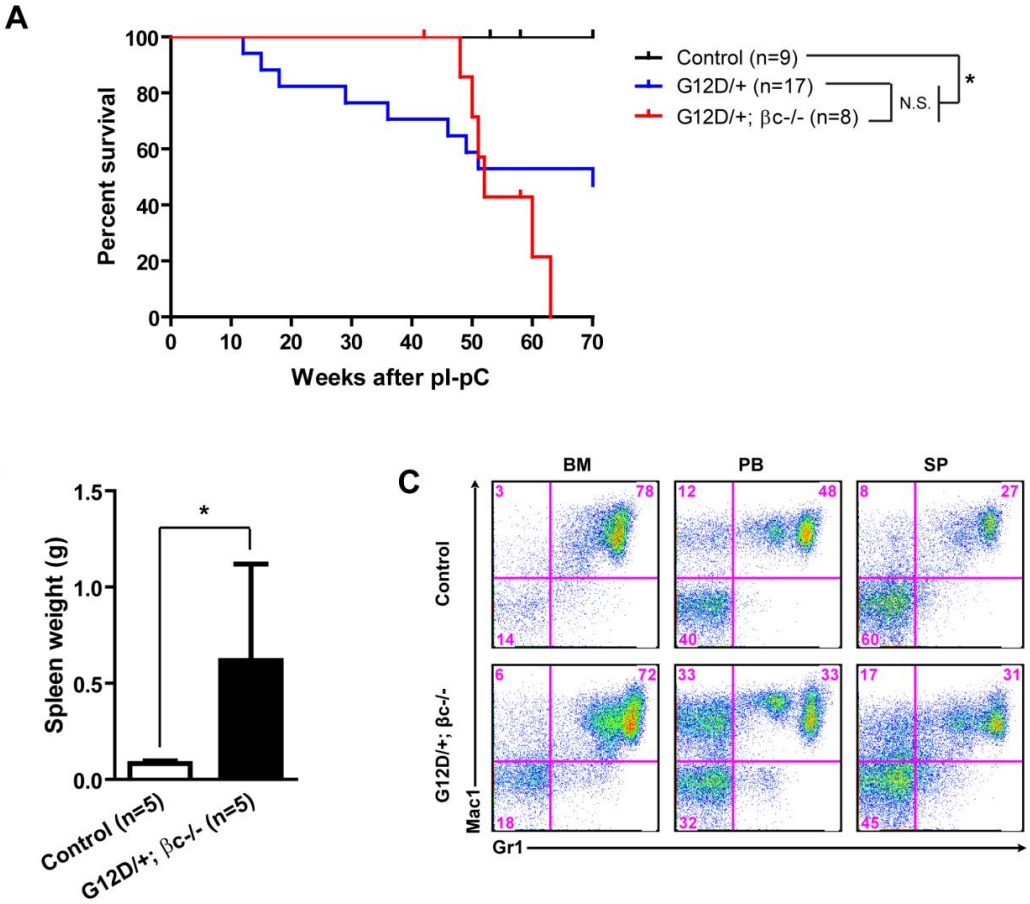

Figure 2-7. Analysis of livers from moribund *Nras*$^{G12D/+}$ and *Nras*$^{G12D/+}$; *βc*$^{-/-}$ mice and age-matched control mice. (A) Representative liver histologic H&E sections. (B) Pan-cytokeratin staining in liver. Skin was used as a positive control (PC) for Keratin staining.

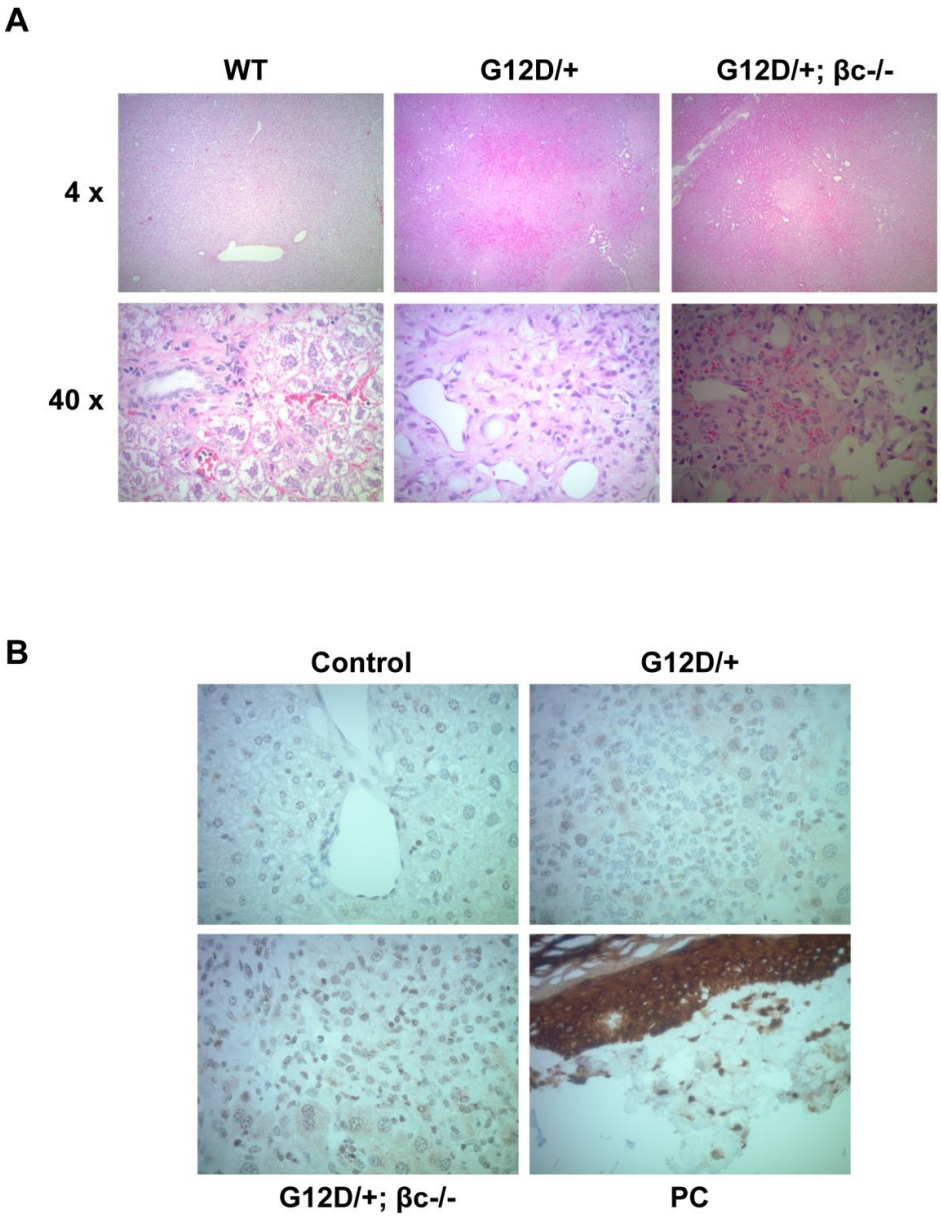

Figure 2-8. Schematic picture illustrating the role of *βc*-mediated signaling in *Nras*$^{G12D/+}$ induced CMML.

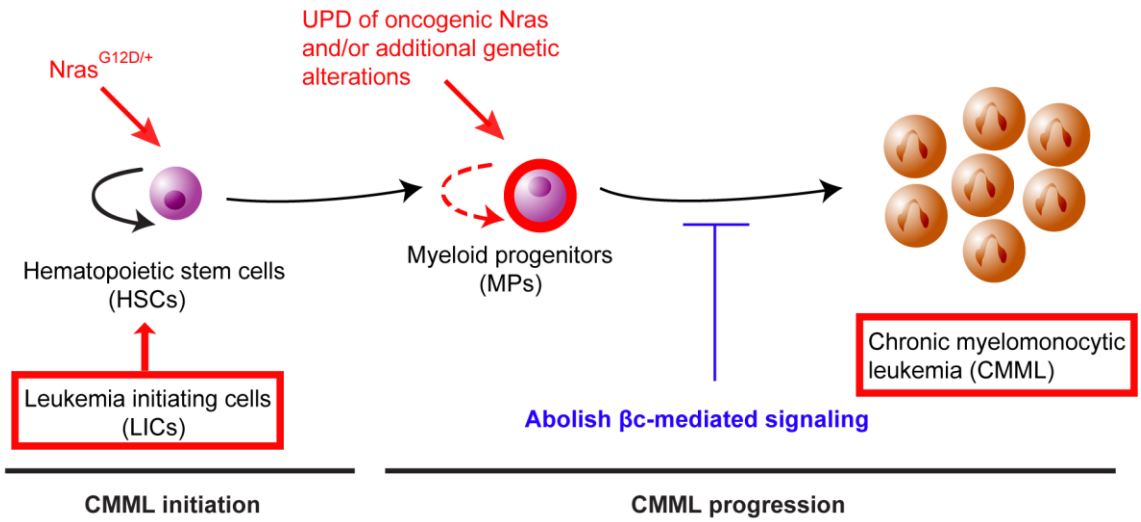

2.7 References

1. Emanuel PD. Juvenile myelomonocytic leukemia and chronic myelomonocytic leukemia. Leukemia 2008;22:1335-42.
2. Elliott MA. Chronic neutrophilic leukemia and chronic myelomonocytic leukemia: WHO defined. Best Pract Res Clin Haematol 2006;19:571-93.
3. Tartaglia M, et al. Somatic mutations in PTPN11 in juvenile myelomonocytic leukemia, myelodysplastic syndromes and acute myeloid leukemia. Nat Genet 2003;34:148-50.
4. Yoshida N, et al. Correlation of clinical features with the mutational status of GM-CSF signaling pathway-related genes in juvenile myelomonocytic leukemia. Pediatr Res 2009;65:334-40.
5. Loh ML, et al. Mutations in CBL occur frequently in juvenile myelomonocytic leukemia. Blood 2009;114:1859-63.
6. Onida F, Beran M. Chronic myelomonocytic leukemia: myeloproliferative variant. Curr Hematol Rep 2004;3:218-26.
7. Chan IT, et al. Conditional expression of oncogenic K-ras from its endogenous promoter induces a myeloproliferative disease. J Clin Invest 2004;113:528-38.
8. Braun BS, et al. Somatic activation of oncogenic Kras in hematopoietic cells initiates a rapidly fatal myeloproliferative disorder. Proc Natl Acad Sci U S A 2004;101:597-602.
9. Zhang J, et al. Oncogenic Kras-induced leukemogeneis: hematopoietic stem cells as the initial target and lineage-specific progenitors as the potential targets for final leukemic transformation. Blood 2009;113:1304-14.

10. Wang JY, et al. Endogenous oncogenic Nras mutation leads to aberrant GM-CSF signaling in granulocytic/monocytic precursors in a murine model of chronic myelomonocytic leukemia. Blood 2010;116:5991-6002.

11. Li Q, et al. Hematopoiesis and leukemogenesis in mice expressing oncogenic NrasG12D from the endogenous locus. Blood 2011;117:2022-32.

12. Wang JY, et al. Endogenous oncogenic Nras mutation initiates hematopoietic malignancies in a dose- and cell type-dependent manner. Blood 2011;118:368-79.

13. Largaespada DA, et al. Nf1 deficiency causes Ras-mediated granulocyte/macrophage colony stimulating factor hypersensitivity and chronic myeloid leukaemia. Nat Genet 1996;12:137-43.

14. Bollag G, et al. Loss of NF1 results in activation of the Ras signaling pathway and leads to aberrant growth in haematopoietic cells. Nat Genet 1996;12:144-8.

15. Le DT, et al. Somatic inactivation of Nf1 in hematopoietic cells results in a progressive myeloproliferative disorder. Blood 2004;103:4243-50.

16. Emanuel PD, et al. Selective hypersensitivity to granulocyte-macrophage colony-stimulating factor by juvenile chronic myeloid leukemia hematopoietic progenitors. Blood 1991;77:925-9.

17. Bowen DT. Chronic myelomonocytic leukemia: lost in classification? Hematol Oncol 2005;23:26-33.

18. Cambier N, et al. Chronic myelomonocytic leukemia: from biology to therapy. Hematol Cell Ther 1997;39:41-8.

19. Hercus TR, et al. The granulocyte-macrophage colony-stimulating factor receptor: linking its structure to cell signaling and its role in disease. Blood 2009;114:1289-98.

20. Shi Y, et al. Granulocyte-macrophage colony-stimulating factor (GM-CSF) and T-cell responses: what we do and don't know. Cell research 2006;16:126-33.

21. Kotecha N, et al. Single-cell profiling identifies aberrant STAT5 activation in myeloid malignancies with specific clinical and biologic correlates. Cancer Cell 2008;14:335-43.

22. Iversen PO, et al. Inhibition of granulocyte- macrophage colony-stimulating factor prevents dissemination and induces remission of juvenile myelomonocytic leukemia in engrafted immunodeficient mice. Blood 1997;90:4910-7.

23. Bernard F, et al. Transient hematologic and clinical effect of E21R in a child with end-stage juvenile myelomonocytic leukemia. Blood 2002;99:2615-6.

24. Birnbaum RA, et al. Nf1 and Gmcsf interact in myeloid leukemogenesis. Mol Cell 2000;5:189-95.

25. Woodcock JM, et al. The human granulocyte-macrophage colony-stimulating factor (GM-CSF) receptor exists as a preformed receptor complex that can be activated by GM-CSF, interleukin-3, or interleukin-5. Blood 1997;90:3005-17.

26. Kim A, et al. Beta common receptor inactivation attenuates myeloproliferative disease in Nf1 mutant mice. Blood 2007;109:1687-91.

27. Wang J, et al. Nras G12D/+ promotes leukemogenesis by aberrantly regulating haematopoietic stem cell functions. Blood 2013;121:5203-7.

28. Li Q, et al. Oncogenic Nras has bimodal effects on stem cells that sustainably increase competitiveness. Nature 2013;504:143-7.

29. Nicola NA, et al. The structural basis of the biological actions of the GM-CSF receptor. Ciba Foundation symposium 1997;204:19-27; discussion -32.

30. Okuda K, et al. Signaling domains of the beta c chain of the GM-CSF/IL-3/IL-5 receptor. Annals of the New York Academy of Sciences 1999;872:305-12; discussion 12-3.

31. Kuhn R, et al. Inducible gene targeting in mice. Science 1995;269:1427-9.

32. Kiel MJ, et al. SLAM family receptors distinguish hematopoietic stem and progenitor cells and reveal endothelial niches for stem cells. Cell 2005;121:1109-21.

33. Kiel MJ, et al. Haematopoietic stem cells do not asymmetrically segregate chromosomes or retain BrdU. Nature 2007;449:238-42.

34. Nishinakamura R, et al. Mice deficient for the IL-3/GM-CSF/IL-5 beta c receptor exhibit lung pathology and impaired immune response, while beta IL3 receptor-deficient mice are normal. Immunity 1995;2:211-22.

35. Du J, et al. Loss of CD44 attenuates aberrant GM-CSF signaling in Kras G12D hematopoietic progenitor/precursor cells and prolongs the survival of diseased animals Leukemia 2013;27:754-7.

36. Matsuura S, et al. Negative effects of GM-CSF signaling in a murine model of t(8;21)-induced leukemia. Blood 2012;119:3155-63.

Chapter 3

Loss of p53 synergizes with enhanced oncogenic *Nras* signaling to promote malignant transformation of chronic myelomonocytic leukemia to acute myeloid leukemia

Li Lu, a postdoctoral in Xuehua Zhong's lab, helped to perform the bioinformatics analysis of the RNA-seq data.

3.1 Abstract

Chronic myelomonocytic leukemia (CMML) is a devastating disease that transforms to acute myeloid leukemia at a fairly high rate. However, the molecular mechanism driving this malignant transformation remains largely unknown. To test potential genetic interaction between *p53* loss and endogenous oncogenic Nras signaling in promoting CMML to AML, we generated $Nras^{G12D/+}$; $p53^{-/-}$ mice. Transplantation of $Nras^{G12D/+}$; $p53^{-/-}$ bone marrow cells resulted in a highly penetrant AML in recipient mice. We found that loss of *p53* profoundly impacted on the function of $Nras^{G12D/+}$ myeloid progenitors (MPs) but not hematopoietic stem cells (HSCs) to promote leukemogenesis. $Nras^{G12D/+}$; $p53^{-/-}$ MPs showed increased quiescence and self-renewal. More importantly, they were transformed to self-renewing AML initiating cells (referred as AML-MPs) and capable to induce AML in serial transplanted recipients. Molecular and cellular characterization identified megakaryocyte-erythroid progenitors (MEPs) as the origin of transformed AML-MPs. RNA-Seq analysis revealed that AML-MPs gained partial signature of HSCs and largely retained MEP signature. The distinct transcriptome of AML-MPs was mainly driven by p53. In addition, we found that AML-MPs acquired overexpression of oncogenic *Nras* through UPD of oncogenic *Nras* allele and possibly epigenetic regulation, which led to hyperactivation of ERK1/2 signaling. Our results demonstrate that *p53* deficiency synergizes with enhanced oncogenic Nras signaling to bolster the leukemogenic transformation of MEPs and drive CMML transformation to AML.

3.2 Introduction

Chronic myelomonocytic leukemia (CMML) and its juvenile counterpart, JMML, belong to the group of "mixed myelodysplastic/myeloproliferative diseases" (MDS/MPD) defined by the WHO [1, 2]. CMML primarily occurs in the elderly with median ages at presentation ranging from 65 to 75 years, whereas JMML exclusively affects children, typically under the age of 4 years. Despite the demographic difference, CMML and JMML share similar clinical features, including monocytosis, hepatosplenomegaly, and the absence of the *BCR-ABL* fusion gene.

In contrast to JMML that is primarily driven by activating *RAS* pathway mutations [1, 3-5], the molecular pathogenetics of CMML is more diverse. Mutations occurring in four major groups of genes are known to drive CMML formation [6]. The first group of genes are signaling molecules, including *FLT3, KIT, NRAS, KRAS, PTPN11, CBL,* and *JAK2*. Among these genes, mutations in *NRAS, KRAS,* and *CBL* are most frequent (10-20%), whereas mutations in other genes are only identified in ~1-3% of CMML patients [1, 2, 7]. The second group of genes are involved in epigenetic regulation of gene transcription (e.g. DNA methylation and chromatin remodeling), such as *DNMT3A, TET2, IDH1/2, ASXL1,* and *EZH2*. Among them, *TET2* and *ASXL1* are most frequently mutated (50-60% and 40%, respectively). The third group of genes include transcription factors, for example, *RUNX1* and *TP53*. The fourth group of genes are involved in RNA metabolism and splicing, including *SRSF2, SF3B1, U2AF1,* and *ZRSF2*.

Associated with heterogeneous molecular abnormalities, CMML exhibits substantial clinical phenotypic diversity, ranging from predominantly "myeloproliferative" (MP-CMML) to predominantly "myelodysplastic" (MD-CMML) CMML [8]. Interestingly, oncogenic *RAS* mutations are particularly enriched in MP-CMML, which is

phenotypically more like JMML than MD-CMML [9]. Consistent with human studies, we previously reported that recipients transplanted with *Nras*$^{G12D/+}$ bone marrow cells develop a highly penetrant CMML-like disease after a prolonged latency [10]. However, none of the recipients with CMML spontaneously transform to acute myeloid leukemia (AML). This is in sharp contrast to CMML patients as ~20% of them develop AML soon after their initial diagnosis. Although acquired uniparental disomy (UPD) or homozygosis of oncogenic *NRAS* allele is observed in CMML patients as well as in our CMML mice [10, 11], it appears to promote CMML progression but is insufficient to induce malignant transformation to AML on its own.

Despite our wealth of knowledge about CMML driver mutations, much less is known about genetic mutations promoting CMML transformation to AML. It has been reported that in the Asian cohort of CMML patients with *RUNX1* mutations, transformation to AML is associated with acquisition of oncogenic *NRAS* mutations [12]. However, this observation has not been functionally validated. We previously reported that knocking down *Tet2* expression does not accelerate *Nras*$^{G12D/+}$-induced CMML or promote its transformation to AML [13]. In contrast, loss of *Dnmt3a* or overexpression of *Evi1* cooperates with *Nras*$^{G12D/+}$ to promote CMML progression to AML [14, 15].

p53 regulates a wide range of biological processes to suppress tumorigenesis, including cell cycle progression, apoptosis, autophagy and cell differentiation [16]. Loss of *p53* cooperates with various genetic lesions, including oncogenic *Ras* and loss of *Pten*, to promote tumorigenesis in various experimental models [17-19]. Although *p53* mutation is prevalent in AML patients with complex karyotype, it is very rare in chronic diseases with largely normal karyotype, such as CMML and myeloproliferative neoplasm

(MPN) [6, 20, 21]. Recent identification of *TP53* mutation as a driver in promoting transformation of *JAK2*^{V617F}-positive MPN to AML indicates an important role of *p53* in development of secondary AML from an antecedent chronic disease [21].

Here, we tested potential genetic interaction between *p53* loss and endogenous oncogenic Nras signaling in promoting CMML to AML. Transplantation of *Nras*$^{G12D/+}$*; p53*$^{-/-}$ bone marrow cells resulted in a highly penetrant AML in recipient mice. Despite the reported role of *p53* in regulating hematopoietic stem cell (HSC) quiescence [22], we found that *p53* was largely dispensable for *Nras*$^{G12D/+}$ HSCs. Rather, loss of *p53* profoundly impacted on the function of *Nras*$^{G12D/+}$ myeloid progenitors (MPs) to promote leukemogenesis. *Nras*$^{G12D/+}$*; p53*$^{-/-}$ MPs showed increased quiescence and self-renewal. More importantly, some of them were transformed to self-renewing AML initiating cells (referred as AML-MPs) and capable to induce AML in serial transplanted recipients. Molecular and cellular characterization identified MEPs as the origin of transformed AML-MPs. RNA-Seq analysis revealed that AML-MPs gained partial signature of HSCs and largely retained MEP signature. The distinct transcriptome of AML-MPs was mainly driven by p53. In addition, we found that AML-MPs acquired overexpression of oncogenic *Nras* through UPD of oncogenic *Nras* allele and possibly epigenetic regulation, which led to hyperactivation of ERK1/2 signaling in AML mice. Our study identified a strong synergy between *p53* loss and enhanced oncogenic Nras signaling to promote leukemogenic transformation of MEPs and drive CMML transformation to AML.

3.3 Materials and methods

Mice

All mouse lines were maintained in a pure C57BL/6 genetic background (>N10). Mice bearing a conditional oncogenic *Nras* (*Nras* $^{Lox\text{-}stop\text{-}Lox\ (LSL)\ G12D/+}$) were crossed to *Mx1-Cre* mice to generate mice carrying both alleles (*Nras*$^{LSL\ G12D/+}$*; Mx1-Cre*). The *p53* conditional knockout mice (*p53*$^{fl/fl}$) were obtained from Jackson Laboratories (stock number 008462) and crossed with *Mx1-Cre* to generate *p53*$^{fl/fl}$*; Mx1-Cre* mice. *Nras*$^{LSL\ G12D/+}$*; p53*$^{fl/fl}$ mice were crossed to *p53*$^{fl/fl}$*; Mx1-Cre* to generate compound mice *Nras*$^{LSL\ G12D/+}$*; p53*$^{fl/fl}$*; Mx1-Cre*. Genotyping of *Nras*$^{G12D/+}$ and *Mx1-Cre* was done as previously described [10]. Genotyping of *p53*$^{fl/fl}$ was performed per the instructions of Jackson Laboratory. CD45.1^{+} congenic recipient mice were purchased from NCI.

To induce Cre expression, 5-7 week old mice were injected intraperitoneally (i.p.) with 100 μg of polyinosinic-polycytidylic acid (pI-pC; GE Healthcare) every other day for three times. The day of the first pI-pC injection was defined as Day 1. All experiments were performed on Day 12. The PCR analysis of recombination efficiency at the *p53* locus was performed as previously described [23]. All experiments were conducted in accordance with the *Guide for the Care and Use of Laboratory Animals* and approved by Animal Care and Use Committee at the University of Wisconsin, Madison. The program is accredited by the Association for Assessment and Accreditation of Laboratory Animal Care.

Murine bone marrow transplantation

2.5 x 10^5 total bone marrow cells (CD45.2^{+}) were mixed with same number of congenic bone marrow cells (CD45.1^{+}) and injected into individual lethally irradiated mice (500 rads x 2, 3 hours apart) as previously described [24].

HSCs, MPPs and MPs were sorted using a FACS AriaII (BD Biosciences) as described [24, 25]. Purified HSCs, MPPs or MPs ($CD45.2^+$) were transplanted with 2 x 10^5 whole bone marrow cells ($CD45.1^+$) into individual lethally irradiated mice.

At the moribund stage, 1 x 10^6 bone marrow or 5 x 10^6 spleen cells from recipients with AMD were transplanted into individual sublethally irradiated mice (650 rads).

Flow cytometric analysis of hematopoietic tissues

For lineage analysis of bone morrow, spleen and peripheral blood, flow cytometric analyses were performed as previously described [24]. HSCs, MPPs, LSK and MPs in bone marrow and spleen were analyzed as previously described [25, 26]. Stained cells were analyzed on a FACS Calibur or LSRII (BD Biosciences).

Directly conjugated or biotin conjugated antibodies against the following surface antigens were purchased from eBioscience: CD45.1 (A20), CD45.2 (104), Mac-1 (M1/70), Gr-1 (RB6-8C5), CD3 (145-2C11), CD4 (RM4-5), CD8 (53-6.7), CD19 (eBio1D3), Thy1.2 (53-2.1), TER119 (TER-119), B220 (RA3-6B2), IgM (eB121-15F9), IL-7Rα (B12-1), CD41 (eBioMWReg30), CD48 (HM48-1), Sca1 (D7), c-Kit (2B8), and CD34 (clone RAM34). FcγRII/III (2.4G2) was purchased from BD Biosciences. CD150 (TC15-12F12.2) was purchased from Biolegend.

Cell cycle analysis

Cell cycle analysis was performed essentially as described [27]. Fixed cells were simultaneously stained with PECy7-conjugated antibodies against CD41, CD48, B220,

TER119 and Gr1, PE-CD150, APC-c-Kit, PerCP Cy5.5-Sca1, FITC-Ki67 (BD Biosciences), and DAPI (Invitrogen). The stained cells were analyzed on a LSRII (BD Biosciences).

EdU incorporation

EdU (Invitrogen) was administered as a single dose of 1 mg injected i.p. EdU incorporation was measured 16 hours later using the Click-It EdU Pacific Blue Flow Kit (Invitrogen) as previously described [27]. $Sca1^{+}$ cells were enriched using an AutoMACS (Miltenyi). Enriched cells were first stained with FITC-conjugated antibodies against CD41, CD48, B220, TER119 and Gr1 and APC-CD150. After Click-It reaction, cells were then stained with PE-c-Kit and PerCP Cy5.5-Sca1. The stained cells were analyzed on a LSRII (BD Biosciences).

Flow cytometric analysis of phospho-ERK1/2 and phospho-Stat5

Phosphorylated ERK1/2 and Stat5 (p-ERK1/2 and p-Stat5) were analyzed in defined $Lin^{-/low}$ $c\text{-}Kit^{+}$ and $Lin^{-/low}$ $c\text{-}Kit^{-}$ cells essentially as previously described [10]. Surface proteins were detected with FITC-conjugated antibodies (BD Biosciences unless specified) against B220 (6B2), Gr-1 (RB6-8C5), CD3 (17A2, Biolegend), CD4 (RM4-5), CD8 (53-6.7), and TER119, and PE-conjugated anti-CD117/c-Kit antibody (eBiosciences, San Diego, CA). p-ERK1/2 was detected by a primary antibody against p-ERK (Thr202/Tyr204; Cell signaling Technology) followed by APC conjugated donkey anti-rabbit F(ab')2 fragment (Jackson ImmunoResearch). p-Stat5 (pY694) was detected by Alexa 647 conjugated primary antibody against p-Stat5 (BD Biosciences).

Complete blood count and histopathology

Complete blood count analysis was performed using a Hemavet 950FS (Drew Scientific). Mouse tissues were fixed in 10% neutral buffered formalin (Sigma-Aldrich) and further processed at the UWCCC Histology Lab.

Colony assay and replating assay

5 x 10^4 bone marrow cells were plated in duplicate in semisolid medium MethoCult M3234 (StemCell Technologies) supplemented with mGM-CSF or mIL-3 (Peprotech, Rocky Hill, NJ) according to the manufacture's protocol. The colonies were counted after 7 to 10 days in culture. Then colonies were harvested to repeat the same procedure for serial replating.

RNA-Seq and data analysis

Total RNAs were isolated from purified MP cells with RNeasy Mini Kit per the manufacturer's instructions (Qiagen). RNA-Seq was performed using an Illumina HiSeq 2000 system at the UW Biotechnology Center. Sequencing data were analyzed by BioInfoRx, Inc. Raw sequencing data quality was evaluated using FastQC , and reads were mapped to the latest mouse genome mm10 using Subread package. Gene level expression values were obtained using FeatureCount from Subread package. Data normalization and differential expression analysis were performed using limma package in R. Aligned RNA-Seq sequencing reads from control and leukemia samples were used

to detect somatic and germline variants. SNP and indel mutations were detected using samtools and varscan. Variants were annotated using SNPEff and SIFT4G softwares.

3.4 Results

Loss of *p53* synergizes with oncogenic *Nras* to induce a highly penetrant acute myeloid leukemia

To test potential genetic interactions between p53 deficiency and oncogenic Nras signaling in leukemogenesis, we generated *Mx1-Cre*, $p53^{fl/fl}$; *Mx1-Cre*, $Nras^{LSL\ G12D/+}$; *Mx1-Cre* and $Nras^{LSL\ G12D/+}$; $p53^{fl/fl}$; *Mx1-Cre* mice (Figure 3-S1A and S1B). At 5-7 weeks old, these mice were administrated with polyinosinic-polycytidylic acid (pI-pC) every other day for three times to induce endogenous interferon production, which stimulates Cre recombinase expression from an interferon-inducible promoter Mx1 in hematopoietic tissues [28]. Subsequently, the Cre recombinase induced oncogenic *Nras* expression from its endogenous locus and simultaneously deleted *p53* expression. The day of the first pI-pC injection is defined as Day 1 and all mice were sacrificed on Day 12 for various analyses. We refer the pI-pC treated compound mice as $p53^{-/-}$, $Nras^{G12D/+}$ and $Nras^{G12D/+}$; $p53^{-/-}$ mice respectively, and pI-pC treated *Mx1-Cre* mice as control mice throughout this chapter. We evaluated *p53* deletion efficiency in $Nras^{G12D/+}$; $p53^{-/-}$ HSCs and whole bone marrow (WBM) cells on Day 12. Single-HSC genotyping revealed that *p53* expression was completely removed in ~50% of HSCs (our unpublished results), while a small fraction of WBM cells still retained floxed p53 allele (Figure 3- S1C).

We transplanted 2.5 x 10^5 bone marrow cells ($CD45.2^+$) isolated from control, $p53^{-/-}$, $Nras^{G12D/+}$, and $Nras^{G12D/+}$; $p53^{-/-}$ mice along with same number of congenic

competitor cells ($CD45.1^+$) into individual lethally irradiated recipient mice ($CD45.1^+$). Consistent with our previous reports, over 90% of the recipient mice transplanted with $Nras^{G12D/+}$ cells developed CMML-like phenotypes with a median survival of 360 days [10], while all the recipients with $p53^{-/-}$ cells developed acute T-cell lymphoblastic leukemia/lymphoma (T-ALL) with a median survival of 168 days (Figure 3-1A and 1B). In contrast, about 88% of the recipients with $Nras^{G12D/+}$; $p53^{-/-}$ cells developed AML and about 67% of the recipients developed T-ALL with a median survival of 111 days, significantly shorter than other groups of recipients; some mice developed both diseases.

The recipient mice with AML displayed prominent monocytosis, anemia, and reduced platelet count in peripheral blood, expansion of myeloid compartment in spleen, and marked hepatosplenomegaly (Figure 3-1C~1E). Both spleen and liver were significantly infiltrated with immature blast cells (Figure 3-1F and our unpublished results). The AML disease was transplantable to secondary recipients (Figure 3-1G). To our surprise, flow cytometric analysis of AML cells demonstrated that in about 90% of the AML mice, the expression of CD45, a protein tyrosine phosphatase that is expressed on almost all hematopoietic cells, and lineage markers was significantly downregulated (Figure 3-S2). Genotyping of AML cells showed that *p53* expression was completely deleted, indicating donor-derived origin of these leukemia cells (Figure 3-S1C). To confirm that these $CD45^{-/low}$ $Lin^{-/low}$ AML cells are transformed from hematopoietic cells, we purified $CD45^+$ bone marrow cells from $Nras^{G12D/+}$; $p53^{-/-}$ mice for transplantation. Indeed, the $CD45^+$ hematopoietic cells generated $CD45^{-/low}$ $Lin^{-/low}$ AML cells in recipients (Table 3-1). Our results demonstrate that $p53^{-/-}$ cooperates with oncogenic *Nras* to promote development of AML.

***p53* is largely dispensable for *Nras*$^{G12D/+}$ HSCs.**

To determine the mechanisms underlying *Nras*$^{G12D/+}$*; p53*$^{-/-}$-induced AML, we analyzed hematopoietic compartment of control, *p53*$^{-/-}$, *Nras*$^{G12D/+}$ and *Nras*$^{G12D/+}$*; p53*$^{-/-}$ mice on Day 12. After acute induction of Cre expression, *p53*$^{-/-}$ mice were grossly indistinguishable from control mice, with normal spleen weight (Figure 3-S3A), unremarkable white blood cell counts, hematocrit, and platelet counts in peripheral blood (Figure 3-S3B), and normal myeloid differentiation in hematopoietic tissues (Figure 3-S3C). Consistent with previous reports [25, 26], *Nras*$^{G12D/+}$ mice showed significantly enlarged spleen and significant expansion of granulocytes and monocytes in spleens compared with control and *p53*$^{-/-}$ mice (Figure 3-S3A and S3C). *Nras*$^{G12D/+}$*; p53*$^{-/-}$ mice were generally comparable to *Nras*$^{G12D/+}$ mice except for moderate granulocytic/monocytic hyperplasia in peripheral blood (Figure 3-S3C).

Because *Nras*$^{G12D/+}$ HSCs serve as CMML initiating cells [25], we evaluated *p53* expression level in these cells. HSCs are defined as Lin$^-$ CD41$^-$ CD48$^-$ c-Kit$^+$ Sca1$^+$ CD150$^+$ as previously described [29]. Surprisingly, we found that the transcriptional level of *p53* tended to be lower in *Nras*$^{G12D/+}$ HSCs (Figure 3-S4A). Although intracellular flow cytometry indicated that p53 protein level in *Nras*$^{G12D/+}$ HSCs and WBM was significantly lower that that in control cells (Figure 3-S4B), it did not lead to down-regulation of p21, an important p53 target gene, in *Nras*$^{G12D/+}$ HSCs (Figure 3-S4C).

We further investigated how *p53* deficiency affects *Nras*$^{G12D/+}$ HSC function. Consistent with previous reports [22, 25], we found that HSC compartment in *p53*$^{-/-}$ and *Nras*$^{G12D/+}$ mice were moderately but significantly expanded (Figure 3-2A). However, we

only observed significant expansion of multipotent progenitor (MPP, defined as Lin$^-$ CD41$^-$ CD48$^-$ c-Kit$^+$ Sca1$^+$ CD150$^-$) and LSK (Lin$^-$ sca1$^+$ c-kit$^+$) compartments in *Nras*$^{G12D/+}$ mice (Figure 3-2B and 2C). Loss of *p53* did not significantly alter the size of HSC and MPP compartments in *Nras*$^{G12D/+}$ mice but further expanded their LSK compartment. Cell cycle profiling using Ki67 and DAPI staining did not reveal significant changes in *p53*$^{-/-}$ HSCs, MPPs, and LSKs compared to control cells (Figure 3-2D-2F). However, EdU incorporation analysis showed that percentages of cycling *p53*$^{-/-}$ HSCs, MPPs, and LSKs were significantly lower than those in control cells (Figure 3-2G~2I). Although *Nras*$^{G12D/+}$*; p53*$^{-/-}$ HSCs were similarly hyperproliferation as *Nras*$^{G12D/+}$ HSCs, it appeared that *Nras*$^{G12D/+}$*; p53*$^{-/-}$ MPPs and LSKs were moderately but significantly more proliferative than *Nras*$^{G12D/+}$ cells (Figure 3-2D~2I). Our data suggest that *p53* is largely dispensable for *Nras*$^{G12D/+}$ HSCs but its deficiency might lead to significant changes in downstream *Nras*$^{G12D/+}$ progenitors, which are enriched in LSKs.

Loss of *p53* induces MP expansion and increases MP self-renewal in *Nras*$^{G12D/+}$ mice

To determine how *p53* deficiency affected *Nras*$^{G12D/+}$ myeloid progenitor (MP) function, we analyzed MP (defined as Lin$^-$ IL7Rα$^-$ Sca1$^-$ c-Kit$^+$) compartment in control, *p53*$^{-/-}$, *Nras*$^{G12D/+}$, and *Nras*$^{G12D/+}$*; p53*$^{-/-}$ mice on Day 12. Compared to control mice, loss of *p53* alone induced MP expansion in spleen but not in bone marrow, which appeared to be due to the expansion of granulocyte-macrophage progenitor (GMP) and megakaryocyte-erythroid progenitor (MEP) compartments in spleen (Figure 3-3A). Consistent with our previous results [26], all *Nras*$^{G12D/+}$ MP compartments, including common myeloid progenitor (CMP), GMP, and MEP, were significantly expanded in both bone marrow

and spleen compared to those in control and/or *p53*$^{-/-}$ mice. In addition, deletion of *p53* resulted in markedly increased number of MPs, owing to increased numbers of GMP and MEP, in both bone marrow and spleen in *Nras*$^{G12D/+}$ mice. Contrary to our expectation, the expansion of MP compartment in *Nras*$^{G12D/+}$*; p53*$^{-/-}$ mice was not due to increased cell proliferation (Figure 3-3B and 3C). Rather, *Nras*$^{G12D/+}$*; p53*$^{-/-}$ MPs showed significantly increased quiescence in G0 stage (Figure 3-3B).

Consistent with our quantification analysis using flow cytometry, *in vitro* colony assay in semi-solid medium showed that *Nras*$^{G12D/+}$*; p53*$^{-/-}$ MPs formed significantly higher number of colonies in the presence of mGM-CSF or mIL-3 than control, *p53*$^{-/-}$, and *Nras*$^{G12D/+}$ MPs, though spontaneous colony formation of *Nras*$^{G12D/+}$*; p53*$^{-/-}$ MPs in the absence of cytokines was indistinguishable from *Nras*$^{G12D/+}$ MPs (Figure 3-3D). To evaluate transient self-renewal capability of MPs, we re-plated them in culture for additional rounds *in vitro*. *Nras*$^{G12D/+}$ MPs showed moderately increased self-renewal than control MPs, while *p53*$^{-/-}$ and *Nras*$^{G12D/+}$*; p53*$^{-/-}$ MPs displayed much higher capability to self-renew *in vitro* (Figure 3-3E). Although *p53*$^{-/-}$ and *Nras*$^{G12D/+}$*; p53*$^{-/-}$ MPs showed indistinguishable self-renewal capability in re-plating assay, we did observe that in each round of culture, the colonies formed by *Nras*$^{G12D/+}$*; p53*$^{-/-}$ MPs were consistently larger than those of *p53*$^{-/-}$ MPs. Together, our data indicate that loss of p53 significantly enhances self-renewal of *Nras*$^{G12D/+}$ MPs *in vitro* and leads to their further expansion *in vivo*.

MEPs deficient for *p53* and expressing oncogenic *Nras* are transformed to AML initiating cells

Because recipients of *Nras*$^{G12D/+}$*; p53*$^{-/-}$ cells developed a highly penetrant AML and *Nras*$^{G12D/+}$*; p53*$^{-/-}$ MPs acquired extensive self-renewal *in vitro*, we investigated whether these MPs are transformed to leukemia initiating cells (LICs) to support AML development *in vivo*. As expected, transplantation of highly purified *Nras*$^{G12D/+}$*; p53*$^{-/-}$ HSCs and MPPs in irradiated recipients led to AML and T-ALL, while transplantation of *Nras*$^{G12D/+}$*; p53*$^{-/-}$ MPs resulted in AML only (Table 3-1). Although *p53*$^{-/-}$ MPs showed comparable self-renewal capability as *Nras*$^{G12D/+}$*; p53*$^{-/-}$ MPs *in vitro*, they failed to initiate AML *in vivo* (Table 3-21), suggesting that the increased self-renewal in *p53*$^{-/-}$ MPs was not leukemogenic. To test for the *in vivo* self-renewal potential of AML initiating cells, we further purified CD45.1^{-} Lin^{-} c-Kit^{+} cells from primary recipients transplanted with *Nras*$^{G12D/+}$*; p53*$^{-/-}$ MPs and transplanted them into secondary and tertiary recipients. In most cases, these cells could efficiently induce AML formation (Figure 3-S5A). Limiting dilution experiment estimated that ~1 out of 300 CD45.1^{-} Lin^{-} c-Kit^{+} cells was AML initiating cell (Figure 3-S5B). These results indicate that *Nras*$^{G12D/+}$*; p53*$^{-/-}$ MPs are transformed to AML initiating cells.

To identify which specific population of MPs was transformed to AML initiating cells, we performed RNA-Seq analysis of Control-MPs and AML-MPs (defined as CD45.1^{-} Lin^{-} c-Kit^{+}). Volcano analysis revealed that 2,453 genes were significantly up-regulated and 3,604 genes were significantly down-regulated in AML-MPs (fold change > 2 and FDR<0.05) (Figure 3-4A and Table 3-3). Gene set enrichment analysis identified that genes regulating erythroid development were significantly up-regulated in AML-MPs (Figure 3-4B), while biological processes involved in immune response and leukocyte function were significantly enriched in the down-regulated genes (our

unpublished results). The latter observation was affirmed by gene ontology analysis of 496 up- and 1697 down-regulated genes (fold change > 16 and FDR < 0.001) (Figure 3-4C). Consistent with RNA-Seq analysis, we found that AML-MPs were Mac1$^-$ F4/80$^-$ and displayed immunophenotypes of MEPs (Figure 3-S2A and S6). Therefore, we isolated GMPs and MEPs from *Nras*$^{G12D/+}$*; p53*$^{-/-}$ mice and transplanted them to irradiated recipients. Consistent with our molecular and cellular characterizations, only *Nras*$^{G12D/+}$*; p53*$^{-/-}$ MEPs but not GMPs induced AML formation *in vivo* (Table 3-1). Similarly as *p53*$^{-/-}$ MPs, none of *p53*$^{-/-}$ MEPs and GMPs could initiate AML in recipient mice (Table 3-2). Our data demonstrate that *Nras*$^{G12D/+}$*; p53*$^{-/-}$ MEPs are transformed to LICs and support AML development *in vivo*.

AML-MPs gain partial HSC signature and largely retains MEP signature

We reasoned that if *Nras*$^{G12D/+}$*; p53*$^{-/-}$ MEPs were transformed to self-renewing AML-MPs, they should display some of the HSC signature and retain part of the MEP signature. To test this hypothesis, we defined HSC gene signature as differentially expressed genes between long term-HSCs (LT-HSCs) and MPPs using previously published microarray data [30]. The HSC signature genes were then hierarchically clustered based on their expression in Control- and AML-MPs (Figure 3-4D). The a1 and a2 blocks of genes were identified based on similar expression patterns (significantly down- or up-regulated respectively) shared by AML-MPs and LT-HSCs. Our results show that AML-MPs display partial HSC signature.

Next, we defined MEP signature as differentially expressed genes in MEP compared to LSK, CMP, and GMP ($P < 0.001$) using another set of published microarray

data [31]. The MEP signature genes were then hierarchically clustered based on their expression in Control- and AML-MPs (Figure 3-4E). The b1 and b2 blocks of genes were identified based on similar expression patterns (significantly up- or down-regulated respectively) shared by AML-MPs and MEPs. We found that MEP signature is largely maintained in AML-MPs.

Differentially expressed genes in AML-MPs are enriched for potential p53 target genes

Because *p53* is a master transcription factor regulating proliferation and differentiation of stem and progenitor cells [32, 33], we investigated whether the transcriptome characteristic of AML-MPs was mainly regulated by *p53*. Using previously published ChIP-Seq data [34] that were collected from mouse embryonic stem cells treated with adriamycin, a widely used DNA damage agent to activate *p53*, we identified 19,257 genes with significant p53 binding peaks within 25 Kb of their loci (upstream and downstream) as potential p53 target genes (Peaks in Figure 3-5A). In the same published study, 3,697 genes were identified as direct p53 target genes that are involved in DNA damage response (Targets in Figure 3-5A). The genes included in Peaks and Targets were further compared with genes differentially expressed in AML-MPs (fold change > 2 and FDR<0.05) (DE in Figure 3-5A). We found that about 78% of the DE genes are potential p53 target genes (Figure 3-5A). Among them, 1,288 DE genes belonged to both Targets and Peaks, while 3,408 DE genes were overlapped with Peaks only. Consistent with this observation, in the top 100 up- and down-regulated DE genes based on fold change, 85 and 75 of them were potential p53 target genes, respectively (Figure 3-5B). Significant

p53 binding peaks were confirmed in a few genes random selected from the list described in Figure 3-5B (Figure 3-5C). These data suggest that p53 is a master regulator driving AML-MP formation.

AML-MPs acquires overexpression of oncogenic *Nras*

Although *p53* deletion contributed to transformation of MEPs to AML-MPs, $p53^{-/-}$ MPs failed to induce AML *in vivo*, suggesting that additional genetic mutation(s), such as oncogenic *Nras* mutation, synergizes with $p53^{-/-}$ to promote AML development. To uncover potential cooperating genetic mutations, we re-analyzed RNA-Seq data from AML-MPs using compiled RNA-Seq results from Control-MPs as baseline. Initial analysis revealed that AML-MPs isolated from 4 AML mice all carried $Nras^{G12D/G12D}$ mutation, indicating that UPD of oncogenic *Nras* allele occurred and was selected during leukemogenesis (Figure 3-6A). Moreover, transcriptional level of oncogenic *Nras* was significantly elevated in AML-MPs, ~2.6 fold of WT *Nras* in Control-MPs (Figure 3-6B). These results suggest that overexpression of oncogenic *Nras* cooperates with *p53* deficiency to promote AML.

To further validate our genetic finding, we measured oncogenic Nras-mediated GM-CSF signaling in MPs (enriched in Lin^- $c\text{-}Kit^+$ cells) and myeloid precursors (enriched in Lin^- $c\text{-}Kit^+$ cells) from different groups of animals. Consistent with previous reports [10, 14], GM-CSF signaling was largely normal in $Nras^{G12D/+}$ cells on Day 12 (Figure 3-6C). Similarly as our colony assay result that *p53* deficiency did not change the spontaneous colony formation of WT and $Nras^{G12D/+}$ cells (Figure 3-3D), GM-CSF signaling in $p53^{-/-}$ cells was comparable to that in control cells, while GM-CSF signaling

in *Nras*$^{G12D/+}$*; p53*$^{-/-}$ cells was indistinguishable from that in *Nras*$^{G12D/+}$ cells (Figure 3-6C). In contrast, compared to *Nras*$^{G12D/+}$ and *Nras*$^{G12D/+}$*; p53*$^{-/-}$ cells, ERK1/2 signaling at both basal level and evoked by GM-CSF was significantly hyperactivated in AML-MPs, which harbored *Nras*$^{G12D/G12D}$ mutation and up-regulated oncogenic *Nras* expression (Figure 3-6C). Together, our data suggest that overexpression of oncogenic *Nras*, through UPD of oncogenic *Nras* allele and possibly epigenetic regulation, leads to hyperactivation of ERK1/2 signaling and synergizes with *p53*$^{-/-}$ to induce AML.

3.5 Discussion

In this study, we show that recipients transplanted with *Nras*$^{G12D/+}$*; p53*$^{-/-}$ bone marrow cells developed a highly penetrant AML. *p53* deficiency leads to increased quiescence at G0 stage and increased self-renewal potential in *Nras*$^{G12D/+}$ MPs. Among mutant MPs, MEPs are transformed to AML initiating cells. These cells acquire partial HSC signature and largely maintain MEP signature. During AML development, transformed MEPs gain UPD of oncogenic *Nras* allele and overexpression of oncogenic *Nras*, which leads to hyperactivation of ERK1/2 signaling in AML cells. Therefore, loss of *p53* synergizes with oncogenic *Nras* to promote CMML transformation to AML (Figure 3-S7).

Our results generated from conditional *p53*$^{-/-}$ mice are not entirely consistent with results from germline *p53*$^{-/-}$ mice [22]. Although both studies observed expanded *p53*$^{-/-}$ HSC compartment, our study found that in conditional *p53*$^{-/-}$ mice, EdU incorporation in *p53*$^{-/-}$ HSCs was significantly lower than that in control HSCs (Figure 3-2G), suggesting that HSC expansion in these mice is likely due to expansion of highly quiescent LT-HSCs and/or increased survival of HSCs. This possibility is supported by a previous

study of *Lnk*$^{-/-}$ HSCs, which undergo significant expansion without increase of proliferation [35]. Similar mechanism might be also applicable on the expansion of *p53*$^{-/-}$ MP compartment. In contrast, previous study using germline *p53*$^{-/-}$ mice showed that *p53*$^{-/-}$ HSCs are hyperproliferative compared to control HSCs, which might lead to HSC expansion [22]. We believe that the difference of our study and the previous study is likely caused by different timing of *p53* deletion. In our study, HSC phenotype was analyzed after acute deletion of *p53*, which likely reflects the direct effect of *p53* deficiency on HSCs. However, in the previous study, HSCs were analyzed 2-3 months after *p53* deletion, which is likely influenced by additional changes accumulated in these cells.

Although p53 is largely dispensable for *Nras*$^{G12D/+}$ HSCs, its deficiency significantly impacts on *Nras*$^{G12D/+}$ MPs. Acute deletion of *p53* induces increased quiescence at G0 stage and increased self-renewal potential in *Nras*$^{G12D/+}$ MPs (Figure 3-3B and 3E). These features are characteristic of HSCs. It is therefore not surprising that AML-MPs gain partial HSC signature (Figure 3-4D). Interestingly, despite that *p53*$^{-/-}$ MPs displayed increased self-renewal *in vitro* as *Nras*$^{G12D/+}$*; p53*$^{-/-}$ MPs (Figure 3-3E), they failed to induce AML *in vivo* (Table 3-3), suggesting that *p53*$^{-/-}$ alone only induces non-leukemogenic self-renewal. Similar observation is also reported in MPs expressing AML1-ETO [36]. Our results suggest that *p53*$^{-/-}$ cooperates with oncogenic *Nras* to promote leukemogenic self-renewal in MPs and induce their transformation to AML initiating cells.

Unlike MLL-AF9 induced AML, in which GMPs are transformed to LICs [31], our data demonstrate that AML-MPs are leukemogenic, self-renewing MEPs. This

conclusion is supported by our results from several independent experiments. First, AML-MPs displayed MEP immunophenotypes (Figure 3-S6). Second, in AML-MPs, genes promoting erythroid development were significantly up-regulated, whereas genes involved in immune response/leukocyte function were significantly down-regulated. Third, purified *Nras*$^{G12D/+}$*; p53*$^{-/-}$ MEPs could initiate AML in transplanted recipients. Fourth, AML-MPs largely retained MEP signature (Figure 3-4E). Fifth, *Gata1* and *Gata2*, two master transcription factors regulating MEP function, were significantly up-regulated in AML-MPs, and so were their downstream target genes promoting megakaryocyte and erythroid cell differentiation (our unpublished results). Interestingly, in a recent study of leukemic transformation of MPN to AML, overexpression of *JAK2V617F* mutant in *p53*$^{-/-}$ bone marrow cells also transforms MEPs to AML initiating cells [21]. Transformed MEPs in our model appeared to block differentiation of megakaryocytes and erythrocytes as the AML mice consistently displayed anemia and significantly lowered platelet count in peripheral blood (Figure 3-1D). Our result is consistent with a recent assessment of erythorid dysplasia in human MDS (including MD-CMML) and AML specimens, which identifies a significant correlation of loss of *TP53* and increased frequency of erythroid abnormalities [37].

Although *p53* mutation is prevalent in AML with complex karyotype [20], it is rare in CMML (2 out of 202) [6], probably because majority of CMML patients carry normal karyotype. Consistent with the published results, we did not detect p53 mutations in our cohort of 7 CMML patients. Rather, we found that all of them carried P72R polymorphism, 6 with homozygous R72 allele and 1 with heterozygous R72 allele (Table 3-4). Although the R72 SNP is not significantly associated with susceptibility to breast

and lung cancers [38, 39], numerous studies report that R72 confers stronger phenotypes than P72, including more active in transactivating the expression of leukemia-inhibitory factor, more effective in inducing apoptosis, and more potent in cooperating with EJ-Ras in transforming primary cells and in neutralizing p73 activity [40]. In addition to the P72R SNP in *TP53*, we also found that 5 CMML patients harbored an oncogenic *RAS* mutation [13], and 1 with monosomy 7. Monosomy 7 is observed in ~30% of JMML patients, a sister disease of CMML and characterized by Ras pathway mutations [41, 42]. In addition, monosomy 7 and Ras pathway mutations frequently coexist in AML, including secondary AML transformed from MDS and congenital neutropenia [43-45]. Monosomy 7 and del(7q) are also common in MDS, but are not associated with Ras pathway mutations in this setting. These data suggest that -7/del(7q) are overlapping with Ras pathway, but also distinct. Therefore, it is interesting to investigate in the future whether the P72R SNP is significantly associated with risk of CMML and/or associated with activating RTK/Ras pathway mutations in CMML.

Although our donor cells began with $Nras^{G12D/+}$, oncogenic Nras is overexpressed in AML-MPs through UPD of oncogenic *Nras* allele and probably epigenetic regulation. The up-regulation of oncogenic Nras signaling might explain the significantly shortened lifespan of recipients transplanted with $Nras^{G12D/+}$; $p53^{-/-}$ cells. Interestingly, although UPD of oncogenic *Nras* allele is identified in human and mouse CMML, it only promotes CMML development on its own and fails to induce AML [10]. Similarly, $p53^{-/-}$ alone does not confer leukemogenic self-renewal of MPs (Table 3-2). Consistent with a previous report showing that *p53* loss enables aberrant self-renewal of $Kras^{G12D/+}$ MPs [19], our study identified a significant synergy between $p53^{-/-}$ and enhanced oncogenic

Nras signaling in transforming MEPs to LICs and promoting CMML transformation to AML.

3.6 Figures and legends

Figure 3-1. *p53* deletion transforms oncogenic *Nras*$^{G12D/+}$-induced CMML to AML. (A-F) Lethally irradiated mice were transplanted with 2.5 x 10^5 total bone marrow cells from control, *p53*$^{-/-}$, *Nras*$^{G12D/+}$ or *Nras*$^{G12D/+}$*; p53*$^{-/-}$ mice along with same number of competitor cells. (A) Kaplan-Meier comparative survival analysis of reconstituted mice. Cumulative survival was plotted against days after transplantation. *P* value was determined by the log-rank test. (B) Disease incidence in recipient mice transplanted with *p53*$^{-/-}$, *Nras*$^{G12D/+}$ or *Nras*$^{G12D/+}$*; p53*$^{-/-}$ cells. (C) Representative flow cytometry analysis of bone marrow (BM), spleen (SP) and peripheral blood (PB) cells from moribund AML-*Nras*$^{G12D/+}$*; p53*$^{-/-}$ and age-matched control mice. (D) Complete blood count was performed on peripheral blood samples collected from moribund AML-*Nras*$^{G12D/+}$*; p53*$^{-/-}$ and age-matched control mice. (E) Spleen and liver weight of moribund AML-*Nras*$^{G12D/+}$*; p53*$^{-/-}$ and control mice. (F) Representative spleen histologic H&E sections from moribund AML-*Nras*$^{G12D/+}$*; p53*$^{-/-}$ and control mice. (G) 1x10^6 bone marrow or 5 x 10^6 spleen cells from moribund AML-*Nras*$^{G12D/+}$*; p53*$^{-/-}$ mice were transplanted into sublethally irradiated mice. Kaplan-Meier comparative survival curve was plotted against days after transplantation. The results are presented as mean ± SD. * $P < 0.05$; ** $P < 0.01$; *** $P < 0.001$.

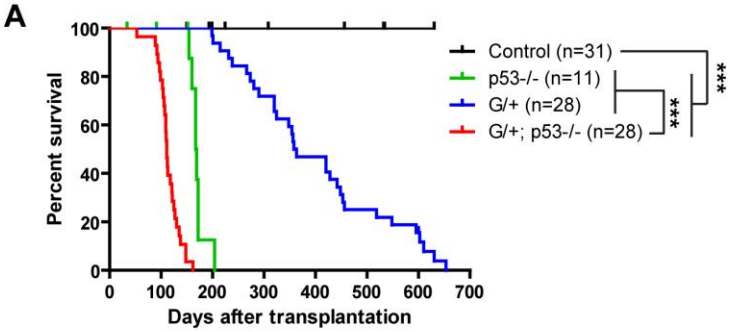

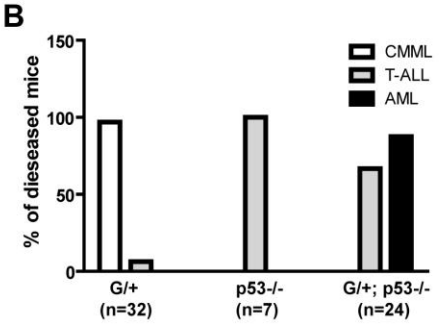

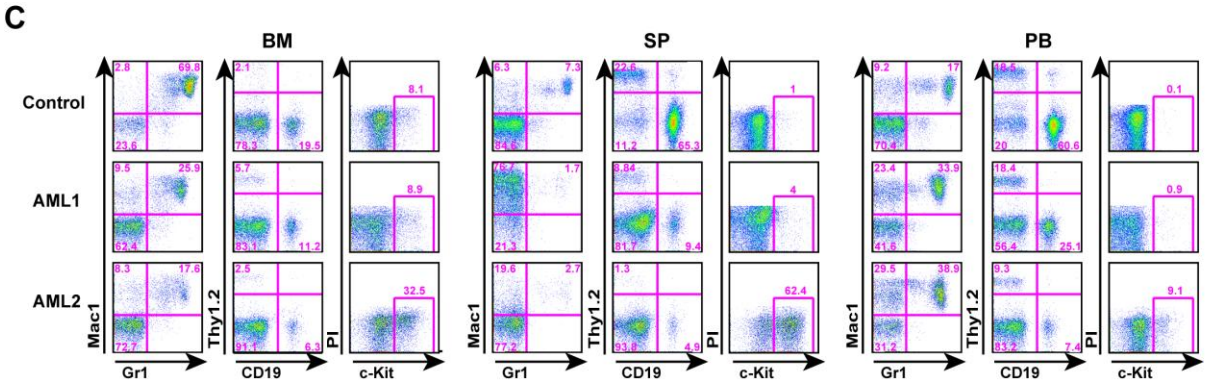

D

	WBC (x10^3/ul)	Hematocrit (%)	Platelet (x10^3/ul)
Control (n=4)	5.4-11.8 (7.4)	42.8-44.4 (43.4)	574-1062 (824)
AML (n=6)	7.2-202 (12.5)	11.4-27.6 (22.4)***	84-366 (122)***

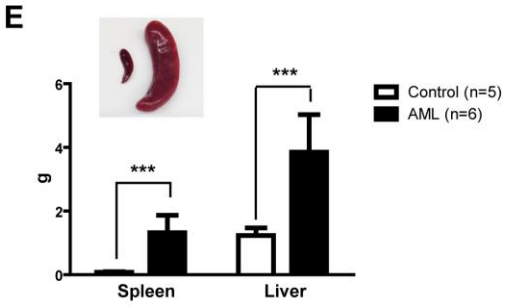

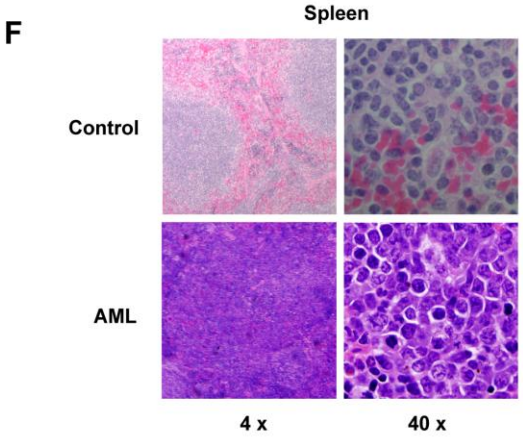

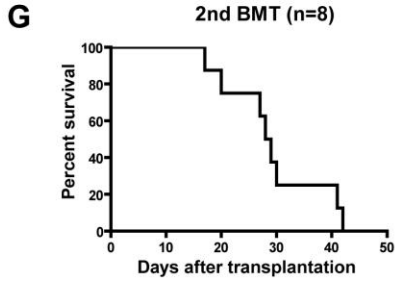

Figure 3-2. Loss of *p53* induces further expansion of LSK compartment in *Nras*$^{G12D/+}$ mice. Control, *p53*$^{-/-}$, *Nras*$^{G12D/+}$ and *Nras*$^{G12D/+}$*; p53*$^{-/-}$ mice were treated with pI-pC and euthanized on Day 12 for analysis as described in Materials and Methods. (A-C) Quantification of HSCs (Lin$^-$ CD41$^-$ CD48$^-$ c-Kit$^+$ Sca1$^+$ CD150$^+$) (A), MPPs (Lin$^-$ CD41$^-$ CD48$^-$ c-Kit$^+$ Sca1$^+$ CD150$^-$) (B), and LSK (Lin$^-$ c-Kit$^+$ Sca1$^+$) cells (C) in bone marrow (BM) and spleen (SP). (D-F) Cell cycle analysis of bone marrow HSCs (D), MPPs (E), and LSKs (F). (G-I) A 16-hour pulse of EdU to quantify proliferating HSCs (G), MPPs (H), and LSKs (I) in bone marrow. Data are presented as mean ± SD. * $P < 0.05$; ** $P < 0.01$; *** $P < 0.001$.

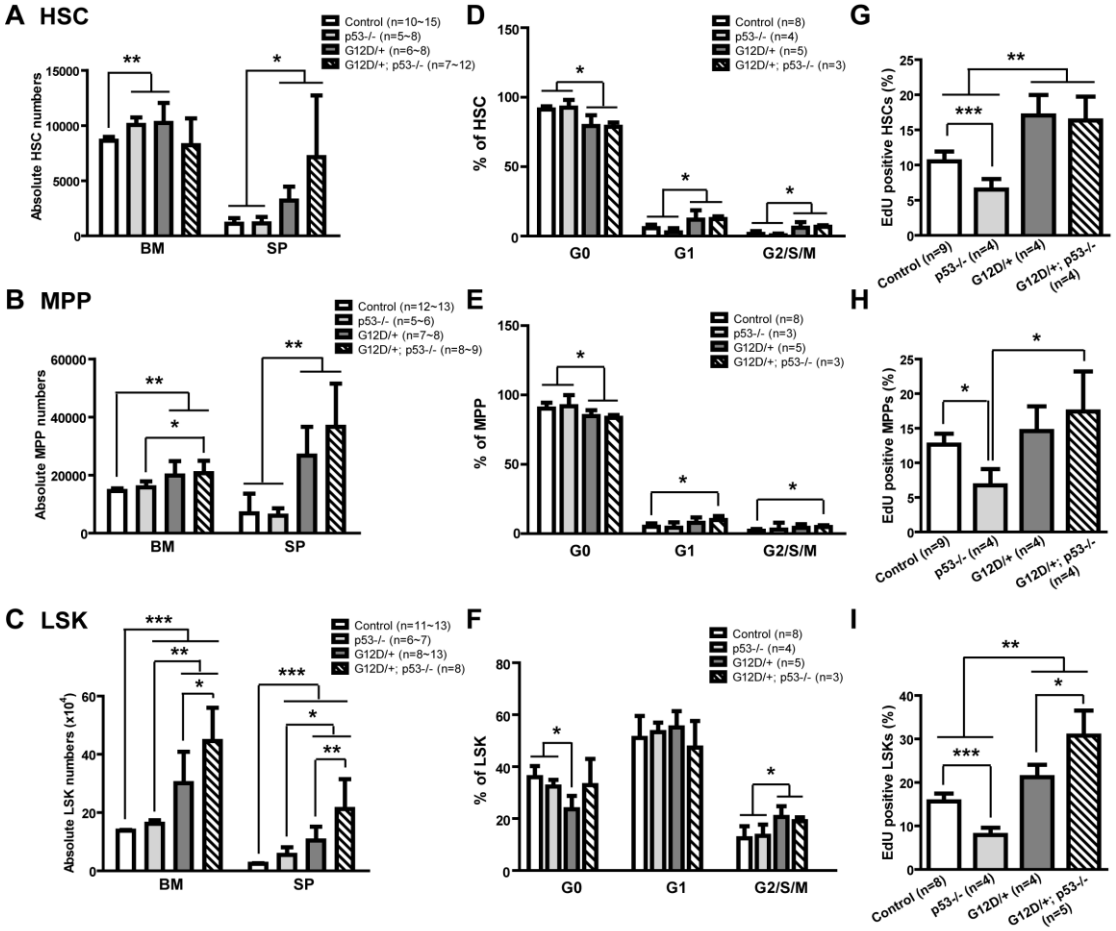

Figure 3-3. *p53* deficiency leads to further expansion and increased quiescence and self-renewal of *Nras*$^{G12D/+}$ myeloid progenitors. Control, *p53*$^{-/-}$, *Nras*$^{G12D/+}$ and *Nras*$^{G12D/+}$*; p53*$^{-/-}$ mice were treated with pI-pC and euthanized on Day 12 for analysis as described in Materials and Methods. (A) Quantification of myeloid progenitors (MPs), common myeloid progenitors (CMPs), granulocyte-macrophage progenitors (GMPs), and megakaryocyte-erythroid progenitors (MEPs) in bone marrow (BM) and spleen (SP). (B) Cell cycle analysis of bone marrow MPs using Ki67/DAPI staining. (C) A 16-hour pulse of EdU to quantify proliferating bone marrow MPs. (D) 5 x 10^4 bone marrow cells isolated from control, *p53*$^{-/-}$, *Nras*$^{G12D/+}$ or *Nras*$^{G12D/+}$*; p53*$^{-/-}$ mice were plated in semisolid medium without cytokines or with 0.2 ng/ml of mGM-CSF or 10 ng/ml mIL-3. Colonies were counted 7-10 days after culture. (E) Methylcellulose culture of 5 x 10^4 bone marrow cells with 10 ng/ml mIL-3 over three rounds of replating. Representative images of colonies are shown. Data are presented as mean ± SD. * $P < 0.05$; ** $P < 0.01$; *** $P < 0.001$.

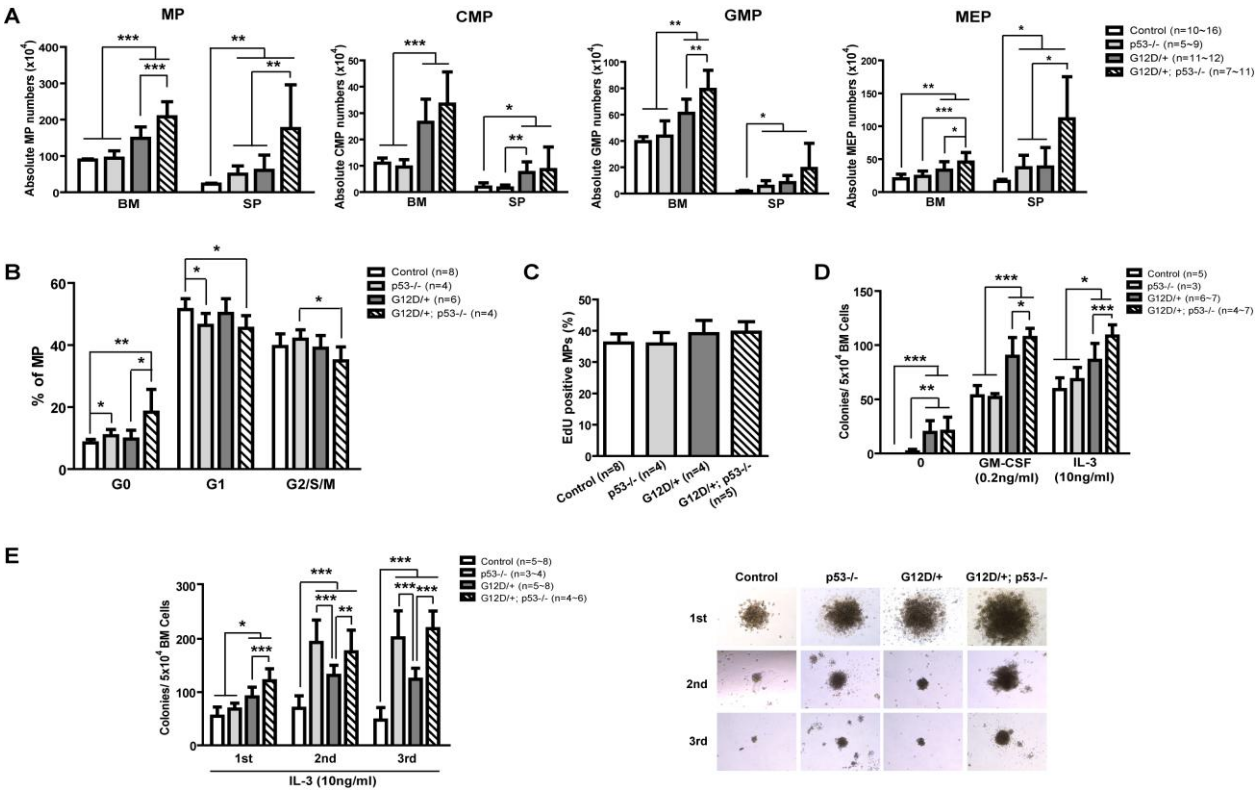
A
MP
CMP
GMP
MEP
Absolute MP numbers (x10⁴)
Absolute CMP numbers (x10⁴)
Absolute GMP numbers (x10⁴)
Absolute MEP numbers (x10⁴)
BM
SP
Control (n=10~16)
p53-/- (n=5~9)
G12D/+ (n=11~12)
G12D/+; p53-/- (n=7~11)
B
% of MP
G0
G1
G2/S/M
Control (n=8)
p53-/- (n=4)
G12D/+ (n=6)
G12D/+; p53-/- (n=4)
C
EdU positive MPs (%)
Control (n=8)
p53-/- (n=4)
G12D/+ (n=4)
G12D/+; p53-/- (n=5)
D
Colonies/ 5x10⁴ BM Cells
0
GM-CSF (0.2ng/ml)
IL-3 (10ng/ml)
Control (n=5)
p53-/- (n=3)
G12D/+ (n=6~7)
G12D/+; p53-/- (n=4~7)
E
Colonies/ 5x10⁴ BM Cells
1st
2nd
3rd
IL-3 (10ng/ml)
Control (n=5~8)
p53-/- (n=3~4)
G12D/+ (n=5~8)
G12D/+; p53-/- (n=4~6)
Control
p53-/-
G12D/+
G12D/+; p53-/-
1st
2nd
3rd

Figure 3-4. Myeloid progenitors isolated from AML mice display partial HSC signature and largely maintain MEP identity. RNA-sequencing based gene expression comparison between control myeloid progenitors (Ctrl-MP) and myeloid progenitors isolated from AML mice (AML-MP). (A) Volcano plot of gene expression in AML-MPs versus control-MPs. Dots located in the upper-left and upper-right sections represent 1697 down- and 496 up-regulated genes respectively (fold change (FC) >16 and false discovery rate (FDR) < 0.001). (B) Gene Set Enrichment Analysis (GSEA) of erythrocyte development gene expression profile. NES, normalized enrichment score. (C) Gene Ontology (GO) analysis of 1697 down-regulated genes (described above) in AML-MPs using DAVID bioinformatics program. The representative biological processes are shown with corresponding FDR. (D) Heat map depicting relative expression of HSC-signature (genes differentially expressed in LT-HSCs versus MPPs; previously described in [30]) in Ctrl- and AML-MPs. Genes in blocks a1 and a2 show similar expression profiles between AML-MPs and LT-HSCs. (E) Heat map showing relative expression of MEP-signature (genes differentially expressed in MEPs versus LSKs, CMPs, and GMPs; previously described in [31]) in Ctrl- and AMD-MPs. Genes in blocks b1 and b2 demonstrate similar expression profiles between AML-MPs and MEPs.

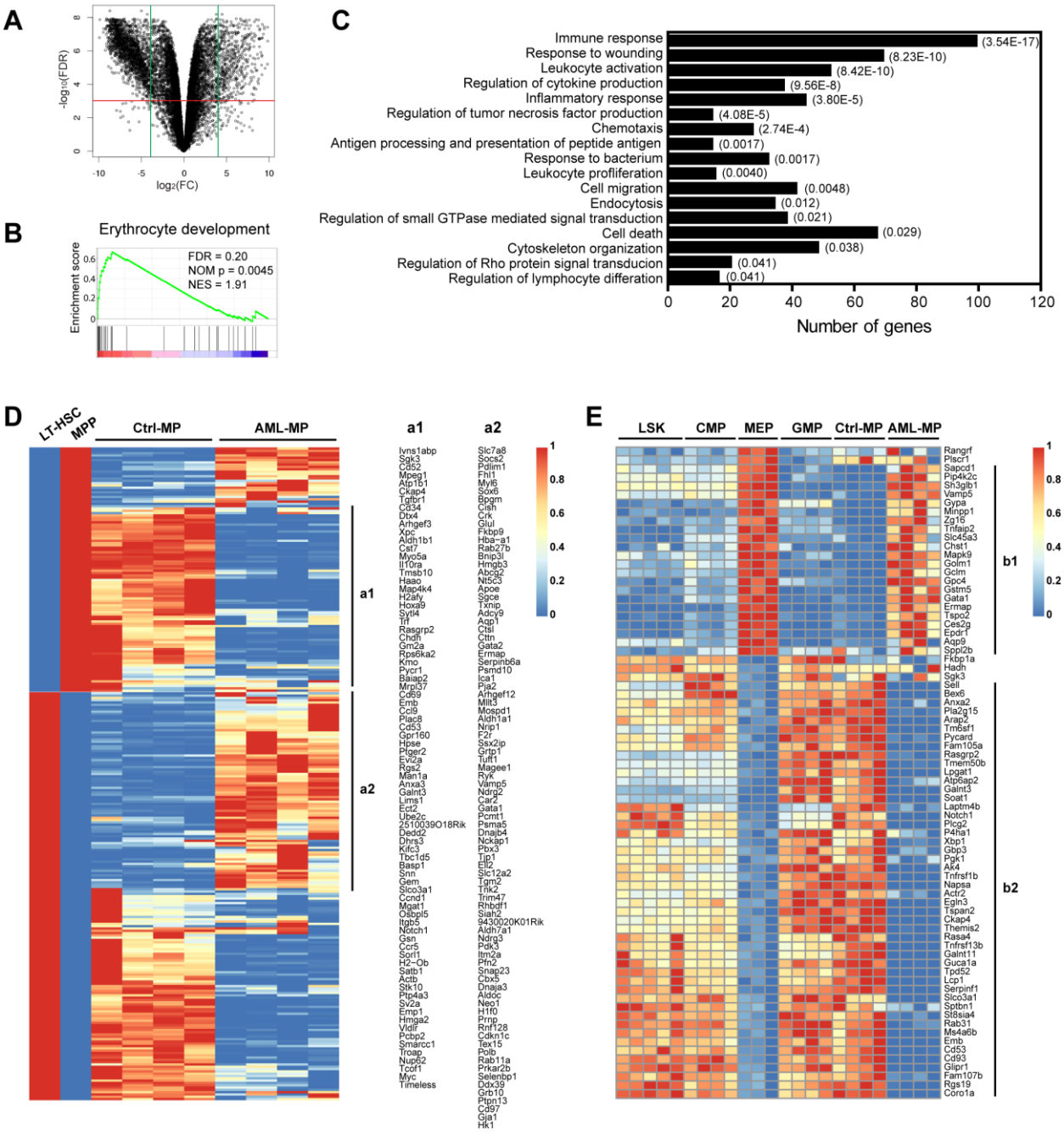
A
-log10(FDR)
log2(FC)
B
Erythrocyte development
Enrichment score
FDR = 0.20
NOM p = 0.0045
NES = 1.91
C
Immune response (3.54E-17)
Response to wounding (8.23E-10)
Leukocyte activation (8.42E-10)
Regulation of cytokine production (9.56E-8)
Inflammatory response (3.80E-5)
Regulation of tumor necrosis factor production (4.08E-5)
Chemotaxis (2.74E-4)
Antigen processing and presentation of peptide antigen (0.0017)
Response to bacterium (0.0017)
Leukocyte profliferation (0.0040)
Cell migration (0.0048)
Endocytosis (0.012)
Regulation of small GTPase mediated signal transduction (0.021)
Cell death (0.029)
Cytoskeleton organization (0.038)
Regulation of Rho protein signal transducion (0.041)
Regulation of lymphocyte differation (0.041)
Number of genes
D
LT-HSC
MPP
Ctrl-MP
AML-MP
a1
a2
E
LSK
CMP
MEP
GMP
Ctrl-MP
AML-MP
b1
b2

Figure 3-5. Genes differentially expressed in AML-MPs are enriched for potential p53 target genes. (A) Venn diagrams illustrating the overlap among differentially expressed genes (DE) in AML-MPs, p53 target genes involved in DNA damage response (Targets), and the genes with p53 binding peaks close to their loci (Peaks). Targets and Peaks are described in [34]. (B) Heat map displaying statistically significant (FDR < 0.001), top 100 up- and down-regulated genes in AML-MPs (based on fold change). Genes in green are p53 target genes involved in DNA damage response, while genes in orange are genes with p53 binding peaks closed to their loci but not regulated by p53 in DNA damage response. (C) Genomic views of p53 binding peaks at 4 representative gene loci.

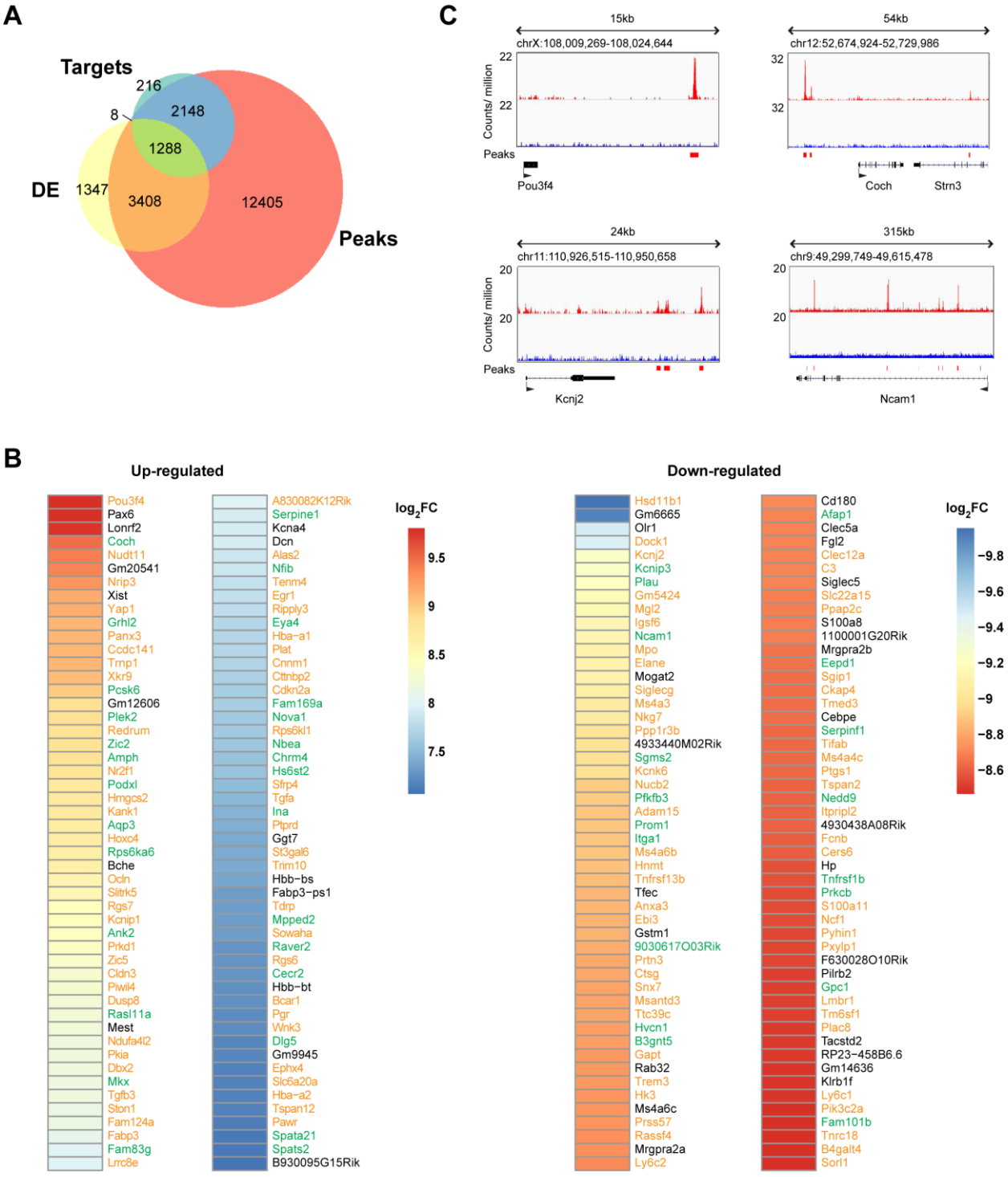
A
Targets
216
2148
8
1288
DE
1347
3408
12405
Peaks
C
15kb
chrX:108,009,269-108,024,644
Counts/ million
Peaks
Pou3f4
54kb
chr12:52,674,924-52,729,986
Coch
Strn3
24kb
chr11:110,926,515-110,950,658
Kcnj2
315kb
chr9:49,299,749-49,615,478
Ncam1
B
Up-regulated
Pou3f4
Pax6
Lonrf2
Coch
Nudt11
Gm20541
Nrip3
Xist
Yap1
Grhl2
Panx3
Ccdc141
Trnp1
Xkr9
Pcsk6
Gm12606
Plek2
Redrum
Zic2
Amph
Nr2f1
Podxl
Hmgcs2
Kank1
Aqp3
Hoxc4
Rps6ka6
Bche
Ocln
Slitrk5
Rgs7
Kcnip1
Ank2
Prkd1
Zic5
Cldn3
Piwil4
Dusp8
Rasl11a
Mest
Ndufa4l2
Pkia
Dbx2
Mkx
Tgfb3
Ston1
Fam124a
Fabp3
Fam83g
Lrrc8e
A830082K12Rik
Serpine1
Kcna4
Dcn
Alas2
Nfib
Tenm4
Egr1
Ripply3
Eya4
Hba-a1
Plat
Cnnm1
Cttnbp2
Cdkn2a
Fam169a
Nova1
Rps6kl1
Nbea
Chrm4
Hs6st2
Sfrp4
Tgfa
Ina
Ptprd
Ggt7
St3gal6
Trim10
Hbb-bs
Fabp3-ps1
Tdrp
Mpped2
Sowaha
Raver2
Rgs6
Cecr2
Hbb-bt
Bcar1
Pgr
Wnk3
Dlg5
Gm9945
Ephx4
Slc6a20a
Hba-a2
Tspan12
Pawr
Spata21
Spats2
B930095G15Rik
log2FC
9.5
9
8.5
8
7.5
Down-regulated
Hsd11b1
Gm6665
Olr1
Dock1
Kcnj2
Kcnip3
Plau
Gm5424
Mgl2
Igsf6
Ncam1
Mpo
Elane
Mogat2
Siglecg
Ms4a3
Nkg7
Ppp1r3b
4933440M02Rik
Sgms2
Kcnk6
Nucb2
Pfkfb3
Adam15
Prom1
Itga1
Ms4a6b
Hnmt
Tnfrsf13b
Tfec
Anxa3
Ebi3
Gstm1
9030617O03Rik
Prtn3
Ctsg
Snx7
Msantd3
Ttc39c
Hvcn1
B3gnt5
Gapt
Rab32
Trem3
Hk3
Ms4a6c
Prss57
Rassf4
Mrgpra2a
Ly6c2
Cd180
Afap1
Clec5a
Fgl2
Clec12a
C3
Siglec5
Slc22a15
Ppap2c
S100a8
1100001G20Rik
Mrgpra2b
Eepd1
Sgip1
Ckap4
Tmed3
Cebpe
Serpinf1
Tifab
Ms4a4c
Ptgs1
Tspan2
Nedd9
Itpripl2
4930438A08Rik
Fcnb
Cers6
Hp
Tnfrsf1b
Prkcb
S100a11
Ncf1
Pyhin1
Pxylp1
F630028O10Rik
Pilrb2
Gpc1
Lmbr1
Tm6sf1
Plac8
Tacstd2
RP23-458B6.6
Gm14636
Klrb1f
Ly6c1
Pik3c2a
Fam101b
Tnrc18
B4galt4
Sorl1
log2FC
−9.8
−9.6
−9.4
−9.2
−9
−8.8
−8.6

Figure 3-6. Overexpression of oncogenic *Nras* leads to hyperactivation of ERK1/2 signaling in AML-MPs. (A) Representative sequencing results from RNA-Seq analysis show uniparental disomy of *Nras G12D* mutation in AML-MPs. (B) Reads per kilobase per million of mapped reads (RPKM) of *Nras* in control- and AML-MPs. (C) Whole bone marrow cells isolated from control, $p53^{-/-}$, $Nras^{G12D/+}$ and $Nras^{G12D/+}; p53^{-/-}$ mice on Day 12 or moribund AML-$Nras^{G12D/+}; p53^{-/-}$ recipients were serum and cytokine starved for 2 hours and stimulated with various concentrations of mGM-CSF (0, 0.32 and 10 ng/ml) at 37°C for 10 minutes. Levels of p-ERK1/2 and p-Stat5 were measured using phosphor-specific flow cytometry. Non-neutrophil bone marrow cells were gated for data analysis. Myeloid progenitors are enriched in $Lin^{-/low}$ c-Kit^{+} cells, whereas myeloid precursors are enriched in $Lin^{-/low}$ c-Kit^{-} cells. Data are presented as mean ± SD. * $P < 0.05$; ** $P < 0.01$; *** $P < 0.001$.

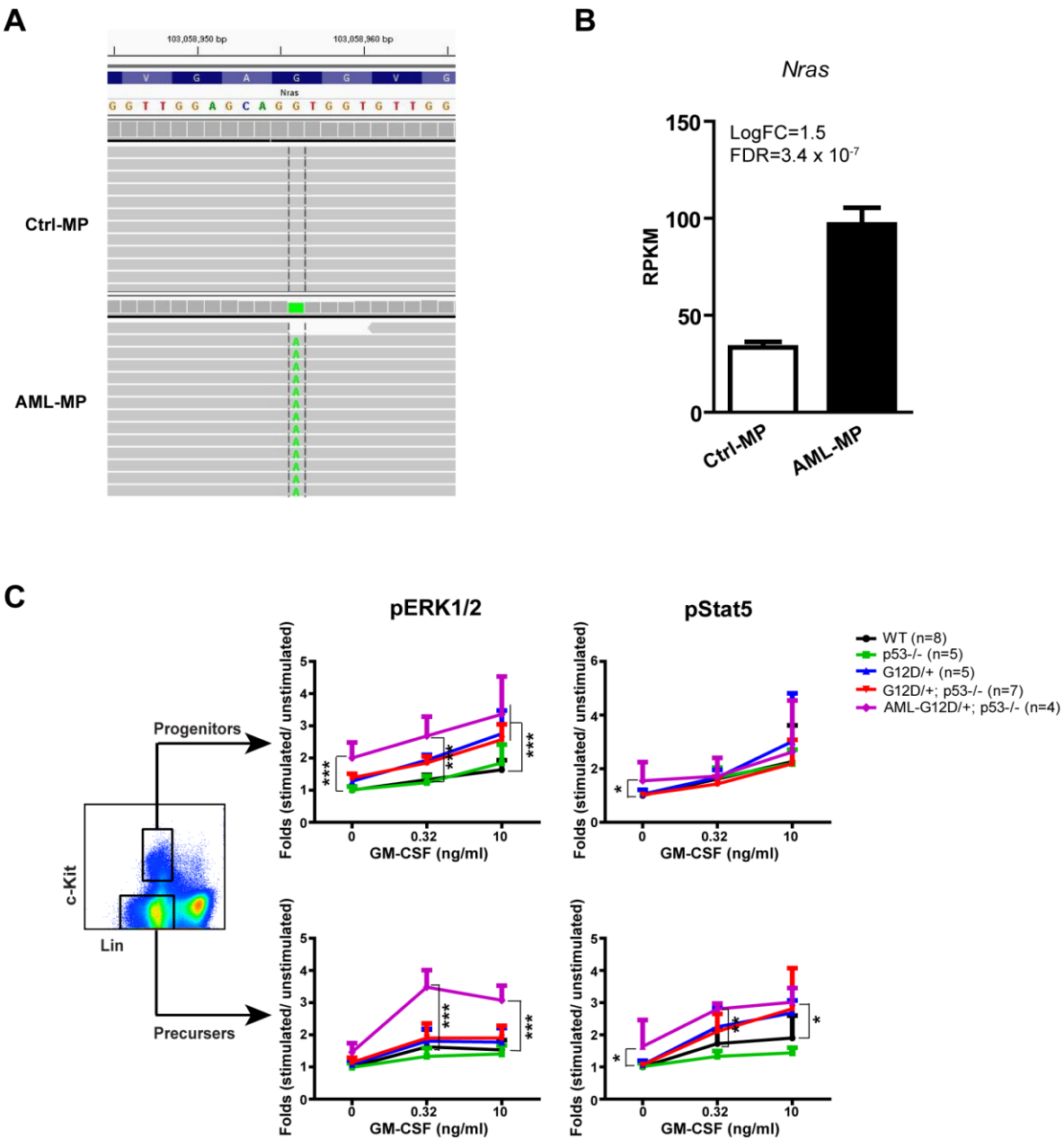
A
103,058,950 bp
103,058,960 bp
Nras
Ctrl-MP
AML-MP
B
Nras
LogFC=1.5
FDR=3.4 x 10-7
RPKM
150
100
50
0
Ctrl-MP
AML-MP
C
pERK1/2
pStat5
Progenitors
Precursers
c-Kit
Lin
Folds (stimulated/ unstimulated)
GM-CSF (ng/ml)
0
0.32
10
WT (n=8)
p53-/- (n=5)
G12D/+ (n=5)
G12D/+; p53-/- (n=7)
AML-G12D/+; p53-/- (n=4)

Figure 3-S1. Generation and characterization of experimental animals. (A) Schematic illustration of the strategy to generate experimental mice. (B) Genotyping analysis of different alleles using genomic DNAs isolated from different groups of animals. (C) Genotyping analysis to evaluate *p53* deletion efficiency in bone marrow cells after pI-pC treatment and in AML cells.

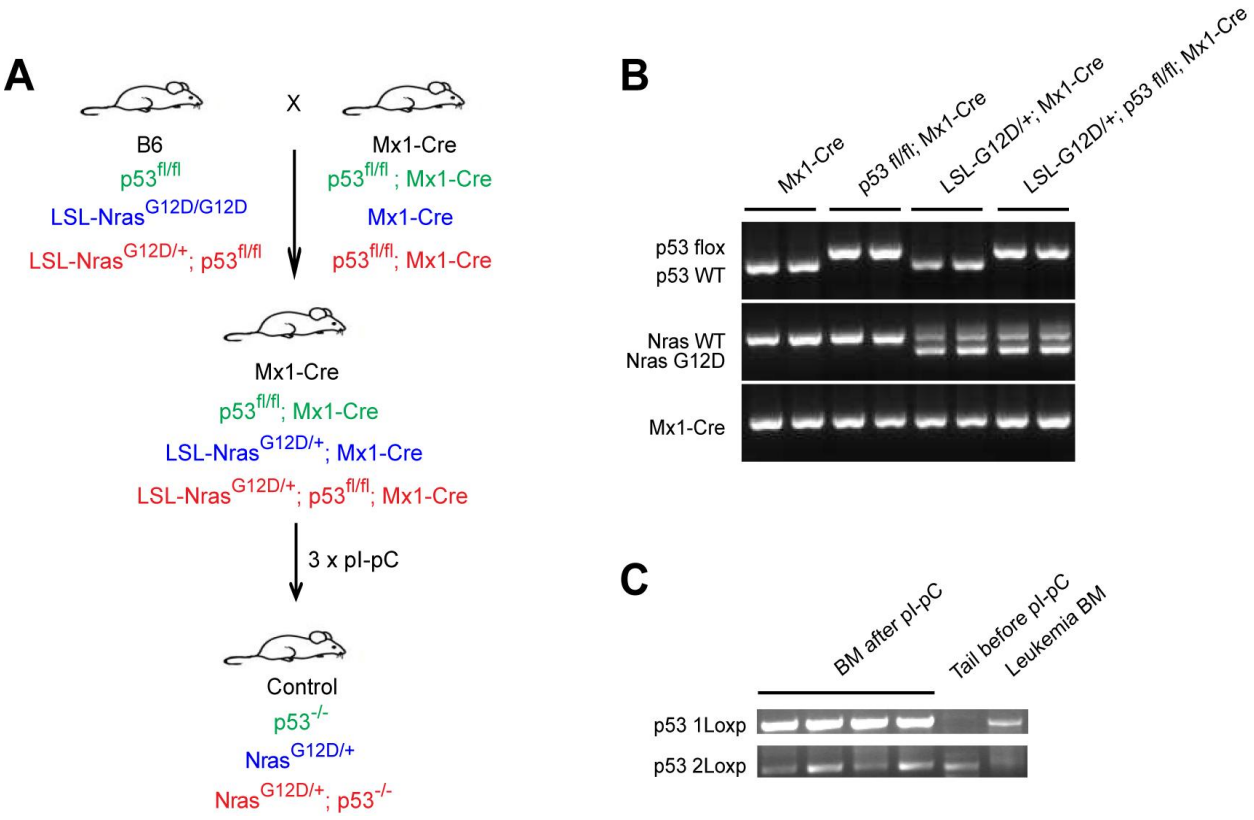

Figure 3-S2. Cellular characterization of *Nras*$^{G12D/+}$; *p53*$^{-/-}$-induced AML. (A-C) Representative flow cytometry analysis of donor-derived (CD45.1^{-}) bone marrow (BM) (A), spleen (SP) (B) and peripheral blood (PB) (C) cells from moribund AML-*Nras*$^{G12D/+}$; *p53*$^{-/-}$ and age-matched control mice.

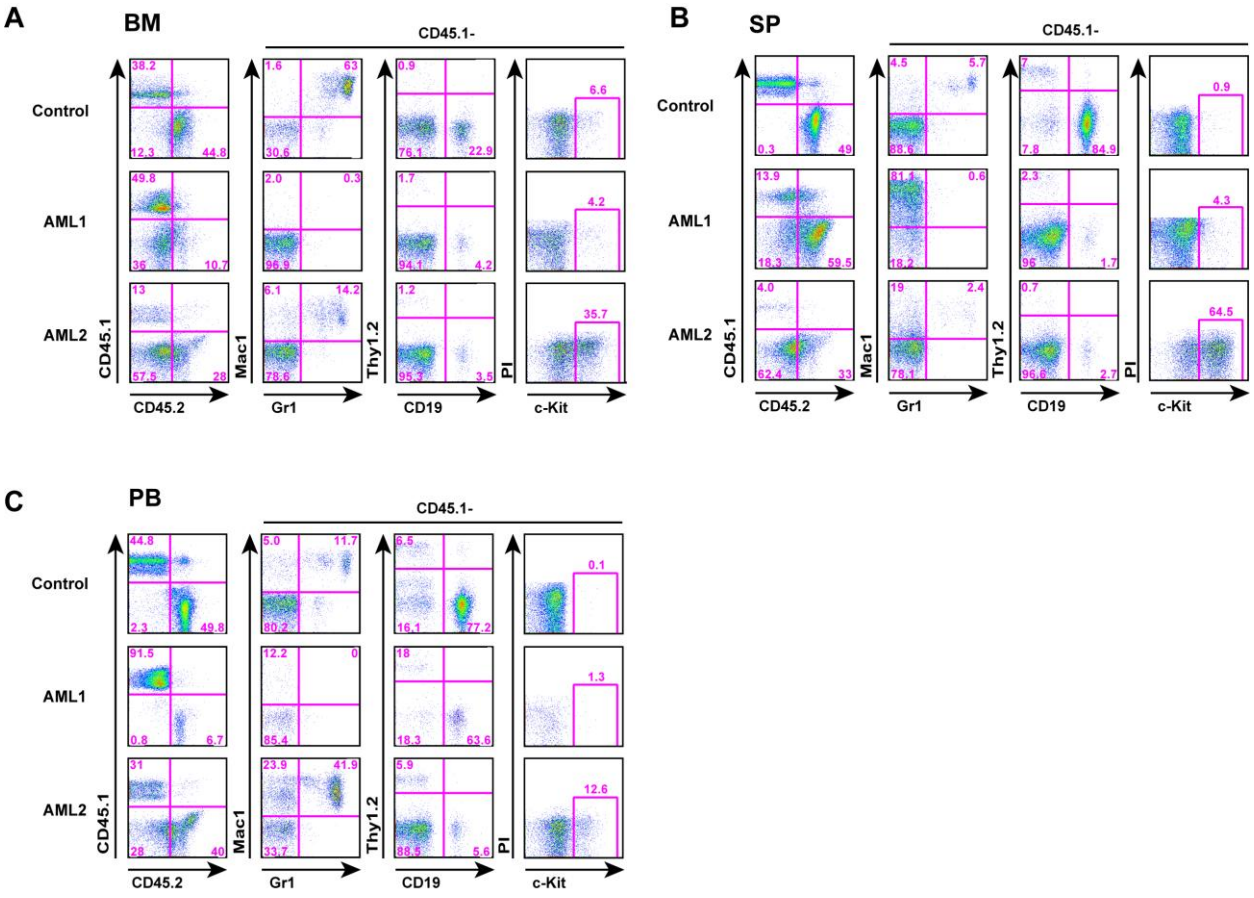

Figure 3-S3. Loss of *p53* increases myeloid cells in the peripheral blood of *Nras*$^{G12D/+}$ mice. Control, *p53*$^{-/-}$, *Nras*$^{G12D/+}$ and *Nras*$^{G12D/+}$*; p53*$^{-/-}$ mice were treated with pI-pC and euthanized on Day 12 for analysis as described in Materials and Methods. (A) The ratio of spleen weight to body weight (BW). (B) Complete blood count analysis of peripheral blood samples. (C) Flow cytometric analysis of myeloid cells in bone marrow (BM), spleen (SP) and peripheral blood (PB). Data are presented as mean ± SD. * $P < 0.05$; ** $P < 0.01$; *** $P < 0.001$.

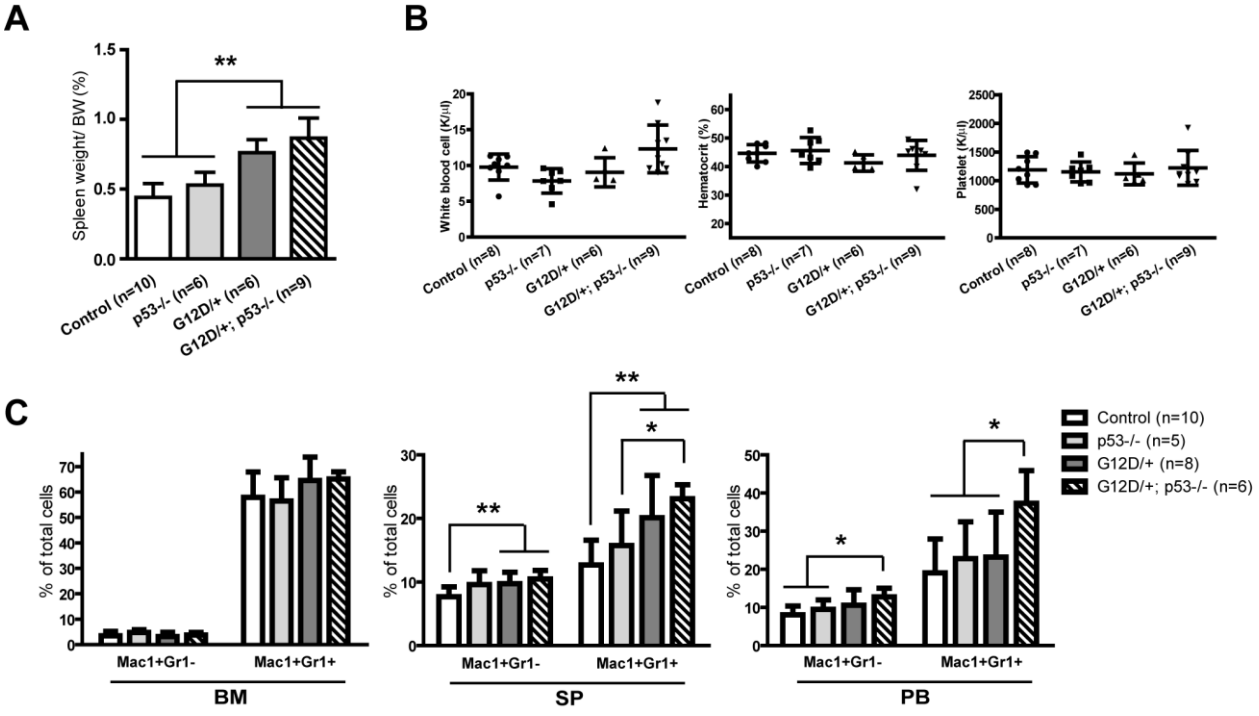

Figure 3-S4. p53 expression level is decreased in *Nras*$^{G12D/+}$ HSCs. Control and *Nras*$^{G12D/+}$ mice were treated with pI-pC and euthanized on Day 12 for analysis as described in Materials and Methods. (A) Relative *p53* mRNA level were quantified by PCR-array in control and *Nras*$^{G12D/+}$ HSCs. (B) Expression levels of p53 protein were quantified by intracellular flow cytometry in control, *Nras*$^{G12D/+}$ and *p53*$^{-/-}$ HSCs (left) and whole bone marrow (WBM) cells (right). WBM cells from wild-type C57BL/6 mice irradiated with 200 rads serve as a positive control (PC). (C) Expression levels of p21 protein were quantified by intracellular flow cytometry in control, *Nras*$^{G12D/+}$ and *p53*$^{-/-}$ HSCs. Data are presented as mean ± SD. * $P < 0.05$.

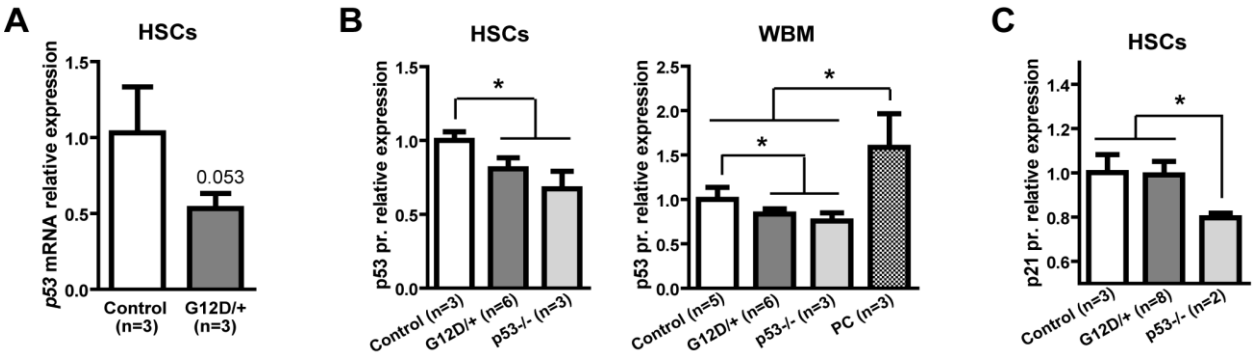

Figure 3-S5. Leukemia initiating cells are enriched in Lin$^-$ c-Kit$^+$ cells. (A) Variant numbers of Lin$^-$ c-kit$^+$ cells were sorted from moribund AML-*Nras*$^{G12D/+}$; *p53*$^{-/-}$ mice and transplanted into sublethally irradiated mice. (B) Limiting dilution analysis of the LIC (leukemia initiating cell) frequency in Lin$^-$ c-Kit$^+$ leukemia cells.

A

Primary transplantation			Secondary transplantation			Tertiary transplantation		
Number of Lin-c-kit+ dornor	AML mice (total mice)	Latency (days)	Number of Lin-c-kit+ dornor	AML mice (total mice)	Latency (days)	Number of Lin-c-kit+ dornor	AML mice (total mice)	Latency (days)
10000	8 (15)	108±27	100000	2 (2)	28±2	1000	1 (1)	63
			1000	4 (4)	47±6	100	0 (2)	N/A
						10	0 (4)	N/A

B

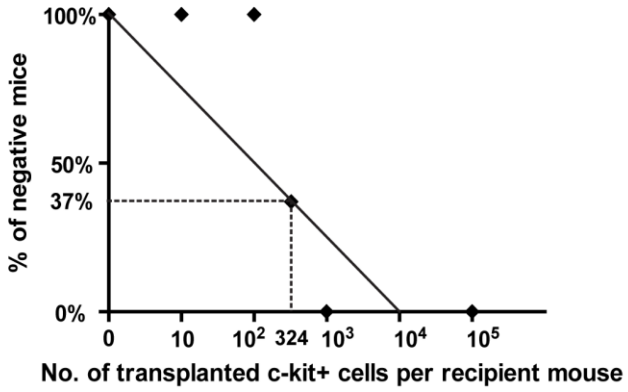

Figure 3-S6. Representative flow cytometry analysis of myeloid progenitors in spleen from moribund AML-*Nras*$^{G12D/+}$; *p53*$^{-/-}$ and control mice.

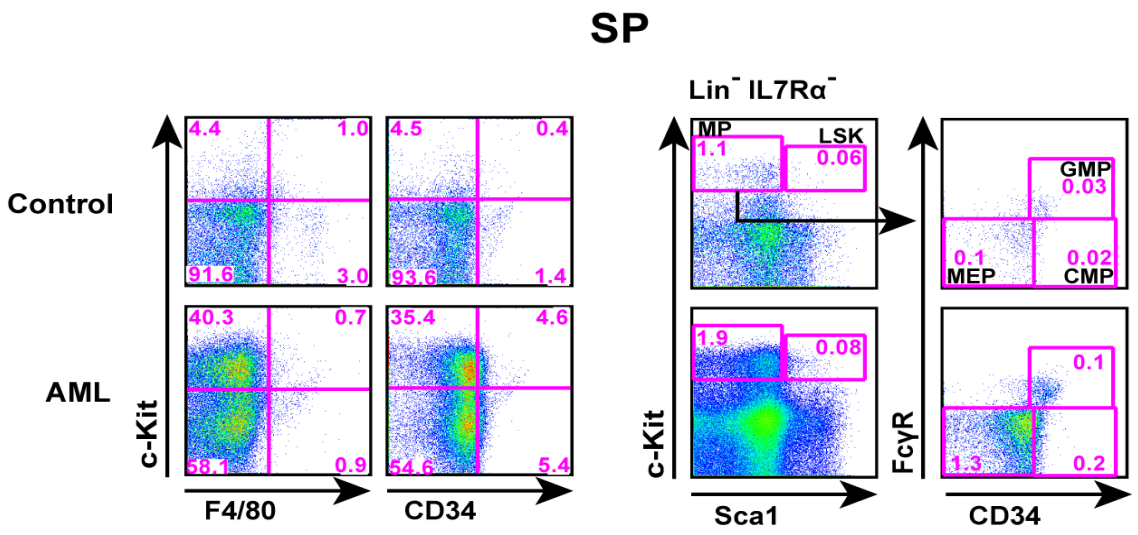

Figure 3-S7. Schematic picture illustrating the generation of leukemia initiating cells in CMML and AML.

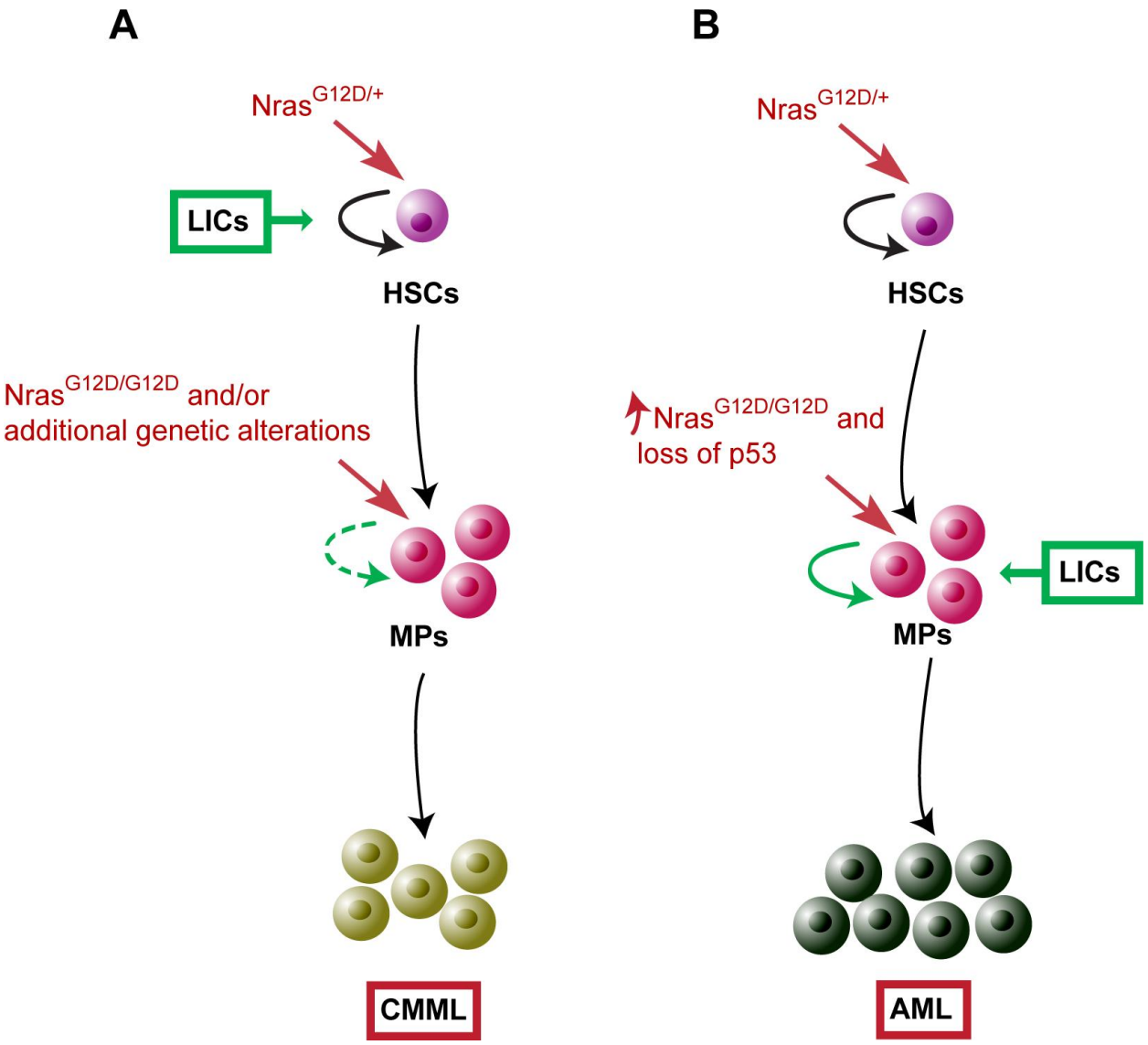

3.7 Tables

Table 3-1. *Nras$^{G12D/+}$; p53$^{-/-}$* MEPs serves as leukemia initiating cells

Donor cell types	Number of donor cells	Number of helper cells	Number of recipient mice	Disease diagnosis	Diseased animals	%
WBM	$2.5x10^5$	$2.5x10^5$	20	AML and TALL	20	100
$CD45^+$ BM	$2.5x10^5$	$2.5x10^5$	4	AML and TALL	4	100
HSC	30	$2x10^5$	10	AMD and TALL	7	70
MPP	30	$2x10^5$	12	AMD and TALL	10	83
MP	10,000	$2x10^5$	15	AMD	8	53
GMP	4,000	$2x10^5$	3	N/A	0	0
MEP	2,000	$2x10^5$	3	AMD	2	67

Various types of cells were isolated from primary *Nras$^{G12D/+}$; p53$^{-/-}$* mice on Day 12 and transplanted with helper cells ($CD45.1^+$) into lethally irradiated mice. Mice without any diseases were monitored for at least one year. WBM, whole bone marrow; HSC, hematopoietic stem cell; MPP, multipotent progenitor; MP, myeloid progenitor; GMP, granulocyte-macrophage progenitor; MEP, megakaryocyte-erythroid progenitor.

Table 3-2. *p53*$^{-/-}$ MPs do not initiate AML *in vivo*

Donor cell types	Number of donor cells	Number of helper cells	Number of recipient mice	Disease diagnosis	Diseased animals	%
WBM	$2.5x10^5$	$2.5x10^5$	20	TALL	20	100
MP	10,000	$2x10^5$	4	N/A	0	0
GMP	4,000	$2x10^5$	8	N/A	0	0
MEP	2,000	$2x10^5$	8	N/A	0	0

Various types of cells were isolated from primary *p53*$^{-/-}$ mice on Day 12 and transplanted with helper cells ($CD45.1^+$) into lethally irradiated mice. Mice without any disease were monitored for at least one year.

Table 3-3. Summarization of differentially expressed genes in AML-MPs

	FDR<0.05		FDR<0.001	
	logFC>1[#]	logFC>4	logFC>1	logFC>4[##]
Up	2453	537	1966	496
Down	3604	1715	3210	1697

# indicates genes used in GSEA analysis (Figure 4C) and in identification of potential p53 target genes (Figure 5A).

indicates genes used in GO analysis (Figure 4B).

Table 3-4. Summary of whole exome sequencing results from 7 CMML patients

Patient	CMML-2	CMML-8	CMML-10	CMML-12	CMML-13	CMML-20	CMML-OSU
Age	73	60	70	77	74	68	42
Gender	Male	Male	Male	Male	Male	Male	Male
Diagnosis	sAML with antecedent of CMML	sAML with antecedent of CMML	CMML-2	CMML-1	CMML-1	CMML-1	CMML-1
Karyotype	46, XY	46, XY	46, XY	46, XY	46, XY	45, X, -Y[6]/14	45, XY, -7[15]/5
WBC ($x10^3$/uL)	7.4	56.1	29.7	32.2	81.6	27.1	53.9
Monocyte ($x10^3$/uL)	0.59	23	2.7	6.1	6.5	5.42	28
BM blasts (%)	20	20	10	2	1	7	N/A
KRAS	V7E (21%)	-	-	G12D (42%)	-	-	-
NRAS	-	G12D (51%)	G12R (19%)	-	G13V (44%)	-	-
TP53	P72R (94%)	P72R (100%)	P72R (43%)	P72R (93%)	P72R (100%)	P72R (100%)	P72R (100%)

3.8 References

1. Emanuel, P.D., Juvenile myelomonocytic leukemia and chronic myelomonocytic leukemia. Leukemia, 2008. **22**(7): p. 1335-42.
2. Elliott, M.A., Chronic neutrophilic leukemia and chronic myelomonocytic leukemia: WHO defined. Best Pract Res Clin Haematol, 2006. **19**(3): p. 571-93.
3. Tartaglia, M., et al., Somatic mutations in PTPN11 in juvenile myelomonocytic leukemia, myelodysplastic syndromes and acute myeloid leukemia. Nat Genet, 2003. **34**(2): p. 148-50.
4. Yoshida, N., et al., Correlation of clinical features with the mutational status of GM-CSF signaling pathway-related genes in juvenile myelomonocytic leukemia. Pediatr Res, 2009. **65**(3): p. 334-40.
5. Loh, M.L., et al., Mutations in CBL occur frequently in juvenile myelomonocytic leukemia. Blood, 2009. **114**(9): p. 1859-63.
6. Itzykson, R., et al., Prognostic score including gene mutations in chronic myelomonocytic leukemia. J Clin Oncol, 2013. **31**(19): p. 2428-36.
7. Reuter, C.W., M.A. Morgan, and L. Bergmann, Targeting the Ras signaling pathway: a rational, mechanism-based treatment for hematologic malignancies? Blood, 2000. **96**(5): p. 1655-69.
8. Bowen, D.T., Chronic myelomonocytic leukemia: lost in classification? Hematol Oncol, 2005. **23**(1): p. 26-33.
9. Onida, F. and M. Beran, Chronic myelomonocytic leukemia: myeloproliferative variant. Curr Hematol Rep, 2004. **3**(3): p. 218-26.

10. Wang, J.Y., et al., Endogenous oncogenic Nras mutation leads to aberrant GM-CSF signaling in granulocytic/monocytic precursors in a murine model of chronic myelomonocytic leukemia. Blood, 2010. **116**(26): p. 5991-6002.
11. Dunbar, A.J., et al., 250K single nucleotide polymorphism array karyotyping identifies acquired uniparental disomy and homozygous mutations, including novel missense substitutions of c-Cbl, in myeloid malignancies. Cancer Res, 2008. **68**(24): p. 10349-57.
12. Kuo, M.C., et al., RUNX1 mutations are frequent in chronic myelomonocytic leukemia and mutations at the C-terminal region might predict acute myeloid leukemia transformation. Leukemia, 2009. **23**(8): p. 1426-31.
13. Chang, Y.I., et al., Evaluation of allelic strength of human TET2 mutations and cooperation between Tet2 knockdown and oncogenic Nras mutation. Br J Haematol, 2014.
14. Li, Q., et al., Hematopoiesis and leukemogenesis in mice expressing oncogenic NrasG12D from the endogenous locus. Blood, 2011. **117**(6): p. 2022-32.
15. Chang, Y.I., et al., Loss of Dnmt3a and endogenous Kras cooperate to regulate hematopoietic stem and progenitor cell functions in leukemogenesis. Leukemia, 2015.
16. Meek, D.W., Tumour suppression by p53: a role for the DNA damage response? Nat Rev Cancer, 2009. **9**(10): p. 714-23.
17. Johnson, L., et al., Somatic activation of the K-ras oncogene causes early onset lung cancer in mice. Nature, 2001. **410**(6832): p. 1111-6.

18. Chen, Z., et al., Crucial role of p53-dependent cellular senescence in suppression of Pten-deficient tumorigenesis. Nature, 2005. **436**(7051): p. 725-30.

19. Zhao, Z., et al., p53 loss promotes acute myeloid leukemia by enabling aberrant self-renewal. Genes Dev, 2010. **24**(13): p. 1389-402.

20. Rucker, F.G., et al., TP53 alterations in acute myeloid leukemia with complex karyotype correlate with specific copy number alterations, monosomal karyotype, and dismal outcome. Blood, 2012. **119**(9): p. 2114-21.

21. Rampal, R., et al., Genomic and functional analysis of leukemic transformation of myeloproliferative neoplasms. Proc Natl Acad Sci U S A, 2014. **111**(50): p. E5401-10.

22. Liu, Y., et al., p53 regulates hematopoietic stem cell quiescence. Cell Stem Cell, 2009. **4**(1): p. 37-48.

23. Marino, S., et al., Induction of medulloblastomas in p53-null mutant mice by somatic inactivation of Rb in the external granular layer cells of the cerebellum. Genes Dev, 2000. **14**(8): p. 994-1004.

24. Zhang, J., et al., Oncogenic Kras-induced leukemogeneis: hematopoietic stem cells as the initial target and lineage-specific progenitors as the potential targets for final leukemic transformation. Blood, 2009. **113**(6): p. 1304-14.

25. Wang, J., et al., Nras G12D/+ promotes leukemogenesis by aberrantly regulating haematopoietic stem cell functions. Blood, 2013. **121**(26): p. 5203-5207.

26. Wang, J.Y., et al., Endogenous oncogenic Nras mutation initiates hematopoietic malignancies in a dose- and cell type-dependent manner. Blood, 2011. **118**(2): p. 368-379.

27. Kong, G., et al., Combined MEK and JAK inhibition abrogates murine myeloproliferative neoplasm. J Clin Invest, 2014. **124**(6): p. 2762-73.

28. Kuhn, R., et al., Inducible gene targeting in mice. Science, 1995. **269**(5229): p. 1427-9.

29. Kiel, M.J., et al., Haematopoietic stem cells do not asymmetrically segregate chromosomes or retain BrdU. Nature, 2007. **449**(7159): p. 238-42.

30. Forsberg, E.C., et al., Differential expression of novel potential regulators in hematopoietic stem cells. PLoS Genet, 2005. **1**(3): p. e28.

31. Krivtsov, A.V., et al., Transformation from committed progenitor to leukaemia stem cell initiated by MLL-AF9. Nature, 2006. **442**(7104): p. 818-22.

32. He, S., D. Nakada, and S.J. Morrison, Mechanisms of stem cell self-renewal. Annu Rev Cell Dev Biol, 2009. **25**: p. 377-406.

33. Pant, V., A. Quintas-Cardama, and G. Lozano, The p53 pathway in hematopoiesis: lessons from mouse models, implications for humans. Blood, 2012. **120**(26): p. 5118-27.

34. Li, M., et al., Distinct regulatory mechanisms and functions for p53-activated and p53-repressed DNA damage response genes in embryonic stem cells. Mol Cell, 2012. **46**(1): p. 30-42.

35. Bersenev, A., et al., Lnk controls mouse hematopoietic stem cell self-renewal and quiescence through direct interactions with JAK2. J Clin Invest, 2008. **118**(8): p. 2832-44.

36. Rhoades, K.L., et al., Analysis of the role of AML1-ETO in leukemogenesis, using an inducible transgenic mouse model. Blood, 2000. **96**(6): p. 2108-15.

37. Eidenschink Brodersen, L., et al., Assessment of erythroid dysplasia by "difference from normal" in routine clinical flow cytometry workup. Cytometry B Clin Cytom, 2015. **88**(2): p. 125-35.

38. Matakidou, A., T. Eisen, and R.S. Houlston, TP53 polymorphisms and lung cancer risk: a systematic review and meta-analysis. Mutagenesis, 2003. **18**(4): p. 377-85.

39. Schmidt, M.K., et al., Do MDM2 SNP309 and TP53 R72P interact in breast cancer susceptibility? A large pooled series from the breast cancer association consortium. Cancer Res, 2007. **67**(19): p. 9584-90.

40. Olivier, M., M. Hollstein, and P. Hainaut, TP53 mutations in human cancers: origins, consequences, and clinical use. Cold Spring Harb Perspect Biol, 2010. **2**(1): p. a001008.

41. Chan, R.J., et al., Juvenile myelomonocytic leukemia: a report from the 2nd International JMML Symposium. Leuk Res, 2009. **33**(3): p. 355-62.

43. Kalra, R., et al., Monosomy 7 and activating RAS mutations accompany malignant transformation in patients with congenital neutropenia. Blood, 1995. **86**(12): p. 4579-86.

44. Stephenson, J., H. Lizhen, and G.J. Mufti, Possible co-existence of RAS activation and monosomy 7 in the leukaemic transformation of myelodysplastic syndromes. Leuk Res, 1995. **19**(10): p. 741-8.

45. McNerney, M.E., et al., The spectrum of somatic mutations in high-risk acute myeloid leukaemia with -7/del(7q). Br J Haematol, 2014. **166**(4): p. 550-6.

Chapter 4

Conclusions and Future Directions

4.1 Introduction

Chronic myelomonocytic leukemia (CMML) is a rare disease that mainly targets the elderly people. The main characteristic of CMML is persistent monocytosis in peripheral blood. In 2008, World Health Organization (WHO) classified CMML as a mixed myelodysplastic/myeloproliferative neoplasm (MDS/MPN) disease because of its overlapping phenotypes between MDS and MPN [1]. While the molecular pathogenesis of CMML is heterogeneous, mutations involved in Ras signaling are predominantly observed in myeloproliferative-CMML (MP-CMML) [2]. Recently our lab developed an oncogenic *Nras* induced CMML mouse model that closely mimics human MP-CMML [3]. Based on this mouse model, we further introduced additional genetic alterations by crossing and generating new compound mice. The work described here contributes to our understanding of molecular, cellular, and signaling mechanisms of CMML initiation, progression and malignant transformation. In the future, additional work could be directed towards the following directions.

4.2 To determine whether CMML initiation is abrogated in $Nras^{G12D/+}$; $\beta c^{-/-}$; $\beta_{IL3}^{-/-}$ mice

Because mice have an additional β_{IL3} subunit, IL-3 signaling is unaffected in *βc* deficient mice. However, this is not the case in human. Therefore, the conclusion drawn in chapter 2 that *βc* deficiency slows down the CMML progression but does not eradicate the disease may not be consistent in CMML patients treated with a βc inhibitor. To further inhibit IL-3 signaling and mimic the situation when treating CMML patients with a βc inhibitor, $Nras^{LSL\ G12D/+}$; *Mx1-Cre;* $\beta c^{-/-}$; $\beta_{IL3}^{-/-}$ mice will be generated. Previous data

indicate that $\beta c^{-/-}$; $\beta_{IL3}^{-/-}$ double mutant mice show grossly normal hematopoiesis as $\beta c^{-/-}$ mice [4].

First, I will confirm that both GM-CSF and IL-3 signaling are abolished in compound $Nras^{G12D/+}$; $\beta c^{-/-}$; $\beta_{IL3}^{-/-}$ mice by phospho-flow assay. Secondly, to determine whether CMML initiation is abrogated, recipient mice transplanted with control, $Nras^{G12D/+}$ or $Nras^{G12D/+}$; $\beta c^{-/-}$; $\beta_{IL3}^{-/-}$ bone marrow cells will be carefully monitored. Finally, I will detect HSC and MP compartments in the three different groups of mice to determine whether $Nras^{G12D/+}$-induced HSC expansion, increased self-renewal, and myeloid differentiation bias in HSCs are affected by deleting both βc and β_{IL3}.

4.3 To determine whether combined MEK and JAK inhibition prolongs the survival of AML mice initiated by $p53^{-/-}$ and $Nras^{G12D/+}$

Over activated Ras signaling plays a central role in juvenile myelomonocytic leukemia (JMML) and MP-CMML development. Our previous data show that combined MEK and JAK inhibition abrogates $Nras^{G12D/G12D}$-induced acute MPN phenotypes for at least 20 weeks and rescues $Nras^{G12D/G12D}$ HSC functions *in vivo* [5]. To investigate whether inhibition of both MEK and JAK signaling abolishes $Nras^{G12D/+}$; $p53^{-/-}$-induced AML, combined AZD1480 (a JAK inhibitor) and AZD6244 (a MEK inhibitor) will be tested.

First, I will test whether combined drug treatment abolishes p-ERK1/2 and p-Stat5 signaling in moribund AML recipient mice by phospho-flow assay. Secondly, I will determine whether combined drug treatment inhibits AML cell growth *in vitro*. Bone marrow cells will be isolated from moribund AML recipient mice and cultured *in vitro* with or without drug treatment. Cell number will be quantified by CellTiter-Glo assay.

Finally, the efficacy of combined drug treatment will be investigated in AML mice. Because AML mice died rapidly in a narrow time window, I will randomly divide recipients to two groups 80 days post transplantation. One group will be treated with combined drug and one with vehicle. All treated mice will be carefully monitored for disease phenotypes.

4.4 To identify novel genetic mutations driving malignant transformation of CMML to AML using next generation sequencing

Unlike JMML, in which mutations in Ras signaling pathway play a central theme in disease development, the molecular pathogenesis of CMML is much more heterogeneous as I discussed in Chapter 1. Benefited from the next-generation sequencing (NGS) technology, large cohorts of CMML and JMML patient samples were sequenced to identify novel pathological mutations [6, 7]. However, little has been done to identify genetic alterations that lead to CMML malignant transformation to AML. Recently Ross L. Levine and his colleagues reported their capture-based NGS results of 33 post-MPN AML samples, in which 13 patients had paired samples before and after transformation [8]. The sequencing results identified several previously reported mutations, such as *ASXL1*, *IDH2*, *SRSF2* and *TP53*, and some novel recurrent mutations, *CALR*, *MYC*, *PTPN11*, *SETBP1*.

In the future, we will continuously collect paired CMML and AML samples for in-depth whole exome sequencing (>150x coverage). This will yield genetic mutations specifically occurring at AML stage as potential driver candidates. However, mutations specifically promoting CMML formation might be missing from this experimental setting.

4.5 Final conclusion

The work described in this thesis contributes to our understanding of the molecular and cellular mechanisms of CMML initiation, progression and malignant transformation. The experimental data using genetically engineered mouse models provide strong evidence that GM-CSF signaling is dispensable for CMML initiation but plays an important role in disease progression, and loss of *p53* synergizes with enhanced oncogenic Nras signaling to bolster transformation of MPs and induce CMML malignant transformation to AML. These findings provide strong evidence to identify mutant *TP53* in small fraction of CMML cells (sequencing CMML samples with super high coverage, e.g. 10,000X) as a prognostic factor predicting high risk of AML transformation and to target oncogenic Ras signaling as a potential therapeutic regimen to prevent and/or treat transformed AML.

4.6 References

1. Vardiman, J.W., et al., The 2008 revision of the World Health Organization (WHO) classification of myeloid neoplasms and acute leukemia: rationale and important changes. Blood, 2009. **114**(5): p. 937-51.
2. Ricci, C., et al., RAS mutations contribute to evolution of chronic myelomonocytic leukemia to the proliferative variant. Clin Cancer Res, 2010. **16**(8): p. 2246-56.
3. Wang, J., et al., Endogenous oncogenic Nras mutation promotes aberrant GM-CSF signaling in granulocytic/monocytic precursors in a murine model of chronic myelomonocytic leukemia. Blood, 2010. **116**(26): p. 5991-6002.
4. Scott, C.L., et al., Reassessment of interactions between hematopoietic receptors using common beta-chain and interleukin-3-specific receptor beta-chain-null cells: no evidence of functional interactions with receptors for erythropoietin, granulocyte colony-stimulating factor, or stem cell factor. Blood, 2000. **96**(4): p. 1588-90.
5. Kong, G., et al., Combined MEK and JAK inhibition abrogates murine myeloproliferative neoplasm. J Clin Invest, 2014. **124**(6): p. 2762-73.
6. Kohlmann, A., et al., Next-generation sequencing technology reveals a characteristic pattern of molecular mutations in 72.8% of chronic myelomonocytic leukemia by detecting frequent alterations in TET2, CBL, RAS, and RUNX1. J Clin Oncol, 2010. **28**(24): p. 3858-65.

7. Sakaguchi, H., et al., Exome sequencing identifies secondary mutations of SETBP1 and JAK3 in juvenile myelomonocytic leukemia. Nat Genet, 2013. **45**(8): p. 937-41.

8. Rampal, R., et al., Genomic and functional analysis of leukemic transformation of myeloproliferative neoplasms. Proc Natl Acad Sci U S A, 2014. **111**(50): p. E5401-10.